Long-term Spatial-temporal Eelgrass (*Zostera marina*) Habitat Change (1932-2016) in the Salish Sea using Historic Aerial Photography and Unmanned Aerial Vehicle

by

Natasha K. Nahirnick

Bachelor of Science (Honours), University of Victoria, 2015

A Thesis Submitted in Partial Fulfillment of the Requirements for the Degree of

Master of Science

in the Department of Geography

University of Victoria

Long-term Spatial-temporal Eelgrass (*Zostera marina*) Habitat Change (1932-2016) in the Salish Sea using Historic Aerial Photography and Unmanned Aerial Vehicle

by

Natasha K. Nahirnick

Bachelor of Science (Honours), University of Victoria, 2015

Supervisory Committee

Dr. M. Costa, Co-supervisor (Department of Geography)

Dr. T. Sharma, Co-supervisor (Department of Geography, Adjunct; Parks Canada)

Dr. R. Canessa, Member (Department of Geography)

Abstract

Eelgrass (*Zostera marina*) is a critical nearshore marine habitat for juvenile Pacific salmon (*Oncorhynchus* spp.) as they depart from their natal streams. Given the poor marine survival of Coho (*O. kisutch*) and Chinook (*O. tshawytscha*) salmon juveniles in recent decades, it is hypothesized that deteriorating eelgrass habitats could contribute to their low survival. The primary goal of this research was to investigate the possible long-term spatial-temporal trends in eelgrass habitat in the Salish Sea and was addressed by two main objectives: (1) Define a methodology for mapping eelgrass habitats using UAV imagery to create a baseline for long-term mapping; and (2) Assess changes in eelgrass area coverage and fragmentation over the period of 1932-2016 using historic aerial photographs and Unmanned Aerial Vehicle (UAV) imagery, and assess the relationship between eelgrass and residential housing density and shoreline activities. Three study sites in the Southern Gulf Islands of the Salish Sea were chosen for analysis. The overall accuracies of eelgrass delineation from UAV imagery were 95.3%, 88.9%, and 90.1% for Village Bay, Horton Bay, and Lyall Harbour, respectively. The UAV method was found to be highly effective for this size of study site, however results were impacted by the environmental conditions at the time of acquisition, namely: sun angle, tidal height, cloud cover, water clarity, and wind speed. The results from the first objective were incorporated into a long-term dataset of historic aerial photography and used to evaluate changes in eelgrass area and fragmentation. All three eelgrass meadows showed a deteriorating trend in eelgrass condition. On average, eelgrass area coverage decreases by 41% while meadow complexity as indicated by the shape index increases by 76%. Shoreline activities (boats, docks, log booms, and shoreline armouring) and residential housing density increased markedly at all sites over the study period. By using a linear correlation model, it was revealed that eelgrass areal coverage and fragmentation (Shape Index) were, in general, very strongly correlated to these landscape-level coastal environmental indicators. While this correlation model is not meant to show a direct causative impact on eelgrass at these sites, these results suggest an overall deterioration of coastal environmental health in the Salish Sea due to a dramatic increase in the use of the coastal zone, as well as likely declines in water quality due to urbanization.

Table of Contents

Supervisory Committee ii
Abstract iii
Table of Contents iv
List of Tables vi
List of Figures vii
Acknowledgements viii
Chapter 1 – Introduction 1
1.1 Overview 1
1.2 Objectives 3
1.3 Thesis Structure 4
1.4 Literature Review 5
1.4.1 Distribution, decline, and recovery of eelgrass landscapes 5
1.4.2 Remote sensing of seagrass habitats 8
1.4.3 Environmental considerations for remote sensing of benthic habitats 9
Chapter 2 – Benefits and challenges of UAV imagery for eelgrass (*Zostera marina*) mapping in small estuaries of the Canadian West Coast 14
2.1 Introduction 15
2.2 Materials and Methods 17
2.2.1 Study Sites 17
2.2.2 Ground Reference Data Collection 18
2.2.3 UAV Image Acquisition and Processing 20
2.2.4 Eelgrass Feature Extraction 22
2.3 Results 24
2.3.1 Village Bay, Mayne Island 25
2.3.2 Horton Bay, Mayne Island 26
2.3.3 Lyall Harbour, Saturna Island 27
2.4 Discussion 29
2.4.1 Visual interpretation of ultra-high resolution UAV imagery 30
2.4.2 Environmental conditions at the time of image acquisition 31
2.4.3 UAV technology in seagrass ecology and conservation 34

2.4.4 Opportunities for future work 36
2.5 Conclusions 37
Chapter 3 – Long-term spatial-temporal eelgrass (*Zostera marina*) habitat change in the west coast of Canada (1932-2016) 38
3.1 Introduction 39
3.2 Materials and Methods 41
3.2.1 Study sites 41
3.2.2 Dataset 42
3.2.3 Eelgrass delineation from aerial photographs 44
3.2.4 Air photo reliability assessment 44
3.2.5 Analysis of eelgrass derived landscape metrics 45
3.2.6 Landscape-level coastal environmental indicators 46
3.2.7 Analysis of the combined dataset 47
3.3 Results 47
3.3.1 Data quality of aerial photography 47
3.3.2 Long-term spatial-temporal trends in eelgrass area and fragmentation 48
3.3.3 Long-term changes in coastal environmental indicators 49
3.3.4 Relationship between eelgrass and environmental indicators 51
3.4 Discussion 58
3.4.1 Data quality and limitations 58
3.4.2 Long-term spatial-temporal trends in eelgrass coverage 59
3.4.3 Comparison to other records of eelgrass change 60
3.4.4 Associated impacts on salmonids 62
3.5 Conclusions 63
Chapter 4 – Summary and Conclusions 65
Bibliography 69
Appendix A – Distribution of training and validation data in Village Bay, Horton Bay, and Lyall Harbour 84
Appendix B – Optimizing UAV Flight Times for Benthic Habitat Mapping 86
Appendix C – Matrix for interpreting benthic habitats in UAV imagery 94
Appendix D – Additional sites mapped by UAV not included in analysis 95

List of Tables

Table 2.1 Summary of environmental conditions by site and zone 24

Table 2.2 Combined error matrices for Village Bay, Horton Bay, and Lyall Harbour. Correctly classified validation points are shaded light grey, overall accuracy is shaded blue. . 25

Table 3.1 Air photo and UAV characteristics. 2014 aerial photography not used in eelgrass mapping due to significant glint. 43

Table 3.2 Scale of air photo quality for eelgrass mapping 45

Table 3.3 Air photo quality scores for three sites from 1932 to 2016 48

Table 3.4 Shoreline activity and alteration counts 56

Table 3.5 Pearson's R values for Correlations between Housing Density and Shoreline Activities and eelgrass Percent Cover and Shape Index at three sites over time period 1932-2016 (all p-values <0.05 except where noted *) 57

List of Figures

Figure 1.1 Eelgrass (Phillips, 1985). 5

Figure 1.2 In situ spectra of eelgrass and green algae (O'Neill et al., 2011). Note the lower green reflectance (550nm) of fouled eelgrass compared with healthy green algae. 10

Figure 1.3 Average above-water reflectance with 95% confidence interval of shallow and deep benthic substrates (adapted from O'Neill et al., 2011). 11

Figure 1.4 Diagram of sun glint (Mount, 2005). 12

Figure 2.1 Study sites showing previous eelgrass mapping by community conservation groups in green.. A) Village Bay; B) Horton Bay; C) Lyall Harbour 18

Figure 2.2 Examples of cover types in kayak video ground reference data and corresponding location in UAV imagery. 20

Figure 2.3 Diagram of image overlap during UAV flight 22

Figure 2.4 Flight lines and image distribution shown in Pix4D software 22

Figure 2.5 Extracted eelgrass features in Village Bay, Mayne Island. 26

Figure 2.6 Extracted eelgrass features in Horton Bay, Mayne Island. Black dashed lines indicate boundaries between zones. 27

Figure 2.7 Extracted eelgrass features in Lyall Harbour, Saturna Island. Black dashed lines delineate boundaries between zones. 28

Figure 2.8 Subset of Village Bay 2cm orthomosaic showing textural differences between eelgrass and Ulva spp. 31

Figure 2.9 (a) Phytoplankton bloom in Lyall Harbour, July 13, 2016; (b) Approximately the same location July 15, 2016. 32

Figure 2.10 Cloud reflectance obscuring eelgrass meadow in Horton Bay, Mayne Island at approximately 50% cloud cover. 34

Figure 2.11 (a) Overcast cloud reflectance in Zone 1 of Lyall Harbour with no enhancement, (b) Same location with a local equalization enhancement. 34

Figure 3.1 Study sites. Eelgrass polygons derived from 2016 UAV imagery (Chapter 2). 42

Figure 3.2 Eelgrass area (ha) over time period 1932-2016 in three sites in the Southern Gulf Islands 52

Figure 3.3 Shape Index over time period 1932-2016 of eelgrass meadows at the three study sites in the Southern Gulf Islands. 52

Figure 3.4 Changes in spatial distribution of eelgrass at Village Bay. 53

Figure 3.5 Changes in spatial distribution of eelgrass at Horton Bay 54

Figure 3.6 Changes in spatial distribution of eelgrass at Lyall Harbour 55

Figure 3.7 Indicators of coastal environmental health at each study site over the period of 1932 to 2014. 56

Acknowledgements

There are several people that I must thank for their assistance and support throughout this project. First I would like to thank my supervisor, Dr Maycira Costa. It has been over four years since I approached her in my undergrad looking to do my honours with her in coastal remote sensing, but really having no idea what I wanted to do, or what it really meant to do coastal remote sensing. With her guidance, unending support, and seemingly bottomless patience, I have learned an incredible amount. I would also like to thank my co-supervisor Dr Tara Sharma from the Gulf Islands National Park Reserve for helping to facilitate this research, providing the majority of the historic aerial photography used in the analysis, and for providing feedback throughout the process.

A giant thank-you must be extended to Paul Hunter and Sarah Schroeder, whose contributions to this research definitely warrant co-authorship. In addition to the help they provided in data collection and analysis, their thoughts and second opinions were utilized frequently. I will be forever in debt to Eve Gordon and Dean Polti, whose time in the field and UAV equipment facilitated the entire data collection comprising Chapter 2.

Further, major gratitude is extended to the Mayne Island Conservancy and the Saturna Island Marine Research and Education Society for graciously hosting us while doing field work on both islands and providing me with their mapping data.

To the current members of the Spectral Lab: Andrea Hilborn, Karyn Suchy, Ziwei Wang, and Nicole Le Baron, for listening to me rant, providing honest opinions, and reading my writing.

Several people deserve mention for their roles in the production of this work. Karen Tinsley, for reading everything I write, and correcting the use of every comma and semi-colon. Terri Evans, for listening to my problems. Dr Olaf Niemann, for his practical insights. Dr David Atkinson, for his immense help in acquiring data and helping write the SAS code in Appendix A.

This research was part of the Salish Sea Marine Survival Project, as such, I thank the Pacific Salmon Foundation and all its supporters for funding. Further funding was provided by NSERC graduate scholarship as well as Mitacs Accelerate.

This work is dedicated to my parents, Neil and Myrna, and to my Auntie Joy, who have always been my biggest supporters, even when they don’t quite understand what I do.

Chapter 1 – Introduction

1.1 Overview

Seagrasses are marine angiosperms with a near-global extent, being found on 6 continents, and include 72 species (Short et al., 2011). They are highly productive ecosystems, ranking among the world's most valuable habitats (Costanza et al., 1997). Seagrass landscapes are a mosaic of components ranging from small, sparse, and highly fragmented patches to large, dense, and nearly continuous 'meadows' (Robbins & Bell, 1994). In the temperate regions of the Atlantic and Pacific Oceans, *Zostera marina*, commonly known as 'eelgrass', is a species of great conservation interest (Thom et al., 2012).

Eelgrass, like other seagrasses, is widely acknowledged for the ecological services it provides. Eelgrass meadows slow coastal erosion and bind sediments with a network of rhizomes, and reduce current and wave velocity with their leaves (Fonseca & Cahalan, 1992; Hansen & Reidenback, 2013). Eelgrass contributes to the oxygenation of water and is a source of detritus, organic matter, and nutrient cycling that contributes to the nearshore marine ecosystem, as well as providing sustenance through the direct consumption of leaves and eelgrass epiphytes (Penhale & Smith, 1977; Phillips, 1985). By reducing wave and current velocity and providing sustenance, eelgrass creates sheltered nursery habitat for fish and invertebrates with protection from predators (Beck et al., 2001; Jackson et al., 2001). Specifically in the Salish Sea, Pacific salmon (*Oncorhynchus* spp.) use eelgrass meadows in estuaries to acclimate to the more saline environment of the ocean, herring (*Clupea pallasi*) often spawn directly on eelgrass blades, and young-of-year Dungeness crab (*Metacarcinus magister*) benefit from the shelter and detritus eelgrass habitats offer (Plummer et al., 2013; Semmens, 2008). Further, eelgrass meadows are important feeding habitat for birds such as black Brant geese (*Branta bernicla*) and great blue heron (*Ardea herodias*) (Huang et al., 2015; Wilson & Atkinson, 1995). Due to the high availability of food materials and the habitat structure, eelgrass meadows tend to support high productivity and biodiversity (Robinson & Yakimishyn, 2011).

Despite the well-recognized importance of seagrass habitats in nearshore marine areas, declines have been documented worldwide (Orth et al., 2006; Waycott et al., 2009). While natural disturbances have resulted in large- and small-scale seagrass losses, human impacts on the coastal zone are now recognized as the primary cause of seagrass habitat loss, accounting for an estimated

2-5% annual loss of seagrass (Short & Wyllie-Echeverria, 1996; Duarte, 2002). Increased use of the coastal zone has resulted in direct physical damage related to boat operation and storage including: boat anchoring and mooring (Collins et al., 2010; Unsworth et al., 2017); dock shading (Gladstone & Courtenay, 2014; Burdick & Short, 1999); propeller scarring and hull dragging (Zieman, 1976); and particularly in British Columbia, scouring and smothering by wood debris from marine log storage (Sedell et al., 1991). Increased urbanization and coastal development leading to changes in nearshore water quality has resulted in loss of seagrasses through: nutrient loading leading to epiphyte growth and eutrophication (Burkholder et al., 2007; Short & Burdick, 1996; van Katwijk et al., 2010); high suspended sediment loads which decrease the amount of light available for photosynthesis (Giesen et al., 1990); and toxic pollutants sourced from fish farming and aquaculture (Holmer et al., 2008; Marba et al., 2006; Tallis et al., 2008). Unfortunately, seagrass losses are expected to continue and accelerate into the future as human population pressure increases (Duarte et al., 2002; Waycott et al., 2009).

Seagrasses are often considered a key indicator of coastal environmental health and marine restoration success because of their importance to nearshore coastal ecosystems and their response to anthropogenic disturbances (Short & Wylie-Echeverria, 1996; Duarte et al., 2002). As such, monitoring is extremely important in order to mitigate further seagrass loss. Metrics for such monitoring include: patch size; number of patches; shoot density; biomass; percent cover; maximum depth; and epiphyte biomass and epiphyte species (McMahon et al., 2013; Wood & Lavery, 2000). These metrics are traditionally measured by ground-based methods, such as boat or diver surveys, which are limited by site accessibility, time, and cost (Neckles et al., 2012). To address these limitations, the use of remotely sensed imagery collected by satellite, manned aircraft, or unmanned Aerial Vehicle (UAV) is proposed as an alternative for seagrass monitoring at larger geographic scales and with greater time and cost efficiency (Hossain et al., 2015).

In the Salish Sea, a lack of historical records on eelgrass distribution has inhibited long-term assessment of change and the extent of human impacts (Levings & Thom, 1994; Waycott et al., 2009). However, shoreline alterations and watershed modifications have been major causes for declines in other coastal habitats, suggesting that eelgrass habitats have suffered as well (Levings & Thom, 1994). Given the poor marine survival of Coho (*O. kisutch*) and Chinook (*O. tshawytscha*) salmon juveniles in recent decades, it is hypothesized that deteriorating eelgrass

habitats could contribute to their low survival (Beamish et al., 2003; Jackson et al., 2001; Simenstad & Cordell, 2000).

1.2 Objectives

The goal of this research was to analyze a time series (1932-2016) of historic aerial photography and contemporary Unmanned Aerial Vehicle (UAV) imagery to investigate the long-term trends in eelgrass habitat distribution in the Gulf Islands of the Salish Sea, and to consider the possible influence of landscape-level coastal environmental indicators of anthropogenic stress. The specific objectives of this research are as follows:

1. Define the current (2016) eelgrass extent at the selected study sites using low-cost consumer-grade UAV technology and concurrent ground reference data. The results of this objective will provide a baseline for the analysis of historic aerial photography.
2. Assess the long-term spatial-temporal eelgrass habitat change from 1932 to 2016 using historic aerial photography and UAV imagery by considering how metrics of eelgrass change: areal cover and Shape Index. Examine the possible influence of residential housing density and shoreline activities on the long-term changes in eelgrass habitats at the selected study sites.

1.3 Thesis Structure

Chapter 1 provides an overview of the importance of seagrass habitats, threats to seagrass decline, and methods of monitoring changes in seagrass habitats, as well as the goals and objectives of this thesis. The remainder of this chapter presents a literature review describing the factors governing the distribution of eelgrass habitats; the processes driving the decline and recovery of seagrass habitats; remote sensing techniques for monitoring seagrass habitats; the role of aerial photography in long-term seagrass assessments; and the environmental factors necessary for consideration when mapping eelgrass using UAV or historic aerial photography.

In Chapter 2, the current (2016) eelgrass areal extent is defined at the study sites using UAV imagery and Object-Based Image Analysis (OBIA). This chapter discusses the development of image acquisition methods tailored to the UAV platform for benthic habitat mapping, and explores the role of environmental conditions at the time of image acquisition on image quality and habitat interpretation.

The results from Chapter 2 are incorporated into a long-term dataset of historic aerial photography in Chapter 3. From this dataset, ranging from 1932 to 2016, eelgrass distribution is delineated and changes in areal extent and fragmentation are analyzed. Changes in residential housing density within adjacent watersheds and nearby shoreline activities were quantified and related to changes in eelgrass areal extent and fragmentation using a linear correlation model.

Chapter 4 summarizes the findings of the two separate investigations, and discusses their respective roles in the future of seagrass conservation and restoration.

To supplement the thesis, several Appendices are included at the end of the text. These include analytical methods for optimizing sun angle and tidal height of image acquisition; a photointerpretive matrix describing the visual attributes of benthic cover types in the UAV imagery; the distribution of training and validation data for Village Bay, Horton Bay, and Lyall Harbour; and results from additional sites mapped by UAV that were not included in the analyses in Chapters 2 and 3.

1.4 Literature Review

This literature review begins with the factors that govern the distribution of eelgrass in the Salish Sea and the decline and recovery of seagrass landscapes. Next, a review of methods for monitoring seagrass landscapes is presented, including ground-based and remote sensing methods. The final section of the literature review will address the environmental considerations for aerial photographic mapping of benthic habitats, which is important for both the UAV image acquisition, as well as the interpretation of historic aerial photography.

Figure 1.1 Eelgrass (Phillips, 1985).

1.4.1 Distribution, decline, and recovery of eelgrass landscapes

The spatial pattern created by eelgrass landscapes is a mosaic of components ranging from small, sparse, and highly fragmented patches to large, dense, and nearly continuous meadows, growing in both intertidal and subtidal areas (Phillips, 1985). For photosynthesis to occur, eelgrass is restricted to a range of water depths in which sufficient light can penetrate the water column, from 1.8m above mean lower-low water (MLLW) up to 6.6m below MLLW in clear waters (Phillips, 1985). Soft coastal sediments, ranging from mud to mixed sand and gravel, allow for anchoring of the eelgrass rhizomes (Figure 1.1; Phillips, 1985). Additionally, exposure to wave energy will further determine the distribution of the eelgrass landscape; sheltered areas tend to support larger continuous meadows while areas exposed to wave dynamics tend to exhibit more elongated patch shapes with less aggregation (Robbins & Bell, 1994; Frederiksen et al., 2004a). The largest eelgrass meadows are typically found in protected estuarine areas, and can tolerate a large range of salinity from 10 to 30 ppt (Phillips, 1985).

Eelgrass landscapes can exhibit large fluctuations in spatial and temporal distribution, and are constantly under transformation as a result of a number of factors (Short and Wyllie Echeverria, 1996). Seagrass declines can be experienced through natural processes such as storms and wave action, herbivore grazing, and disease. Storms and wave action can damage seagrass meadows by

damaging leaves and uprooting entire plants, while excessive wave motion causes the resuspension of sediments that limit light availability and may bury seagrass once settled (Short & Wylie-Echeverria, 1996). Larger and denser eelgrass patches are able to withstand greater wave and current action stress due to improved anchoring, mutual physical protection, and physiological integration among shoots (Olesen & Sand-Jensen, 1994; Bos and van Katwijk, 2007). Herbivores, such as geese, dugongs, manatees, and green turtles, can cause reduced leaf cover or loss of entire plants (Ward et al., 2005; Nakaoka & Aioi, 1999). In terms of disease, perhaps the most prolific is the *Labyrinthula* spp. slime mold, infecting *Z. marina*, which has caused massive historical die-backs. This 'wasting disease' was responsible for losses of up to 90% in Atlantic North America and Europe in the 1930s (Dexter, 1985; Frederiksen et al., 2004a,b; Orth & Moore, 1984).

While natural disturbances have been shown to cause large losses of seagrasses, human-induced disturbances are considered to be primarily responsible for the sustained decline in seagrasses worldwide (Short & Wyllie-Echeverria, 1996). Watershed characteristics such as land use and land cover affect water quality of coastal estuaries by altering the sediment and chemical loads entering stream and riverine systems (Basnyat et al., 1999). Nutrient loading into estuarine habitats from agricultural runoff, residential septic systems, urban areas, and sewage outfalls promotes eutrophication, the excessive growth of epiphytes, algae, and phytoplankton (Drake et al., 2003; Valiela et al., 1992). These species compete for the solar radiation necessary for photosynthesis, and have been linked to losses of *Z. marina* and other seagrasses (Larkum & West, 1990; Short & Burdick, 1996). For example, Short & Burdick (1996) found that watersheds contributing more nitrogen from residential sources experienced greater rates of competitive algae (epiphytes, macro algae, and phytoplankton), resulting in declines in eelgrass habitat, while drainage areas isolated from groundwater nitrogen inputs experienced little or no change in eelgrass extent.

Suspended sediments, a consequence of natural erosion, dredging, and runoff from agricultural tilling and harvested forest lands will also affect water quality (Anderson & Lockaby, 2011; Giesen et al., 1990; Karr & Schlosser, 1978; Riemann & Hoffman, 1991). High sediment concentrations lessen the light available for photosynthesis and have been shown to cause reductions in shoot density, biomass, and canopy height (Longstaff & Dennison, 1999). In addition to being sensitive to eutrophication and suspended sediments, seagrasses are sensitive to heavy

metal bioaccumulation, herbicide toxicity, and petrochemicals (Negri et al., 2015). As such, impervious surfaces in urban and residential areas can be a major source of contaminants entering the nearshore marine system and are considered to be a key environmental indicator (Arnold & Gibbons, 1996). Nutrients, sediments, and other contaminants entering the aquatic environment from diffuse sources are collectively known as non-point source (NPS) pollutants.

In addition to large scale changes in water quality, localized activities on the shoreline can have severe impacts on seagrass meadows (Orth et al., 2006). Harbour and dock building can cause direct physical disturbance and continue to shade seagrasses after they have been built (Shafer, 1999). Eelgrass beds growing under and adjacent to docks exhibit lower shoot density and canopy structure (Burdick & Short, 1999; Gladstone & Courtenay, 2014). Boat moors, anchors, and propellers produce scours in seagrass meadows (Collins et al., 2010; Unsworth et al., 2017; Walker et al., 1989; Zieman, 1976). For example, the severe impacts associated with swinging chain moors produce circular scars in seagrass meadows that can reach sizes of 122 to 314m^2 per moor (Unsworth et al., 2017; Walker et al., 1989). Protective infrastructure such as breakwaters, dykes, and shoreline armouring alter the flow of water and sediments through nearshore and estuarine ecosystems (Patrick et al., 2016). Recently, Dethier et al. (2017) examined the impact of shoreline armouring in the Salish Sea, finding a consistent association between armouring and reductions in beach width, numbers of accumulated logs, beach wrack and associated invertebrates, and shoreline riparian vegetation. Marine timber storage, a consequence of the forest harvest industry, has been widespread in the Salish Sea and results in direct scarification of the substrate; it also smothers seagrasses with woody debris and detritus (Jackson, 1986; Sedell & Duval, 1985). Seagrass bed fragmentation contributes to the large-scale declines because smaller patches more susceptible to disturbances (Olesen & Sand-Jensen, 1994).

The rate of recovery of damaged or degraded seagrass habitats depends on intrinsic growth characteristics and attributes of the plant itself. This includes: rhizome growth rate, branching frequency and angle; plant demographic processes, such as shoot recruitment and mortality; and competition between species (Olesen and Sand-Jensen, 1994). After a disturbance, the growth characteristics and attributes of the plant itself will govern the rate of seagrass recolonization. Expansion of *Z. marina* patches by horizontal rhizome growth is relatively slow compared to other seagrass species and has been measured to be between 16 to 26cm/year (Marba & Duarte, 1998;

Olesen & Sand-Jensen, 1994). As an angiosperm, *Z. marina* additionally has seed dispersal strategies for reproduction. However, the seeds are negatively buoyant and drop to the sediment quickly, and thus are likely limited to short-distance dispersal from the parent stock but can result in rapid expansion rates following major disturbance (Olesen & Sand-Jensen, 1994; Orth et al., 1994). However, as with seagrass disturbances, there are both natural and anthropogenic factors to seagrass recovery. Much energy has been invested by academics and communities in methods for seagrass restoration (Bos & van Katwijk, 2007; Lee & Park, 2008; Nakashita et al., 2017; van Katwijk et al., 2016) and in the alleviation of anthropogenic stressors on seagrass habitats (Rehr et al., 2014).

1.4.2 Remote sensing of seagrass habitats

Because of the high value of seagrass ecosystems and their susceptibility to anthropogenic disturbances and pressures, seagrass ecosystems are often considered an indicator of coastal environmental health and as such, monitoring of seagrasses is of high priority for coastal and marine conservation (Krause-Jensen et al., 2005; Orth et al., 2006). Metrics for such monitoring of seagrasses include: patch size; number of patches; percent cover; shoot density; biomass; percent cover; and epiphyte biomass and epiphyte species (Robinson & Yakimishyn, 2005; Short et al., 2014). Ground based methods, such as by boat or diver, have often been employed by ecologists, biologists, and community volunteers because they are well characterized, require minimal equipment, and do not necessitate technical knowledge for image analysis. However, ground-based methods are limited by site accessibility, time, and cost. An alternative to ground-based methods for eelgrass monitoring is the use of remotely sensed imagery, which can be a cost and time efficient method to cover large and inaccessible areas.

It is now common to use remotely sensed satellite imagery to assess many of the metrics traditionally sampled in the field at spatial scales larger than can be assessed using ground-based measurements. Moderate resolution satellites at the 10-30m scale, such as the Landsat or SPOT series, have been a cost effective way of assessing eelgrass extent and biomass over large geographic areas (Hogrefe et al., 2014; Pasqualini et al., 2005; Schweizer et al., 2005;). The applications of moderate resolution satellites to study seagrass patch shape are limited by spatial resolution and are most effective when meadows are large, continuous, and of a single species

(Dekker et al., 2006). High resolution satellites and multispectral or hyperspectral airborne sensors in the 1-5m range, such as the Quickbird, Worldview, and IKONOS satellite series or the aircraft-mounted CASI imaging spectrometer, often provide sufficient spatial and spectral resolution for addressing monitoring metrics such as number of patches, patch shape, leaf area index, species composition, and epiphyte density (Fyfe, 2003; Lyons et al., 2015; O'Neill et al., 2013; Phinn et al., 2008; Reshitnyk et al., 2014). Currently on the cutting edge of remote sensing of seagrasses is the use of small Unmanned Aerial Vehicles (UAVs). Using these remotely piloted low-altitude aircraft, ultra-high resolution imagery of seagrass meadows can be used to assess patch dynamics at spatial scales and repeat frequencies not possible with other remote sensing platforms (Barrell & Grant, 2015; Duffy et al., 2018; Ventura et al., 2016).

However, these highly advanced technologies are severely limited by temporal resolution. Earth observation satellite data availability began in 1972 with Landsat 1 (Lyons et al., 2012), high resolution satellites are further restricted to generally post-2000 (Roelfsema et al., 2014), and UAVs are even further limited to generally post-2010 for small-scale patch dynamics (Barrell & Grant, 2015). In order to assess longer time frames of seagrass change, it is necessary to consider an often overlooked source of data (Dekker et al., 2006). Archived aerial photography dating back to as early as the 1920's creates the longest possible remote sensing time series and has been valuable tool in the many fields interested in the spatial-temporal dynamics of landscapes (Rango et al., 2008). While historic aerial photography is unable to assess metrics like biomass and leaf area index, there has been great success in measuring changes in areal extent, fragmentation, impact assessment, and investigating linkages between seagrass loss and ecological consequences (Ball et al., 2014; Frederiksen et al., 2004a,b; Martin et al., 2010; Pillay et al., 2010; Short & Burdick, 1996).

1.4.3 Environmental considerations for remote sensing of benthic habitats

This section will introduce the remote sensing considerations pertinent to the acquisition of through-water aerial photography for benthic habitat mapping, including: the phenology and detectability of target and non-target SAV species; water column conditions of tidal height and turbidity; surface effects created by sun angle and wind speed; and cloud cover and atmospheric

effects (Finkbeiner et al., 2001). Examining these conditions is important for mission planning for UAV image acquisition, as well as in the interpretation of historic aerial photography.

Submerged Aquatic Vegetation (SAV)

The best time to acquire imagery of any Submerged Aquatic Vegetation (SAV) is during the season of peak biomass of the species of interest. In the Salish Sea, the time of peak biomass of eelgrass is June – August (Phillips, 1985). However, reliability problems may arise when other SAV species are present that can be mistaken for eelgrass. In the Salish Sea, it may be difficult to differentiate between eelgrass and species of green algae, such as *Ulva fenestrate* and Filamentous *Enteromorpha* ssp., due to their similar spectral profiles (Figure 1.2) (O'Neill et al., 2011). These SAV species contain the photosynthetic pigment chlorophyll-a, which absorbs heavily in the blue and red regions of the spectrum. Consequently, all of these species exhibit an observed green hue in aerial imagery. However, during this time of SAV peak biomass, epiphytic (biofouled) conditions are more likely, resulting in decreased green reflectance and increased red reflectance in eelgrass (Figure 1.2) (Drake et al., 2003; O'Neill et al., 2011). Eelgrass biofouling is likely to occur at a greater rate during the summer months when eelgrass is at maximum biomass and when nutrient, light, and temperature conditions are optimal for epiphyte growth (Phillips, 1985).

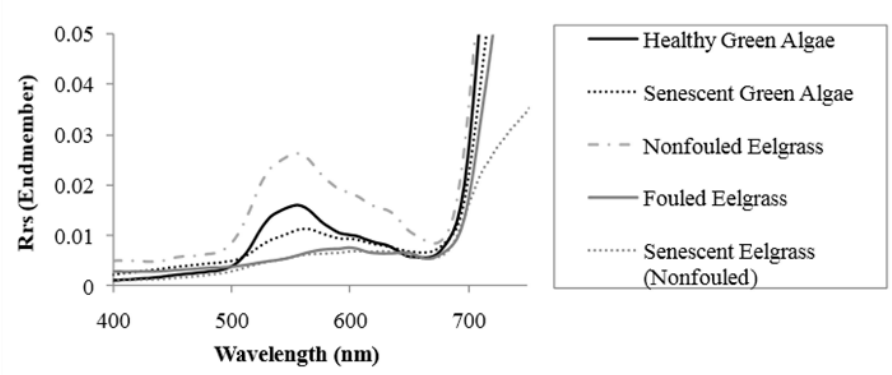

Figure 1.2 In situ spectra of eelgrass and green algae (O'Neill et al., 2011). Note the lower green reflectance (550nm) of fouled eelgrass compared with healthy green algae.

Tidal height & turbidity

The characteristics of the water column, such as tidal height and turbidity, control the depth of light penetration through the water, and in turn, the visibility of target benthic habitats. As shown in Figure 1.3, light attenuation in the water column reduces the contrast and ability to differentiate between eelgrass, other SAV, background sediments (O'Neill et al., 2011; Roelfsema et al., 2009).

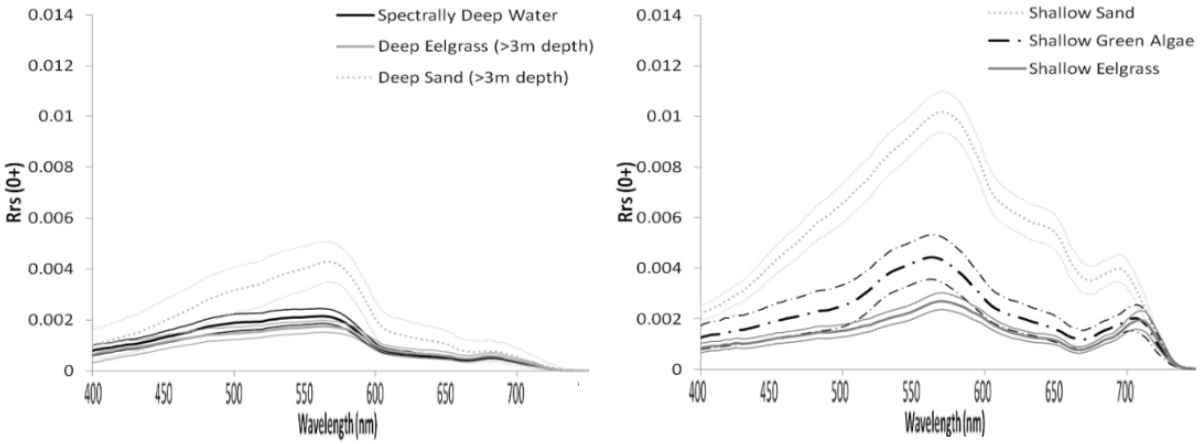

Figure 1.3 Average above-water reflectance with 95% confidence interval of shallow and deep benthic substrates (adapted from O'Neill et al., 2011).

Sea water absorbs nearly all of the near-infrared light within 1m of the surface, with decreasing absorbance (increasing reflectance) moving towards the blue end of the spectrum, which is able to penetrate the water column up to 100m (Jerlov, 1976; Wozniak & Dera, 2007). In addition to the attenuation properties of the sea water itself, the elevated presence of suspended material (organic detritus, inorganic sediments, and phytoplankton) and colour dissolved organic matter (CDOM) (Babin et al., 2003; Wozniak & Dera, 2007), further decreases the depth of light penetration and benthic visibility.

Collecting aerial photography of benthic habitats should be avoided after rain events, as turbidity increases with additional terrestrial runoff, and freshwater input can initiate algal blooms in the summer (Wilber, 1983). Therefore, aerial photography of benthic habitats should be acquired within approximately two hours of low tide under high water clarity conditions (Finkbeiner et al., 2001).

Surface effects: sun angle & wind speed

Sun angle controls in part the illumination of benthic features and the amount of glint present in aerial photography acquired (Mount, 2005). Sun glint is direct specular reflection of sunlight from an optically smooth surface such as water, creating a bright spot in imagery that obscures benthic features and overexposes the photograph. As shown in Figure 1.4, when the incident sun zenith angle (Θ_z) equals the angle of incoming light at the focal point of the camera (S_{sp}), sun glint occurs (Kay et al., 2009; Mount, 2005). At sun angles that would otherwise not produce sun glint, wind can cause small ripples or waves, which can create sun glitter by reflecting sunlight into the camera. Sun glint is thus a function of sun angle, camera position, and surface water roughness.

While sun glint corrections exist for multispectral imagery with NIR bands (Kay et al., 2009), aerial surveys employing standard analogue or digital photography need to minimize sun glint and glitter by optimizing flight times for sun angles. Sun angles ranging between 30 degrees and 45 degrees are recommended to provide sufficient benthic illumination while avoiding significant sun glint for standard aerial cameras with 94° field of view (Finkbeiner et al., 2001; Mount, 2005). Further, to avoid significant sun glitter, wind speeds below 8km/h are optimal (Finkbeiner et al., 2001).

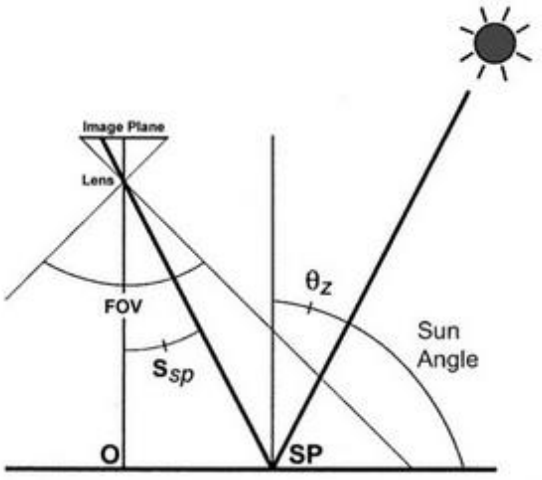

Figure 1.4 Diagram of sun glint (Mount, 2005)

Cloud cover & atmospheric effects

Lastly, it is best to have clear, cloudless skies with little haze when acquiring benthic aerial imagery. Clouds and fog non-selectively scatter incoming solar radiation, blocking visibility of ground features. In addition, cloud shadows can significantly reduce illumination of benthic features and results in decreased contrast between seagrass and background substrate or other SAV. Finkbeiner et al. (2001) recommend a maximum cloud cover of 5%. Atmospheric haze should be minimized as it scatters extraneous light into the camera sensor, thereby reducing the optical contrast within the scene of the image. Haze is the product of Rayleigh scattering, shorter wavelengths of light scattered by gas molecules (O_2, N_2), and Mie scattering, longer wavelengths of light scattered by particulates such as dust, pollen, and water vapour in the atmosphere (Chavez, 1996; Paine & Kaiser, 2012). Removal of extraneous blue light in aerial photography is achieved through the use of a yellow-filter (Finkbeiner et al., 2001). The effects of atmospheric haze increase with altitude of aircraft, because light has to pass through more haze to get to the sensor, requiring a darker yellow filter (Paine & Kaiser, 2012). Post-processing techniques for removal of atmospheric scattering exist for multispectral airborne and satellite imagery (Chavez, 1996), however most of these techniques use near-infrared reflectance correction and thus are not applicable to natural colour film or digital aerial photography (Hedley et al., 2005; Kay et al., 2009). Methods investigated for this project have not implemented any kind of atmospheric correction on their aerial photography prior to analysis (Ball et al., 2014; Fletcher et al., 2009; Lathrop et al., 2014).

Chapter 2 – Benefits and challenges of UAV imagery for eelgrass (*Zostera marina*) mapping in small estuaries of the Canadian West Coast

Abstract - Seagrasses are a fundamental component of nearshore marine habitats and as such, concerted effort has been put into developing remote sensing methods for mapping and monitoring these important habitats. However, in the small coastal bays of the Salish Sea, traditional aerial or satellite remote sensing can be cost-prohibitive or lack sufficient spatial resolution to detect the small, fringing, and often patchy eelgrass (*Zostera marina*) meadows. Bridging the gap between remotely sensed data and ground-based mapping techniques, aerial imagery collected by Unmanned Aerial Vehicle (UAV) is revolutionizing the study of fine-scale ecological phenomena. This chapter presents a method for collection and processing of UAV imagery to map eelgrass at three small coastal estuaries in the Salish Sea of British Columbia. A quad-copter style XAircraft X650 UAV equipped with a rectilinear GoPro Hero 3+ was used to acquire images with a ground resolution of 2 cm. Pix4D Pro software was used to orthorectify, georeference, and mosaic UAV imagery into continuous orthomosaics. Ground reference data was collected in the form of underwater videography collected by kayak. A manual classification approach of segmented image objects was used to classify eelgrass on a presence or absence basis. Mapping accuracies of 96.3%, 86.5%, and 89.7% were achieved for Village Bay, Horton Bay, and Lyall Harbour respectively. Mapping accuracies were found to be related to the environmental conditions at the time of image acquisition. This study presents a first evaluation of the role of environmental conditions at the time of UAV image acquisition in relation to eelgrass mapping accuracy, and how these conditions may differ from published guidelines for manned aerial photography.

2.1 Introduction

Seagrasses are a fundamental component of nearshore marine ecosystems, supporting complex food webs, stabilizing coastal sediments, and providing nursery habitat for a multitude of fish and invertebrate species (Beck et al., 2001; Phillips, 1985). However, seagrasses around the world have shown marked declines in response to both natural and anthropogenic stressors (Duarte, 2002; Short & Wyllie-Echeverria, 1996), and as such, mapping and monitoring seagrass habitat is critical for the success of coastal conservation and restoration initiatives (Nagendra et al., 2013).

A number of remote sensing techniques have been developed to assess the spatial extent of seagrasses, typically relying on aerial photography or multispectral satellite imagery (Lathrop et al., 2014; Hogrefe et al., 2014; O'Neill & Costa, 2013; Reshitnyk et al., 2014). The benefit of these remote sensing techniques is in their ability to map large, monospecific, and continuous seagrass ecosystems synoptically from an aerial view, and typically at a lower cost per unit area than field surveys alone (Klemas, 2016). However, widely available low-cost satellite imagery, such as the Landsat or SPOT series, lack the spatial resolution required to resolve sparse, fringing, or patchy seagrass meadows (Hogrefe et al., 2014; Lyons et al., 2012; Pasqualini et al., 2005). On the other hand, high resolution commercial aerial photography or satellite imagery, such as IKONOS, Quickbird, or the Worldview series, which have been highly successful for mapping and monitoring seagrasses at small spatial scales and in complex environments, remain prohibitively expensive for ecologists and community conservation groups working with small budgets (Knudby & Norlund, 2009; O'Neill & Costa, 2013; Phinn et al., 2008; Reshitnyk et al., 2014). As such, ground-based seagrass mapping and monitoring methods are often employed, which are highly limited in spatial extent and may be time consuming and labour intensive (Precision Identification, 2002).

Bridging the gap between remotely sensed data and ground-based mapping techniques, aerial imagery collected by Unmanned Aerial Vehicle (UAV) is revolutionizing the study of fine-scale ecological phenomena (Anderson & Gaston, 2013; Klemas, 2015). Platforms such as rotorcopters, balloons, and blimps are now widely used in many environmental mapping applications, and show promising results for use in nearshore coastal environments. High resolution data collected by UAV allows for the study of fine-scale ecological patterns that would

be difficult to assess with standard remote sensing technologies. For example, Barrell & Grant (2015) used multi-temporal balloon-mounted aerial photography with a resolution of 4.5 cm to assess density and internal gap dynamics of seagrass patches less than 5 m in diameter. Further, ultra-high resolution has allowed for detection and analysis of spatial distribution of lugworm (Arenicola spp.) mounds and cockle shells (Cerastoderma edule) across an entire seagrass landscape (Duffy et al., 2018). High resolution data can assist in the classification of certain algae species which exhibit textural characteristics at ultra-high resolution that allow them to be distinguished from other spectrally similar species (Bryson et al. 2013). Consumer grade technology, such as the DJI Phantom 4 quad-copter and GoPro Hero camera used by Casella et al. (2017) for coral reef mapping, is inexpensive compared to manned aircraft or high resolution satellite. The decreased operational cost of UAVs allows for repeat surveys on a frequent basis, a substantial benefit for ecological monitoring (Bryson et al., 2013; Casella et al., 2017; Duffy et al., 2018; Guichard et al., 2000; Ventura et al., 2016).

For coastal applications, the high flexibility of UAVs for task-specific flight planning is of considerable benefit, given the highly dynamic nature of the intertidal and nearshore marine area. For instance, Bryson et al. (2013) was able to study mud flat phytobenthos species because imagery could be captured at a specific time in the tidal cycle, a feat that would be difficult with traditional remote sensing in a rapidly changing dynamic intertidal ecosystem. When it comes to mapping ecological features beneath a column of water, such as coral reefs and seagrasses, this high flexibility is invaluable to time data acquisition for specific wind, tide, and sun angle conditions (Casella et al., 2017). With further investigation into the methods of image acquisition, UAV imagery may present a new way of assessing spatial-temporal change, impact assessment, and restoration success of eelgrass habitats in the small coastal bays where traditional remote sensing tools are impractical.

The goal of this research was to assess the performance of a low-cost UAV and consumer-grade digital camera for mapping eelgrass habitats in the Salish Sea. To exemplify the successes and challenges associated with the use of UAVs for eelgrass mapping, the methodology and results are presented from three aerial surveys of eelgrass meadows in the Southern Gulf Islands, British Columbia, Canada.

2.2 Materials and Methods

The methods of this analysis are organized into four sections. Following the rationale for site selection, the methods employed for ground reference data collection, UAV image acquisition and post-processing, and eelgrass feature extraction are described.

2.2.1 Study Sites

The three study areas for UAV mapping of eelgrass were Village Bay and Horton Bay on Mayne Island, and Lyall Harbour on Saturna Island, in the Southern Gulf Islands of British Columbia (Figure 2.1). The larger marine region in which these sites are located is known as the Salish Sea, a transnational water body encompassing the Strait of Georgia, Juan de Fuca Strait, and Puget Sound. The Southern Gulf Islands are located in the Strait of Georgia, the local dynamics of which are dominated by a mixed tidal regime and estuarine circulation primarily driven by the discharge of the Fraser River (Masson, 2002). Further, the Fraser River inputs significant amounts of particulate and organic matter that can influence the optical properties of the Salish Sea (Loos & Costa, 2010). The Strait of Georgia is considered to be one of the most diverse temperate marine regions in the world, hosting over 200 species of fish, hundreds of seabirds, 500 species of plant life, and 1500 species of invertebrates (Georgia Strait Alliance, 2017).

The three sites are part of a long-term spatial-temporal eelgrass study using maps derived from historic aerial photography, with this UAV mapping providing the final installment in the time series dataset (Chapter 3). As such, site selection was largely based on data availability and quality of historic aerial photographs, as well as several site characteristics. The selected sites have bright background sediments, and to account for potential differences in spatial-temporal dynamics as a result of exposure or salinity, they are all protected from wave action and have a perennial freshwater stream input (Frederiksen et al., 2004; Salo et al., 2014). Further, the sites reflect a range of sizes from 200m to 600m maximum flight distance from the ground station. Eelgrass mapping previously conducted by local community groups using ground-based methods was utilized to plan UAV image acquisition (Mayne Island Conservancy Society (MICS), 2016; Saturna Island Marine Resource and Education Society (SIMRES), 2016).

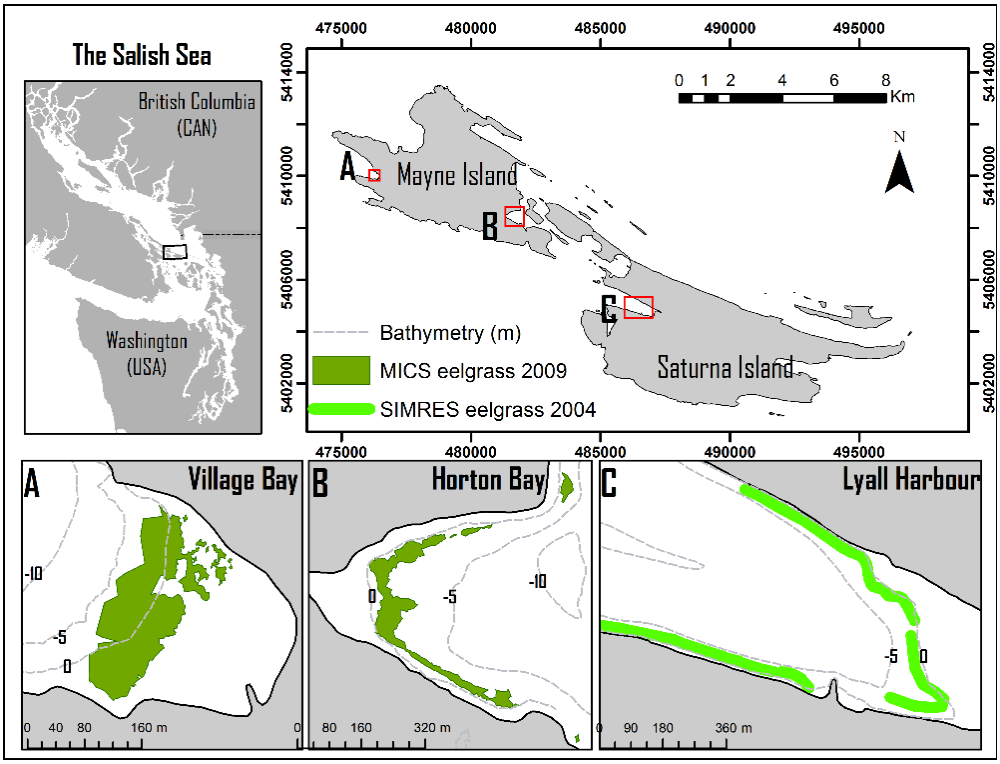

Figure 2.1 Study sites showing previous eelgrass mapping by community conservation groups in green. A) Village Bay; B) Horton Bay; C) Lyall Harbour

2.2.2 Ground Reference Data Collection

Reference data were collected in the form of underwater kayak videography. A GoPro Hero 3+ camera affixed to the bottom of a kayak continuously collected video while a Garmin GPSMAP 64 handheld unit (accuracy ~3m) recorded concurrent GPS coordinates along the track. GPS waypoint coordinates were synchronized with the kayak camera footage according to the timestamps, and video frames at the matched timestamps were classified according to the submerged vegetation present. While eelgrass is mapped on a presence or absence basis, classification of the videography included the following five classes for the purposes of interpretation: eelgrass, green algae (*Ulva* spp., *Enteromorpha* spp.), brown algae (*Saccharina luminaria*, *Sargassum muticum*) and unvegetated substrate. Eelgrass was further differentiated into 'dense' and 'sparse' categories. This refined classification of the ground reference data was important to understand specifically what cover types result in errors during eelgrass mapping process. If cover type was not discernible in the video due to water depth or turbidity, the point was removed from the dataset. Examples of each class, represented by a kayak videography frame

with paired location in the final UAV orthomosaic are provided in Figure 2.2. A stratified random approach was used for defining training and validation samples used in the UAV classification. Half of the videography points for each vegetation class were randomly selected for training (Village N=106; Horton N=171; Lyall N=120), with the other half retained for validation (Village N=107; Horton N=171; Lyall N=117). The distribution of training and validation points for each site are provided in Appendix A.

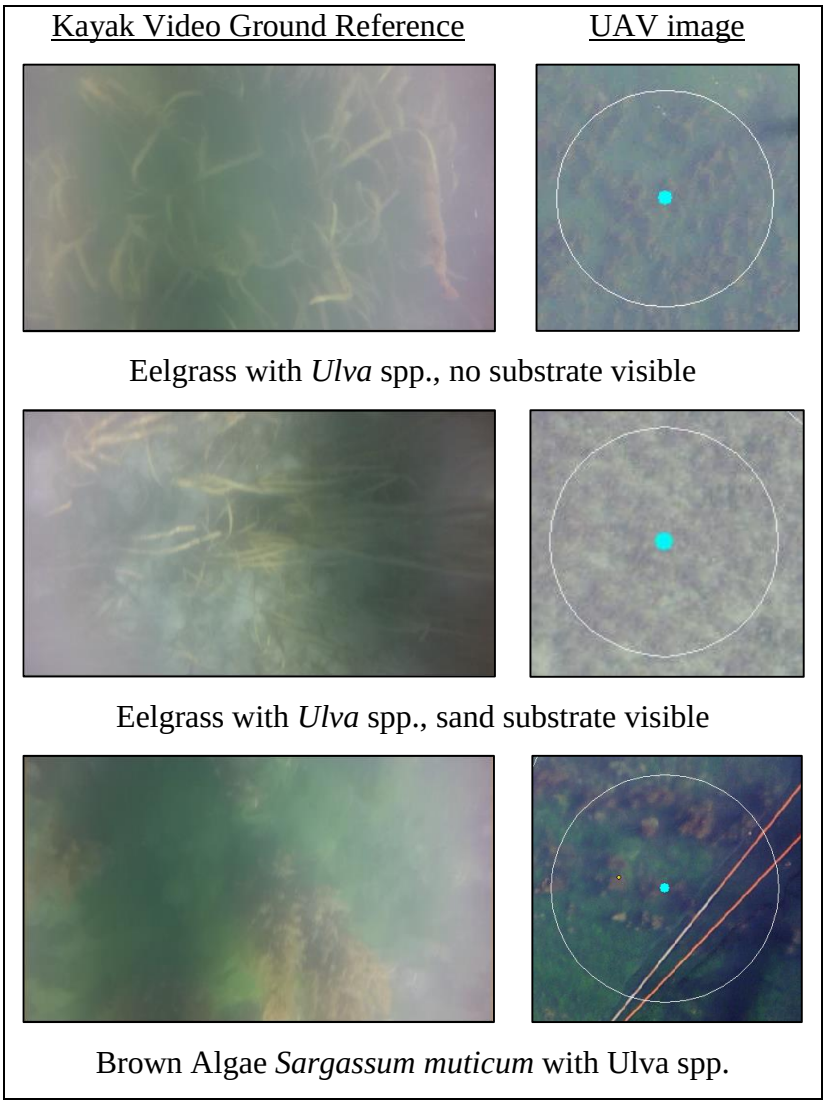

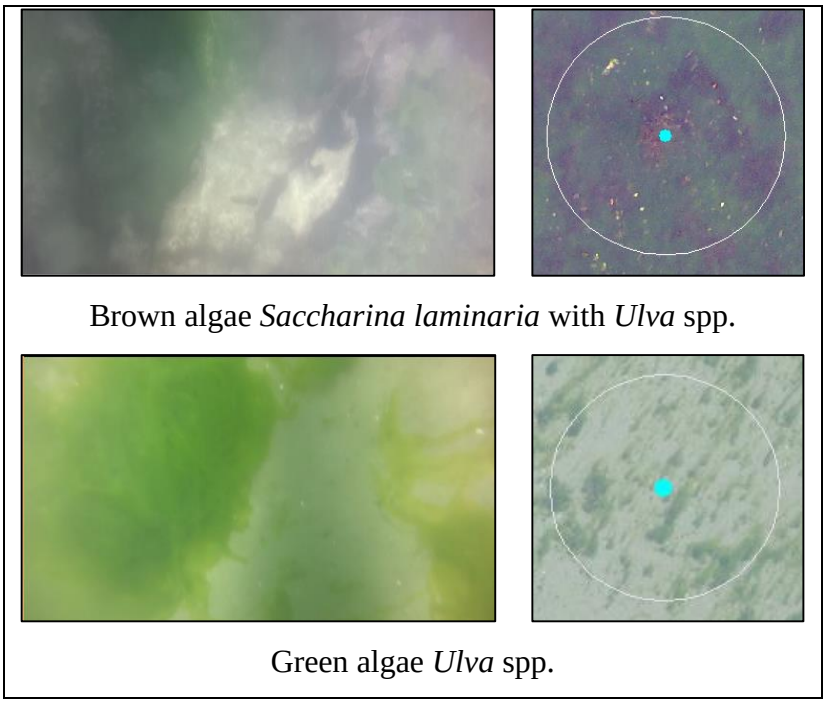

Figure 2.2 Examples of cover types in kayak video ground reference data and corresponding location in UAV imagery

2.2.3 UAV Image Acquisition and Processing

Flight Planning and Clearance Logistics were handled by the Flight Team from High Angle UAV (Victoria, BC). All operations were conducted with clearance from Transport Canada, and in accordance with Civil Aviation and Privacy laws. High Angle UAV holds a Standing Special Flight Operations Certificate (SFOC), a document administered by Transport Canada detailing operational requirements, restrictions, emergency procedures, permitted areas of operation, and minimum liability insurance coverage required for the operation. Flight Plans were reviewed with NAV Canada, a private entity that helps to ensure safe operation of manned and unmanned aircraft in Canada's Airspace. On the day of the flight, the Flight Team coordinated with local Air Traffic Control (ATC) services, and manned aircraft in the area, to ensure no risk was posed to other aircraft operating in the area. During the flight operation, High Angle deployed a set of pre-flight and post-flight checklists to ensure the airworthiness of the UAV, and all operation requirements were met before liftoff, and maintained through the duration of the flight operation.

Image acquisition was planned considering eelgrass phenology, sun angle, tidal height, water clarity, cloud cover, and wind speed, in accordance with the recommendations for benthic

habitat mapping with aerial photography detailed by Finkbeiner et al. (2001). Imagery was collected in June and July of 2016, during the time of peak biomass of *Z. marina* in the Salish Sea. Survey times were scheduled in advance to within 2 hours of low tide and between sun angles of 30° to 45°, using tidal height predictions (Fisheries and Oceans Canada, 2016) and sun angle calculations (United State Naval Observatory, 2016), as described in Appendix B. Unpredictable environmental conditions such as Secchi depth as a proxy for water clarity, cloud cover, and wind speed were recorded on-site throughout each survey.

In order to georeference the orthomosaic during post-processing, a minimum of three ground control points (GCPs) were distributed across each site prior to flight. GCPs consisted of black crosses painted on white corrugated plastic boards of dimensions 0.45 m x 0.60 m. GCP coordinates were collected using Garmin GPSMAP 64 handheld units with 3m accuracy using the waypoint averaging function until 100% sample confidence was achieved. When available, other distinct invariant landmarks, such as corners of piers and distinct rock formations, were used as additional GCPs.

Images were collected using a GoPro Hero 3+ Silver RGB digital camera mounted on a stabilizing gimbal beneath an "off the shelf" XAircraft X650 Pro quad-copter UAV. The standard fisheye GoPro lens was replaced with a 5.4mm rectilinear lens, which was a simple and inexpensive way to avoid the need for significant distortion correction later in post-processing. The flights were manually controlled by an experienced pilot, with one observer monitoring image coverage from the ground station in real-time to ensure coverage of the target area, while a second observer visually scanning airspace and the area surrounding the ground station for unexpected aircraft and other hazards. Nadir angle images, with an approximate ground resolution of 2 cm per pixel at an altitude of 65 m, were collected at a frequency of one image every two seconds, resulting in a single image covering roughly 75 x 55 m on the ground with 85% endlap between consecutive images. Flight lines were set 15m apart to achieve 85% sidelap between flight lines (Figure 2.3). Overlaps were increased above general guidelines for aerial photography because of the small footprint of each photo in relation to the relatively large size of homogenous features in coastal areas (Casella et al., 2017; Ventura et al., 2016). This ensured adequate feature detection for image stitching in the mosaicking process. The UAV flight lines and distribution of individual images is shown in Figure 2.4.

Orthomosaics were prepared using Pix4D Mapper Professional, a photogrammetry engine that orthorectifies, mosaics, and georeferences mosaics by first reconstructing the 3D scene, before projecting the image data to a specified system. Due to the apparent parallax of ground features when collecting aerial photography at such low altitudes, traditional photogrammetry software is not applicable to UAV imagery. Because of this, structure from motion (SfM) has become the method to construct 2D orthomosaics from imagery collected by low-altitude UAV (Casella et al., 2017; Turner et al., 2012; Ventura et al., 2016). The general workflow for orthomosaic construction in Pix4D includes: 1) input imagery and telemetry data (geolocation, altitude, attitude of sensor, etc); 2) automatic tie points between images are then matched against other images in the dataset to create a sparse point cloud; 3) a texture atlas is created from the images and their derived locations, and projected onto the sparse point cloud to create the orthomosaic; and 4) orthomosaic is exported with geographic projection information (NAD 1983 UTM Zone 10N) in GeoTIFF format. All unnecessary visual data were removed from the orthomosaics, including houses and yards of the properties surrounding the sites if captured in frame.

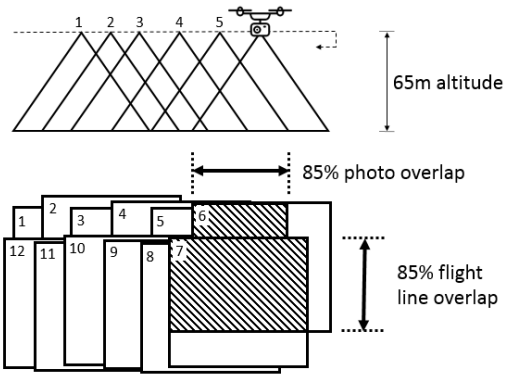

Figure 2.3 Diagram of image overlap during UAV flight

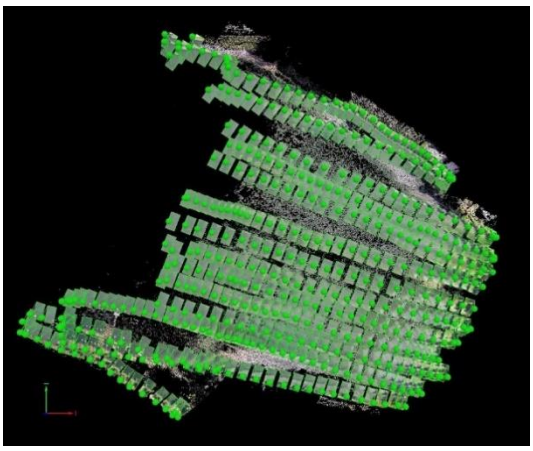

Figure 2.4 Flight lines and image distribution shown in Pix4D software

2.2.4 Eelgrass Feature Extraction

Eelgrass areas were defined based on object-based segmentation followed by visual interpretation and manual classification of segmented image objects. Object-based image analysis (OBIA) is an effective method for analyzing high resolution UAV imagery where the pixel size is much smaller than the target features, making pixel-based classifiers impractical due to spectral

heterogeneity within feature boundaries (Blaschke et al., 2014; Husson et al., 2016; Ventura et al., 2016; Wan et al., 2014). In contrast to pixel-based classifiers, in OBIA an image is first segmented into non-overlapping 'objects' before classification (Blaschke, 2010, Evans & Costa, 2014). The analyst controls the results of the segmentation by adjusting the scale, shape, and compactness parameters; a larger value in the scale parameter results in larger image objects, the shape parameter controls the weighting of spectral or colour information, while the compactness parameter determines how clustered object pixels will be (Kavzoglu & Yildiz, 2014).

Prior to the segmentation step, the orthomosaics were organized according to radiometric differences within the image. Village Bay was analyzed as one full orthomosaic, while the orthomosaics of the two larger sites, Horton bay and Lyall Harbour, were split into zones of fairly similar environmental and radiometric conditions. Orthomosaics were further resampled from 2cm to 10cm using the pixel aggregate algorithm, which significantly reduced processing time required for image segmentation, while still producing good segmentation results. Resampling was followed by digital enhancement techniques. In addition to standard linear enhancements, imagery was transformed into the Hue Saturation Value (HSV) colour space (Fletcher et al., 2009), decorrelates colour features into components that can help make features more readily apparent compared to RGB imagery alone (Andreadis et al., 1995; Fletcher et al., 2009). From the RGB and HSV bands, a combination of individual layers which visually appeared to best separate eelgrass were exported to eCognition for image segmentation. For segmentation, the scale and compactness parameters were defined using a trial and error approach until a balance between detail and objects large enough for quick classification was attained (Scale 50, shape 0.1, compactness 0.5) (Kavzoglu & Yildiz, 2014; Lathrop et al., 2014).

Due to inconsistent radiometric conditions within the resulting orthomosaics, a manual object classification in eCognition was employed instead of an automated classification of segmented image objects (Lathrop et al. 2006; Lathrop et al., 2014). The analyst used the photointerpretive characteristics of the image (tone, texture, etc.; Morgan et al., 2010), in reference to the training samples of the kayak videography, to manually identify image objects that were characterized as "eelgrass". Further, the original 2cm imagery was also used as reference in order to classify eelgrass objects that were created by segmentation of the downsampled 10cm imagery.

To assess the accuracy of the resulting eelgrass maps, extracted eelgrass features were compared to the half of the ground reference data retained for validation on an eelgrass presence or absence basis. Ground reference data points were considered to be classified correctly if they were within the 3m expected accuracy of their mapped classification, to account for the expected accuracy of the handheld GPS unit. Accuracy is reported as a modified error matrix consisting of two rows representing eelgrass presence or absence as mapped from the UAV imagery, and five columns representing the classified ground reference data. The error matrix includes overall, producer's, and user's accuracies. Overall accuracy is the percentage of correctly classified validation points for all cover classes, producer's accuracy is the percentage of validation points within each cover class that were correctly classified (the probability that each cover type was classified correctly), and user's accuracy is the percentage of correctly classified validation points on an eelgrass presence or absence basis (the probability that the map actually represents that cover class on the ground) (Congalton, 1990).

2.3 Results

The results of this analysis are first presented as summary tables describing the environmental conditions at each site (Table 2.1) and the accuracy assessments (Table 2.2). Following these, each site is addressed individually in relation to the results in Tables 2.1 and 2.2, and the final eelgrass delineation provided.

Table 2.1 Summary of environmental conditions by site and zone

Site	Date	Zone	Time	Sun angle	Tide	Cloud Cover	Wind Speed	Secchi Depth	Overall accuracy
Village	June 28, 2016	1	8:15-10:00am	29° – 44°	1.7 – 2.0 m	0%	0 – 4 km/h	4.75 m	96.3%
Horton	July 20, 2016	1	9:15-9:30am	35°	1.2 m	60%	6.5 km/h	4.25 m	86.5%
		2	9:30-10:00am	40°	0.9 m	50%	2.8 km/h		
		3	10:15-10:45am	45°	0.6 m	50%	8.4 km/h		
Lyall	July 15, 2016	1	8:45-9:15am	30°	0.9 m	95%	4.7 km/h	2.5 m	89.7%
		2	9:30-10:45am	42°	0.9 m	30%	4.5 km/h	2.5 m	
		3	11:00-11:30am	54°	1.2 m	30%	8.0 km/h	1.0 m	

Table 2.2 Combined error matrices for Village Bay, Horton Bay, and Lyall Harbour. Correctly classified validation points are shaded light grey, overall accuracy is shaded blue.

	Ground reference data					
UAV	Dense EG	Sparse EG	Brown A	Green A	Unveg	User's
Village Bay (N= 107)						
EG present	23	7	0	0	0	88.2%
EG absent	1	3	11	52	10	100%
Producer's	95.8%	70.0%	100%	100%	100%	96.3%
Horton Bay (N= 171)						
EG present	50	9	0	2	0	73.8%
EG absent	13	8	8	47	34	97.8%
Producer's	79.4%	52.9%	100%	95.9%	100%	86.5%
Lyall Harbour (N= 117)						
EG present	24	32	0	3	1	87.5%
EG absent	1	7	3	35	11	92.5%
Producer's	96.0%	82.1%	100%	92.1%	91.7%	89.7%

2.3.1 Village Bay, Mayne Island

The environmental conditions experienced at Village Bay were considered consistently optimal throughout the UAV survey and thus the site could be analyzed as one full orthomosaic. The produced eelgrass map for this site resulted in the highest overall accuracy of 96.3% (Figure 2.5; Table 2.2). The high accuracy at this site is due to the optimal environmental conditions experienced during image acquisition. Sky conditions were optimal with sun angle between the recommended values (29° to 44°), cloud cover consistently 0% throughout the survey, and wind speed low (0 – 4km/h). As a result, no surface effects on the water are observed in the Village Bay imagery. While the tidal height was not particularly low (1.8m), water clarity was high enough with a 4.75m Secchi depth to detect the deep-water edge of the eelgrass meadow at approximately -2.7m. The error in overall accuracy was entirely a result of errors of omission of eelgrass from the classification, and primarily of sparse eelgrass. Producer's accuracies for eelgrass was 95.8% for dense eelgrass and 70.0% for sparse eelgrass, versus 100% for all non-eelgrass cover classes (Table 2.2).

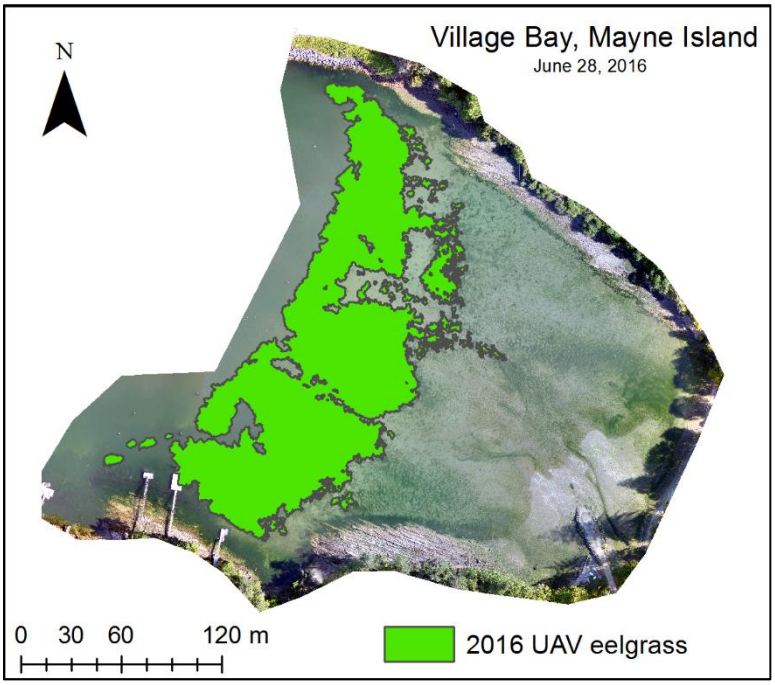

Figure 2.5 Extracted eelgrass features in Village Bay, Mayne Island.

2.3.2 Horton Bay, Mayne Island

Because of the variable environmental conditions experienced during UAV acquisition at Horton Bay, the orthomosaic was split into 3 zones of relatively similar radiometry and classified separately (Figure 2.6). For this medium sized site, the produced eelgrass map showed the lowest overall accuracy of 86.5% (Table 2.2). Sky conditions were highly variable throughout this flight, resulting in water surface effects not observed in Village Bay. Data collection at Horton Bay took longer than expected, causing sun angle to exceed the recommended maximum value of 45° (35° to 48°), which resulted in sun glint as shown in Figure 2.6 location (a). Cloud cover, which remained consistently around 50 – 60%, created an additional reflective surface effect, further discussed and illustrated in Section 2.4. While water clarity was reasonable at Secchi depth 4.25m, the UAV imagery was unable to resolve eelgrass beyond a depth of approximately -2.1m below chart datum. For comparison, the MICS 2015 ground-based mapping for the deep region of Zone 2 affected by sun glint is provided in Figure 2.6, which reaches a depth of approximately -2.5m below chart datum. Given the tidal height of 1.1m at the time of UAV image acquisition, eelgrass at -2.5m below chart datum would be at -3.6m depth below surface, which is feasibly detectable given the Secchi depth of 4.25m. In this case, the detection of the deep eelgrass edge was impeded

by surface effects created by sun glint and cloud reflectance. In terms of sources of error, producer's and user's accuracies of non-eelgrass points were almost as high as for Village Bay, with two green algae points being erroneously classified as eelgrass. The accuracies of the eelgrass classes were much lower, achieving a producer's accuracy of 79.4% for dense eelgrass, as a result of omitting deep eelgrass that was part of the main bed or dense patches of shallow eelgrass mixed with other SAV, and 52.9% for the sparse eelgrass class, entirely as a result of omitting small stands of patchy sparse eelgrass mixed with other SAV.

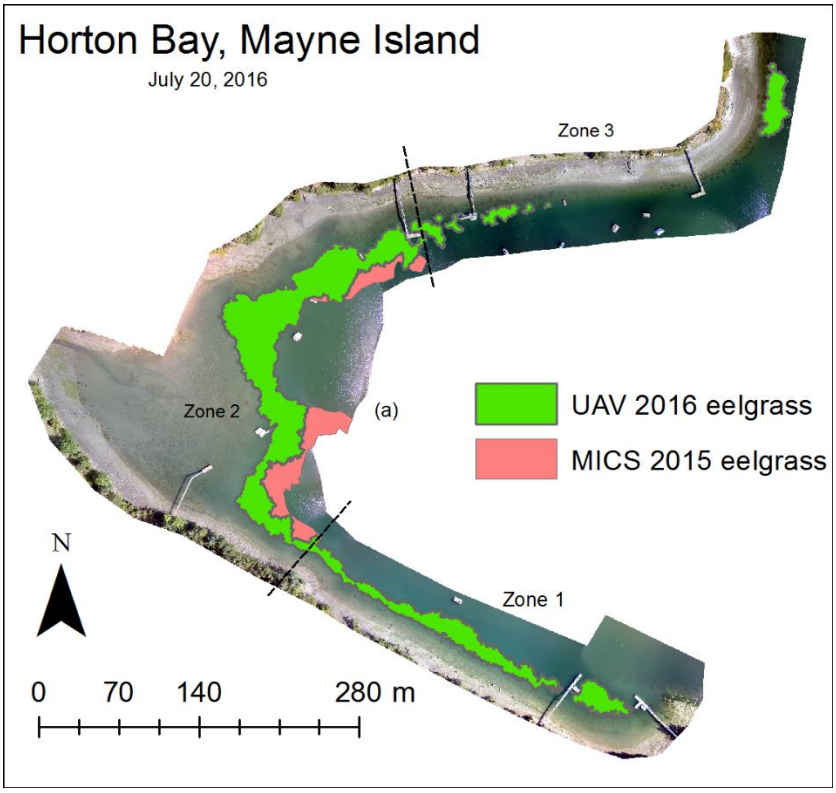

Figure 2.6 Extracted eelgrass features in Horton Bay, Mayne Island. Black dashed lines indicate boundaries between zones.

2.3.3 Lyall Harbour, Saturna Island

The largest site, Lyall Harbour (Figure 2.7), and produced an eelgrass mapping accuracy of 91.1% (Table 2.2). While overall environmental conditions were highly variable at this site, there are clear radiometric distinctions between zones. Sun angle remained within the recommended values throughout Zone 1 and Zone 2 (30° – 45°), but exceeded the maximum recommended sun angle (45° – 54°) in Zone 3, resulting in sun glint (Finkeiner et al., 2001). Cloud

cover started at 95% for Zone 1, and cleared to 30% for Zones 2 and 3. Water clarity was highest in Zones 1 and 2 with Secchi depth of 2.5m, while Zone 3 had very poor water clarity of 1.1m Secchi depth, remnant of a large phytoplankton bloom that had occurred July 13, 2016. In summary, Zone 2 had the most optimal environmental conditions with high water clarity and low cloud cover, while Zones 1 and 3 experienced poor conditions for opposite reasons: Zone 1 had high cloud cover with good water clarity, while Zone 3 had low cloud cover with poor water clarity. Classification errors in Lyall Harbour occurred primarily as a result of omitting patches of sparse eelgrass, as shown by the 82.1% producer's accuracy for sparse eelgrass. Dense eelgrass achieved a greater producer's accuracy of 96.0%, as a result of omitting one small patch of dense eelgrass from the classification. For the non-eelgrass categories, green algae had the lowest Producer's accuracy of the three sites at 92.1%, resulting from dense accumulations of green algae at the shallow edge of the eelgrass meadow erroneously committed to the eelgrass class. Lyall Harbour is the only site in which an error of commission of unvegetated substrate into the eelgrass classification was made, resulting in the only producer's accuracy below 100% for unvegetated of the three sites, at 91.7%. This error was made at the deep edge of the eelgrass meadow, in Zone 3 affected by turbidity.

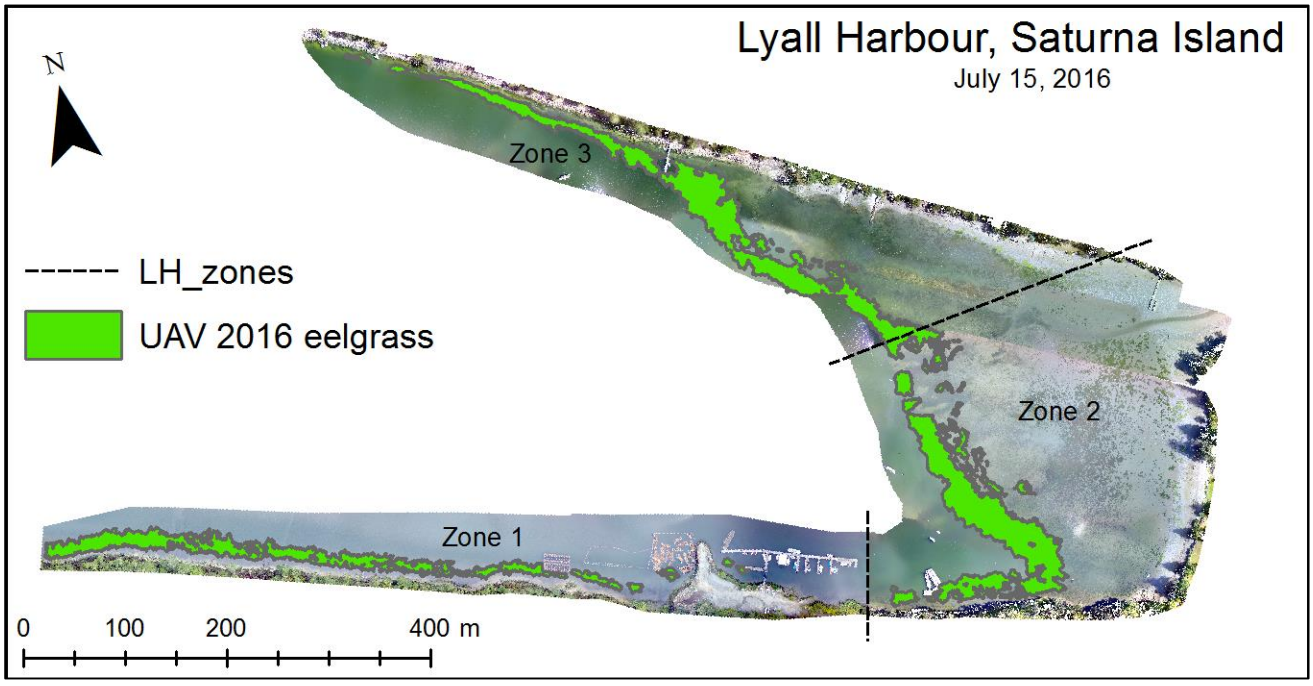

Figure 2.7 Extracted eelgrass features in Lyall Harbour, Saturna Island. Black dashed lines delineate boundaries between zones.

2.4 Discussion

The objective of this study was to utilize low-cost consumer-grade UAV technology to delineate eelgrass extent at three small estuaries in the Southern Gulf Islands, British Columbia. The method was found to be effective, achieving overall accuracies of 96.3%, 86.5%, and 89.7% for Village Bay, Horton Bay, and Lyall Harbour, respectively (Table 2.2). Further, this study presents a first evaluation of the role of environmental conditions at the time of UAV image acquisition in relation to eelgrass mapping accuracy (Table 2.1). UAV imagery at Village Bay was collected under optimal conditions and achieved the highest overall accuracy of the three sites. The primary source of error at Village Bay was the omission of sparse patches of eelgrass mixed with green algae. The larger sites, Horton Bay and Lyall Harbour, experienced more variable environmental conditions as compared to Village Bay, which was reflected in the overall accuracy of the eelgrass mapping. In Horton Bay, omission of deep eelgrass occurred in waters where tidal height and Secchi depth would have otherwise allowed for detection, if not for the detrimental effects of sun glint and cloud reflectance. In the turbid Zone 3 of Lyall Harbour, errors occurred through the omission of deep eelgrass and commission of dense shallow green algae into the eelgrass class. In the larger sites, errors of omission of sparse patches of eelgrass occurred similarly to at Village Bay. The results show that interpretation, and therefore accuracy, of the produced eelgrass maps depends on the environmental characteristics at the time of acquisition, as well as site-specific characteristics such as density of the eelgrass meadow and the presence of other submerged vegetation.

As a result of changing environmental conditions throughout each UAV flight, inconsistent radiometric properties became a major impediment to conducting automated classification of eelgrass in the UAV orthomosaics. While image-to-image colour balancing was applied prior to mosaicking, this did not remove localized cloud reflectance, or account for differences in illumination resulting from 20+° changes in sun angle between the start and end time of survey. As such, we adopted the object-based, manual classification approach for seagrass mapping with aerial photography using eCognition described by Lathrop et al. (2006), combined with digital image enhancements in ENVI software. This method balanced the high visual interpretability of the UAV imagery with a time-efficient process for classifying target features with varying radiometric properties in different parts of the image as a result of changing sun angle, tidal height, water clarity, and cloud cover.

2.4.1 Visual interpretation of ultra-high resolution UAV imagery

While image enhancements contributed to the differentiation between eelgrass and other substrates, especially in portions of Horton Bay and Lyall Harbour, much of the eelgrass could be visually identified without enhancement when environmental conditions were reasonable. This was the case in Village Bay (Figure 2.5), where environmental conditions were optimal and enhancements would not have been necessary (Table 2.1). In all remote sensing methods, submerged vegetation is generally classified by the low reflectance compared to adjacent bare substrates (O'Neill et al., 2011). However, classification errors occur frequently between eelgrass and green algae due to their similar spectral characteristics even when using 'high spatial resolution' satellites such as Worldview-2 (2m spatial resolution) or IKONOS (4m spatial resolution) (O'Neill & Costa, 2013; O'Neill et al., 2011; Reshitnyk et al., 2014). In the high resolution UAV imagery analyzed, eelgrass and green algae were easily distinguishable by visual interpretation through differences in texture and shadow. Individual eelgrass blades create a distinct 'sinuous' texture with significant shadowing within the bed due to the height of the blades, while dense collections of the bladeless green algae exhibit a fine homogenous 'flat' texture with no shadowing (Figure 2.8). The presence of eelgrass epiphytes is a further consideration for differentiating eelgrass from green algae. As was the case in Village Bay, areas of eelgrass with heavy epiphytes present on the blades visually appeared much darker and slightly red in hue compared to green algae, due to strong absorption of incident light by the epiphytes (Drake et al., 2003; O'Neill et al., 2011).

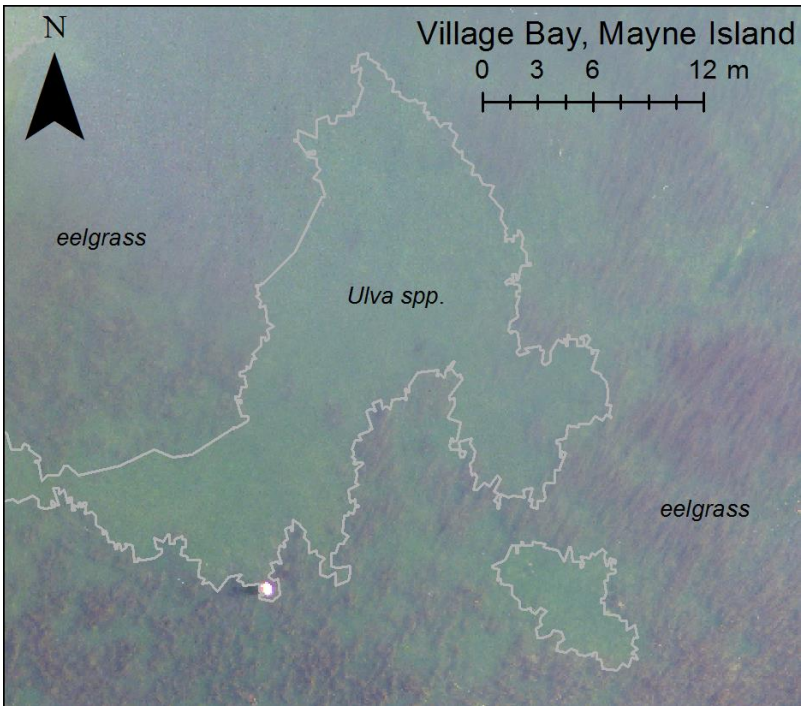

Figure 2.8 Subset of Village Bay 2cm orthomosaic showing textural differences between eelgrass and Ulva spp.

2.4.2 Environmental conditions at the time of image acquisition

The high operational flexibility associated with UAV aerial surveys was certainly beneficial for meeting the task-specific environmental parameters necessary for aerial photographic benthic habitat mapping (Finkbeiner et al., 2001; Klemas, 2015). However, even with this increased flexibility, the balancing act between optimal conditions outlined by Finkbeiner et al. (2001) was difficult to achieve. The first two environmental parameters, sun angle and tidal height, are predictable and were optimized in advance of data collection by selecting for flight windows within 2 hours of the low tide of the day, and at a minimum sun angle of 30° to provide sufficient illumination of the benthos and a maximum sun angle of 45° to avoid sun glint caused by specular reflection (Finkbeiner et al., 2001). Flights at Horton Bay and Lyall Harbour took longer than expected, resulting in sun glint and reduced eelgrass detection in deeper areas. However, it was clear that even when sun was at the minimum recommended angle, illumination was more than sufficient for eelgrass detection. This suggests the minimum sun angle required for low altitude UAV mapping may be lower than that recommended for manned aircraft, and that the window of opportunity for data collection may be larger than initially thought if flights started earlier in the day.

However, even at low tide, light attenuation in the water column reduces the contrast and ability to differentiate between eelgrass, other SAV, and background sediments (O'Neill et al., 2011; Reshitnyk et al., 2014; Roelfsema et al., 2009). The elevated presence of suspended material (organic detritus and inorganic sediments), phytoplankton, and colour dissolved organic matter (CDOM) decreases the optical depth of the water and reduces benthic visibility (Babin et al., 2003; Dekker et al., 2006). While this is not generally a problem in tropical areas for coral reef or seagrass mapping (Casella et al., 2016; Ventura et al., 2017), in a temperate region such as the Salish Sea water clarity is certainly a limiting factor in benthic habitat mapping (O'Neill et al., 2011). The analyzed sites are highly influenced by the nearby Fraser River, the largest river on the west coast of Canada, which discharges a highly turbid plume of particles and organic matter into the Salish Sea (Loos and Costa, 2010). While it is not possible to predict turbidity and water clarity conditions, Secchi depth can be recorded in the field as a proxy for water clarity to assist the interpretation of the imagery, and the use of image enhancements can be useful when water clarity was not optimal during image collection. In the case of an ephemeral, intense algae bloom, UAV flights could be postponed or redone with relative ease within the allocated field dates, compared to manned aircraft or satellite overpasses. For example, an intense algal bloom occurred the day of the initial scheduled flight for Lyall Harbour, creating water clarity conditions of 0.5m (Figure 2.9a). The flight was postponed until several days later when the bloom had substantially cleared to a Secchi depth of 2.5m (Figure 2.9b). The turbidity in Zone 3 of Lyall Harbour was remnant of this phytoplankton bloom (Figure 2.7).

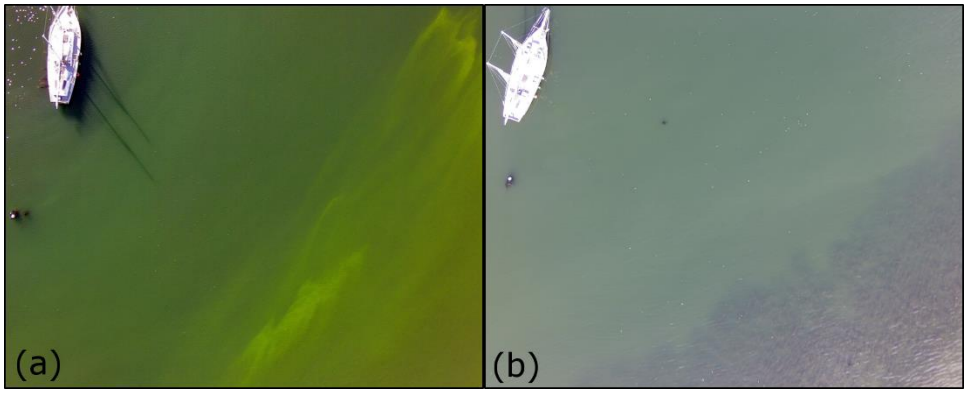

Figure 2.9 (a) Phytoplankton bloom in Lyall Harbour, July 13, 2016; (b) Approximately the same location July 15, 2016.

Cloud cover is another consideration that is also of particular importance in this region, where the influence of the Pacific Ocean and the rainshadow effect of the Vancouver Island and Olympic mountain ranges create frequently cloudy conditions. Guidelines for aerial photographic mapping of benthic habitats outlined by Finkbeiner et al. (2001) recommend cloud cover should be below 10%, because it blocks visibility of target features and creates shadows when the sensor is above the clouds. When mapping terrestrial features, low altitude UAV platforms are beneficial because imagery can still be collected when cloud cover would normally inhibit traditional remote sensing techniques (Getzin et al., 2012; Paneque-Gálvez et al., 2014). When mapping submerged benthic features with UAVs, however, cloud cover poses a different problem than when using traditional remote sensing platforms. When the sensor is between the target and the clouds, as is the case when mapping eelgrass with a UAV, specular reflectance of the clouds occurs on the surface of the water and obscure benthic features. This issue presented itself in two different ways during image collection in Horton Bay and Lyall Harbour. In Horton Bay, cloud cover was 50-60%, creating patches of bright cloud reflectance (Figure 2.10), while in Lyall Harbour, 95% cloud reflectance in Zone 1 created an "overcast" effect equally across the image (Figure 2.11a). While image stitching removed the bright cloud features from the orthomosaics in Horton Bay, the resulting radiometry was still difficult to enhance because of its inconsistencies caused by changing cloud conditions. In Lyall Harbour, the consistently overcast cloud reflectance in Zone 1 was much easier to enhance (Figure 2.11b), suggesting that complete overcast conditions may be better for benthic habitat mapping than intermittent sun and cloud.

Figure 2.10 Cloud reflectance obscuring eelgrass meadow in Horton Bay, Mayne Island at approximately 50% cloud cover.

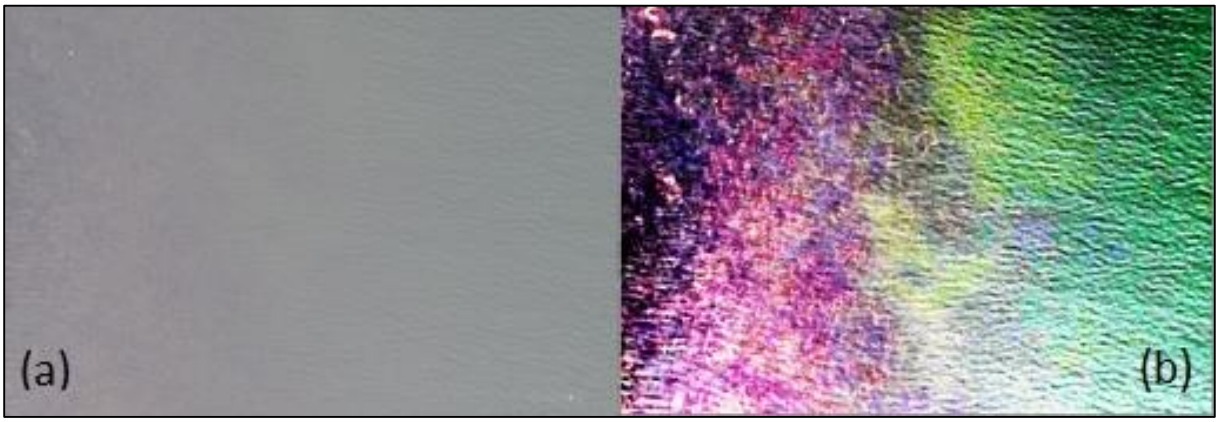

Figure 2.11 (a) Overcast cloud reflectance in Zone 1 of Lyall Harbour with no enhancement, (b) Same location with a local equalization enhancement.

2.4.3 UAV technology in seagrass ecology and conservation

Intertidal vegetated landscapes can be highly complex and dynamic habitats, whose variability over spatial and temporal scales can be difficult to assess with traditional remote sensing techniques (Barrell and Grant, 2015). The high resolution of UAV imagery, combined with reduced operating costs compared to conventional remote sensing, may support many research advances in vegetation dynamics and ecosystem processes of intertidal habitats (Anderson and

Gaston, 2013; Klemas, 2015). The ease of repeatability of UAV surveys would allow tracking changes in bed formation, expansion and loss at relevant temporal scales, whether monthly, seasonally, or annually, as defined by the investigator. Ecologists may find UAV technology extremely valuable for studying seagrass density dynamics, landscape ecology, and for assessing ecological status of seagrass meadows using parameters that can be measured from an aerial perspective (Nagendra et al., 2013). For example, Barrel & Grant (2015) were able to study landscape metrics of eelgrass habitats at the patch scale over a period of time, made possible by the very high resolution imagery and low-cost deployment of UAVs. When studying the persistence and stability of fish assemblages within specific eelgrass meadows (Robinson & Yakimishyn, 2013; Robinson et al., 2011), the spatial heterogeneity and arrangement of eelgrass habitats as derived from UAV imagery could be considered. Beyond ecosystem process research, UAVs can produce data of importance relevance for ecological conservation and restoration value of seagrass ecosystems. Due to the high resolution and low cost of repeated surveys, UAVs would be a valuable tool for exploring impact assessment of coastal activities such as boat mooring and dock construction (Demers et al., 2013; Gladstone et al., 2014). Finally, because of the accessibility of UAV technology beyond academia, coastal restoration site planning and monitoring could find great utility in the adoption of UAVs (Klemas, 2013; Thom et al., 2014).

A major challenge for the adoption of UAV technology by researchers and conservationists is the regulatory and legal framework governing UAV flight operations. It is important for conservation societies and academic institutions to adhere to the regulatory framework in order to conduct operations safely and avoid any negative social impacts in the community. The increased presence of UAVs pose concerns for safety, privacy, and psychological wellbeing, and disregarding the regulations may undermine conservation effectiveness in the long term (Sandbrook, 2015). Although in Canada some UAV operators have considered the available *Exemptions* as an avenue for avoiding the need to apply for the SFOC, this is not practical for operational mapping and monitoring by research or community organizations, as they apply specifically to “fun of flight” operations in Class G airspace. As this research is conducted in Canada, all UAV flights are subject to Transport Canada Guidance and Civil Aviation Regulations (CARs). Commercial and research operations, such as those detailed within, require additional authorization and liability insurance to be conducted legally. In general, this requires the operator to apply for and receive a Special Flight Operations Certificate (SFOC), a document administered

by Transport Canada detailing operational requirements, restrictions, emergency procedures, permitted areas of operation, and minimum liability insurance coverage required for the operation (Transport Canada, 2016).

2.4.4 Opportunities for future work

While this work demonstrates the benefits and challenges of UAV technology for seagrass mapping in small coastal bays where traditional remote sensing data may be inappropriate, there are several avenues for improvement and further work. Further testing is required to determine how the environmental conditions at the time of image acquisition affect the ability to map eelgrass. While parameters such as sun angle, tidal height, turbidity, and wind speed have been thoroughly explored within the scientific literature (Finkbeiner et al., 2001, Kay et al., 2009; Mount, 2005) for traditional remote sensing technologies, the specific guidelines must be adapted to low-altitude UAV platforms. For example, the role of cloud cover clearly differs from both guidelines for aerial photography for benthic habitat mapping, as well as the experiences encountered by other researchers using UAVs for emergent wetland vegetation or terrestrial applications (Getzin et al., 2012; Paneque-Gálvez et al., 2014). Additionally, minimum sun angle requirements need to be explored, as a 30° minimum sun angle is likely higher than necessary and optimal flight windows could be increased by starting flights earlier in the day. The environmental conditions measured in the present study were not recorded with the intention to analyze their specific effects on eelgrass interpretation or mapping accuracy. As such, future work should evaluate these environmental conditions at many sites over a range of environmental conditions. Choosing smaller sites and using an autopilot system would allow for faster image acquisition, and therefore more consistent environmental conditions over the entire site. From the suggested analysis, the development of a mapping reliability scale as described by Pasqualini et al. (1997) for seagrass mapping with aerial photography could be adapted for UAV mapping. In addition to the environmental conditions, further factors could be assessed, such as the size, shape, fetch, and bathymetric slop of the prospective site, as well as the role of eelgrass density and the presence of other submerged vegetation.

2.5 Conclusions

Using a low-cost quad-copter UAV and consumer-grade digital camera, eelgrass was mapped in three small coastal estuaries in the Southern Gulf Islands of British Columbia, Canada. Inconsistent environmental conditions and image radiometry throughout each survey made it impossible to define a universally applicable pixel- or object-based classification. As such, eelgrass feature extraction consisted of manual classification of segmented image objects, which was found to be fast and effective for delineating eelgrass meadow boundaries in UAV imagery with inconsistent radiometry. High mapping accuracies of 96.3%, 86.5%, and 89.7% for Village Bay, Horton Bay, and Lyall Harbour respectively were achieved on an eelgrass presence or absence basis. Environmental conditions at the time of image acquisition were found to play a significant role in the accuracy of the eelgrass mapping, with the highest accuracy achieved for the site that experienced optimal environmental conditions, while the sites with variable environmental conditions experienced far more classification errors. Further research is necessary to develop guidelines for UAV mapping of eelgrass, specifically the role of environmental conditions and site-specific characteristics on mapping accuracy, as several of these factors clearly differ from published guidelines for manned aerial photography. There are many benefits to eelgrass mapping with UAVs compared to conventional remote sensing, including high resolution imagery, high flexibility for achieving optimal environmental conditions, and low-cost for repeated surveys over time when working at small geographic scales.

Chapter 3 – Long-term spatial-temporal eelgrass (*Zostera marina*) habitat change in the west coast of Canada (1932-2016)

Abstract - Eelgrass (*Zostera marina*) is a critical nearshore marine habitat for juvenile Pacific salmon (*Oncorhynchus* spp.) as they depart from their natal streams. Given the poor marine survival of Coho (*O. kisutch*) and Chinook (*O. tshawytscha*) salmon juveniles in recent decades, it is hypothesized that deteriorating eelgrass habitats could contribute to their low survival. For three small estuaries in the Southern Gulf Islands of British Columbia, changes in eelgrass area coverage and shape index over the period of 1932-2016 were assessed using historic aerial photographs and Unmanned Aerial Vehicle (UAV) imagery. In addition, changes in eelgrass area and shape index were evaluated in relation to landscape-level coastal environmental indicators, namely shoreline activities and alterations and residential housing density. All three eelgrass meadows showed a deteriorating trend in eelgrass condition; on average, eelgrass area coverage decreases by 41% while meadow complexity as indicated by the shape index increases by 76%. Shoreline activities (boats, docks, log booms, and armouring) and residential housing density increased markedly at all sites over the study period, which are moderately to strongly correlated to eelgrass area coverage and shape index. Changes in these landscape-level indicators over this time period corroborate the observed decline in eelgrass habitat condition, as they suggest an overall deterioration of coastal environmental health in the Salish Sea due to drastically increased use of the coastal zone as well as declines in water quality due to urbanization.

3.1 Introduction

Seagrasses are a fundamental component of the nearshore marine ecosystems of tropical, temperate, and sub-arctic regions, ranking similarly to mangroves and coral reefs as some of the world's most productive coastal habitats (Short & Wyllie-Echeverria, 1996). Beyond high productivity, seagrasses provide physical structure, refuge from predation, and support complex trophic food webs, as well as serving as nursery habitat for a multitude of fish and invertebrate species (Jackson et al., 2001; Larkum et al., 2007). Eelgrass (*Zostera marina*), the primary seagrass of the Salish Sea, is particularly important in the lifecycle of many commercially important fisheries species, including Pacific salmon (*Oncorhynchus* spp.), herring (*Clupea pallasi*), and Dungeness crab (*Metacarcinus magister*) (Kennedy et al., 2018; Plummer et al., 2013; Robinson & Yakimishyn, 2013). With the mortality of juvenile Coho and Chinook salmon high and variable (Beamish et al., 2003), there is great concern that deteriorating nearshore habitats could be a contributing factor as coastal population pressure and industrial development in this region increases (Carr-Harris et al., 2015; Levings & Thom, 1994; Spromberg et al., 2011).

Seagrass habitats experience natural fluctuations in spatial-temporal distribution. The intrinsic rate of expansion of rhizome growth and seed dispersal is mediated by the various disturbances acting on seagrass meadows in varying intensity and frequency, including wave action, sea ice formation, disease, and herbivore grazing (Ball et al., 2014; Frederiksen et al., 2004a,b; Olesen & Sand-Jensen, 1994). While natural disturbances have resulted in large- and small-scale seagrass losses, human impacts on the coastal zone are now recognized as the primary cause of seagrass habitat loss (Short & Wyllie-Echeverria, 1996).

Through eutrophication and sediment loading, reductions in light penetration through the water column decrease the amount of light available for photosynthesis, sources of which include residential and urban land use runoff; offshore sewage release; industrial waste discharge; and dredging (Giesen et al., 1990; Orth & Moore, 1984; Short & Burdick, 1996). Seagrass losses have been linked to nutrient loading from coastal watersheds as a result of upland residential septic systems and sewage disposal (Basnyat et al., 1999; Hauxwell et al. 2003; Valiela et al., 1992). Short & Burdick (1996) found dramatic losses of eelgrass (*Z. marina*) and overproliferation of epiphytes, phytoplankton, and macroalgae in sites with higher housing density (Short & Burdick,

1996). High concentrations of these algae block sunlight and limits photosynthesis in seagrasses, leading to reduced shoot density and growth (Short et al., 1995).

Further, direct physical damage related to boat operation and storage impact seagrasses through propeller scarring; hull dragging; damage and shading from dock and harbour building; and scarring caused by moor/buoy chains and anchors (Collins et al., 2010; Gladstone & Courtenay, 2014; Unsworth et al., 2017; Walker et al., 1989; Zieman, 1976). Eelgrass under and directly adjacent to docks have shown reduced shoot density and canopy structure (Burdick & Short, 1999), up to a 90% decline of nearby *Z. muelleri* 26 months after dock installation (Gladstone & Courtenay, 2014). Further, shoreline armouring has been found to alter nearshore hydrology, water clarity and sediment composition, leading to losses of eelgrass (Patrick et al., 2014; Patrick et al., 2016), although no areas of eelgrass loss in the present study could be directly associated with any shoreline armouring such as riprap or groynes. Coastal forest harvest has been significant in British Columbia and the most economical method of log storage and transportation has been marine. In addition to direct physical damage and uprooting of eelgrass through log scouring and reduction of photosynthesis through shading, marine log storage also deposits large amounts of bark to the benthos, which smothers eelgrass and changes the chemical composition of the sediments (Sedell et al., 1991). Direct physical damage to seagrasses at small scales can lead to bed fragmentation and contribute to large-scale declines (Burdick & Short, 1999).

Despite the importance of seagrass habitat in nearshore marine areas and the increasing impact of human activities, there is often a lack of historical data with which to assess long-term trends in seagrass distribution. One such region wherein very little quantitative data exists is the Salish Sea, a transnational semi-enclosed body of water shared by British Columbia, Canada, and Washington, United States (Levings & Thom, 1994; Thom & Hallum, 1990; Waycott et al., 2009). The objective of this research is to assess the long-term spatial-temporal dynamics of eelgrass habitats in the Salish Sea over the time period of 1932 – 2016 using historic aerial photography and Unmanned Aerial Vehicle (UAV) imagery. Eelgrass area and meadow complexity (Shape Index) are described at three small estuaries in the Southern Gulf Islands of British Columbia. Two landscape-level indicators of coastal environmental health, residential housing density and shoreline activity and alterations, are used to describe the magnitude of stress on the nearshore marine ecosystem throughout time. This research contributes to the understanding of the spatial-

temporal trends in eelgrass habitats in order to address marine conservation issues related to anthropogenic impacts on the coastal zone.

3.2 Materials and Methods

3.2.1 Study sites

The study sites are located within the Strait of Georgia, in the Southern Gulf Islands, part of the Salish Sea, which is a transnational water body comprised of the Strait of Georgia, Juan de Fuca Strait, and Puget Sound (Figure 3.1). The Strait of Georgia is dominated by a mixed tidal regime and estuarine circulation, primarily driven by the discharge of the Fraser River (Masson, 2002). The area is considered to be one of the most diverse temperate marine regions in the world, hosting over 200 species of fish, hundreds of seabirds, 500 species of marine plants, and 1500 species of invertebrates (Georgia Strait Alliance, 2017). While this region has been utilized by Coast Salish Peoples since time immemorial, European settlement in the 1860s brought major changes in land use practices, including clearing of land for agriculture, large scale forest harvest, and widespread residential and urban development (Elliot, 1984).

In the Southern Gulf Islands, eelgrass is the predominant seagrass in soft sandy sediments, with reports of small amounts of the introduced Japanese eelgrass (*Z. japonica*) found in the upper intertidal (Emmett et al., 2000; Ruesink et al., 2010). Eelgrass is a fundamental component of nearshore coastal marine ecosystems, supporting high fish diversity as many species rely on eelgrass for part or all of their life cycle, including juvenile Pacific Salmon (Kennedy et al., 2018 *in press*; Phillips, 1984). Monitoring of eelgrass meadows in the nearby Gulf Islands National Park Reserve observed epiphytic algae, filamentous diatoms and *Smithora* spp., colonizing eelgrass blades in high densities (Robinson & Yakimishyn, 2005). Other submerged vegetation common in the region includes green algae (*Ulva* spp., *Enteromorpha* spp., and filamentous green algae) and brown algae (Saccharina laminaria, Sargassum muticum,) in small patches less than $1m^2$ (Nahirnick et al., 2018, *in prep*.; O'Neill et al., 2013).

Three sites, Village Bay, Horton Bay, and Lyall Harbour were selected for this analysis, considering their similar biophysical characteristics and quality of available data. Each site is protected from wave action and longshore drift, and has a perennial source of freshwater input. Sites with bright sandy sediments were chosen to increase the reliability of separation of eelgrass

from background sediments. Most of the eelgrass at these sites is found in the shallow bathymetric range between +1.0m and -3.0m (Chapter 2.). Further, all sites selected had previous ground-based mapping data by local community conservation groups available for reference (Wright et al., 2014).

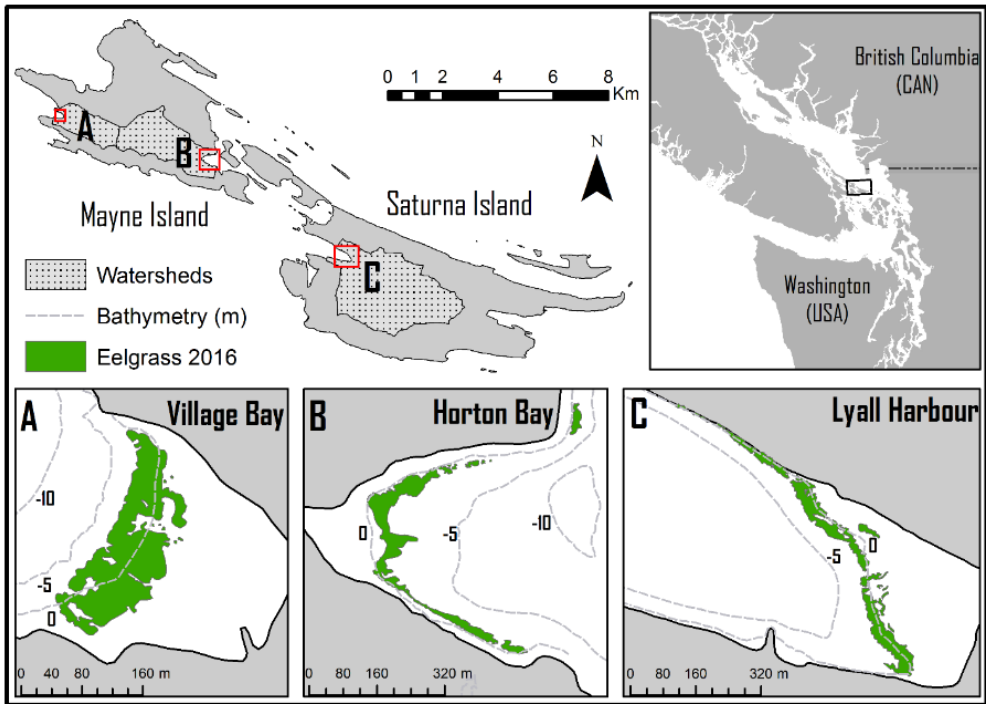

Figure 3.1 Study sites. Eelgrass polygons derived from 2016 UAV imagery (Chapter 2)

3.2.2 Dataset

Data used for the long-term eelgrass habitat and associated landscape indicator change consisted of: aerial photographs acquired from the Gulf Islands National Park Reserve (Parks Canada, 2015) and the Province of British Columbia (GeoBC, 2015) in the form of georeferenced orthomosaics; aerial photograph prints from the University of British Columbia Geographic Information Center (UBC GIC, 2016) scanned at a resolution of 1200 dpi; and imagery collected by Unmanned Aerial Vehicle (UAV) in 2016 (Chapter 2). UAV imagery collected in 2016 was further utilized in order to understand the effect of environmental conditions, eelgrass density, and the presence of other submerged vegetation on the eelgrass delineation. The final dataset was comprised of the years 1932, 1950, 1975, 2004, 2010, and 2016. Aerial photographs were in black

and white from 1932 – 1975 and in colour from 2004 – 2014, with pixel sizes ranging from 0.1 to 1.0m (Table 3.1). Metadata for the orthomosaic datasets and many of the hardcopy photographs were unavailable, however, all aerial photography was acquired during leaf-on season and thus, the assumption was made that seasonality did not influence the eelgrass delineation significantly.

Table 3.1 Air photo and UAV characteristics. 2014 aerial photography not used in eelgrass mapping due to significant glint.

Year	Spatial Resolution	Spectral resolution	Source
1932	0.5m	Black & White	Parks Canada
1950	0.5m; 0.3m	Black & White	Parks Canada; UBC GIC
1975	0.2m; 0.76m	Black & White	Parks Canada; UBC GIC
2004	0.1m	RGB	Parks Canada
2010	0.15m	RGB	Parks Canada
2014	1.0m	RGB + NIR	GeoBC
2016	0.02m	RGB	High Angle UAV

Ground truth data obtained from georeferenced underwater videography were collected by kayak concurrently with the 2016 UAV image acquisition (Chapter 2). While only eelgrass features are mapped from the aerial photography, classification of the videography included the following four classes for the purposes of interpretation: eelgrass, green algae (*Ulva* spp.), brown algae (*Saccharina luminaria* and *Sargassum muticum)*, and unvegetated substrate. A secondary vegetation species was identified if present, and a density category (Sparse or Dense) assigned to each vegetation type.

Previous eelgrass mapping data collected by local community groups using ground-based methods were available for additional reference data. Sites on Mayne Island were mapped by kayak and diver survey: in 2009 at Village Bay; and in 2009, 2012, and 2015 at Horton Bay (Mayne Island Conservancy Society (MICS), 2016). Lyall Harbour, on Saturna Island, was mapped by boat using a transect method parallel to the shore in 2004, describing the general density and form of the eelgrass along each transect segment (Saturna Island Marine Resource and Education Society (SIMRES), 2016).

3.2.3 Eelgrass delineation from aerial photographs

Aerial photographs and UAV imagery were resampled to a common pixel size of 1m x 1m using a pixel aggregate technique (Ball et al., 2014; Frederiksen et al., 2004b). Digital image enhancements such as contrast stretching, Principal Component Analysis (PCA) and colour-space transformations (Red Green Blue to Hue Saturation Value), were tested for their ability to increase the contrast between eelgrass and background sediments using ENVI image analysis software (Ball et al., 2014; Fletcher et al., 2009). When additional enhancements were required in localized areas, GNU Image Manipulation Program (GIMP) was used to apply equalization contrast stretches on small parts of the image. Following image enhancements, eelgrass was delineated manually using visual photointerpretation in ArcGIS 10.3. Most of the aerial photography was collected and curated for the purposes of land-use mapping, and as such, imagery was not conducive to the use of automated methods of benthic habitat mapping: brightness levels varied significantly within and between photographs and image stitching seams in orthomosaics were not placed appropriately for nearshore analysis. Using image enhancements and manual photointerpretation allowed for the optimal use of expert knowledge in the decision-making process of eelgrass classification. Eelgrass delineation was first conducted on the most recent 2016 UAV imagery, in order to utilize the ground reference surveys collected concurrently with the imagery. All ground reference points were used for air photo interpretation (number of points: Village Bay 213; Horton Bay 342; Lyall Harbour 237).

3.2.4 Air photo reliability assessment

To provide an indication of the relative degree of mapping error possible in each aerial photograph, a scale index modeled after the mapping reliability scale described by Pasqualini et al. (1997) was developed. The index is based on three parameters which are known to impede accurate delineation of submerged habitats, namely tidal height, eelgrass visualization, and surface effects such as sun glint and wind ripples (Dobson et al., 1995; Finkbeiner et al., 2001). Tidal height indicates how much water is above the eelgrass, and was determined in the aerial photography through overlaying the water line on bathymetric data. Eelgrass visualization describes how much image enhancement was required in order to map the eelgrass. Sun glint and wind ripple are surface effects which obscure the benthic features below the water, and this parameter is described based on how much of the eelgrass bed is affected. Each parameter is gauged on a scale from 1 to 4, for a total of 12 points (Table 3.2).

Table 3.2 Scale of air photo quality for eelgrass mapping

Factors	4 points	3 points	2 points	1 point
Tide	< 1.0m	1.0 to 2.0m	2.0 to 3.0m	> 3.0m
Eelgrass visualization: contrast between SAV and background sediments	High contrast, deep edge is confidently delineated without enhancements	Moderate contrast, deep edge is delineated with some minor enhancements	Poor contrast, reasonable delineation with major enhancements	Very little contrast even with enhancements
Surface effects: specular reflection & wave plane	None	Small amounts that do not significantly inhibit interpretation	Small amounts which significantly inhibit interpretation in localized areas	Large amount which significantly inhibits interpretation
Total	12	-	-	-

3.2.5 Analysis of eelgrass derived landscape metrics

To describe the changing spatial composition and configuration of the eelgrass meadows throughout the study period, two metrics derived from landscape ecology were calculated: eelgrass meadow size (areal coverage) and Shape Index (Frederiksen et al., 2004a; Forman & Godron, 1981). Areal coverage was calculated for each eelgrass meadow and reported in hectares (ha). As a visual representation of the spatial changes in areal coverage, eelgrass areas gained, lost or remaining unchanged between consecutive mapping years were defined using ArcGIS Union operation between eelgrass meadow polygons (Frederiksen et al., 2004a).

In addition to areal coverage, Shape Index was defined to provide a measure of shape complexity, a proxy for eelgrass meadow fragmentation. The Shape Index has been used in preference to the simple perimeter-area ratio for measuring the shape complexity or edge effect of a landscape patch because of the size dependency problem associated with the perimeter-area ratio: when holding the shape constant, an increase in patch size will cause a decrease in the perimeter-area ratio (Barrell & Grant, 2015; Frederiksen et al., 2004a). Shape Index overcomes this problem by measuring the shape complexity in comparison to a standard shape: a square. Here, Shape Index is used to measure the relative changes in shape complexity of the eelgrass beds, which can be considered analogous to fragmentation or “edge effect”. The formula is as follows (Frederiksen et al., 2004):

$$SI = \frac{0.25P}{\sqrt{A}}$$

Where P is the perimeter and A is the area of the eelgrass meadow. The lower limit of the SI is 1, where the shape is a square, and increases without an upper limit as the shape becomes more complex or irregular.

3.2.6 Landscape-level coastal environmental indicators

'Landscape-level coastal environmental indicators' are used to describe the overall state of coastal environmental health at these study sites (Klemas, 2001). These indicators can be quantified from the same aerial photography used to map eelgrass in order to estimate the magnitude of stress on the nearshore coastal marine environment. The landscape-level coastal environmental indicators quantified here are shoreline activities and alterations, and residential housing density.

Shoreline activities and alterations are used as an indicator of the magnitude of potential physical disturbance in the immediate proximity of the eelgrass meadow. These were assessed according to four categories, including: docks; boats and mooring buoys; bulkhead, armouring, groynes, and built land; and marine timber storage in the form of log booms. These categories were chosen for their documented detrimental impact on seagrass meadows and other natural habitats (Bulleri & Chapman, 2010; Eriander et al., 2017; Gladstone & Courtenay, 2014; Patrick et al., 2014; Sedell et al., 1991; Unsworth et al., 2017). It is understood that not all shoreline activities will impact eelgrass in the same way or to the same magnitude. However, it is difficult to determine which of these activities, if any, could be having an impact at these particular sites when the only data available are photographic snapshots in time. While this indicator is reported by type as described above, the impact on eelgrass of shoreline activities and alterations were not considered on a type-by-type basis, but rather as an overall number of incidences to characterize the magnitude of shoreline stress. As such, shoreline activities as reported here only represent the moment in time when the eelgrass was photographed and subsequently mapped. Furthermore, although docks and built structures are more or less permanent, boat traffic varies from day to day.

Residential housing density is used as an indicator of the magnitude of non-point source nutrient runoff entering each site (Short & Burdick, 1996). Seagrass losses have been linked to nutrient loading from coastal watersheds as a result of upland residential septic systems and

sewage disposal (Basnyat et al., 1999; Valiela et al., 1992). Residential housing density was defined based on the number of houses within a drainage area. First, the drainage area of each site was derived from a Digital Elevation Model using ArcGIS, and the number of houses within each drainage area was determined by direct counts from aerial photography. Housing density was then calculated by dividing the number of houses by the size of the associated drainage area (Short & Burdick, 1996). Due to the limited extent of the 2016 UAV imagery, aerial photography from 2014 (GeoBC, 2015) was used to derive housing density under the assumption that housing density did not significantly change over the two year period.

3.2.7 Analysis of the combined dataset

Four simple linear correlation analyses were performed considering eelgrass area and Shape Index as dependent variables, and housing density and shoreline activities as independent variables. The first analysis included housing density and eelgrass area; the second analysis included housing density and eelgrass Shape Index; the third analysis included shoreline activities and eelgrass area; and the fourth analysis included shoreline activities and eelgrass Shape index. By assessing the relationships between these indicators and eelgrass metric change over time, it is not meant to suggest these indicators are direct causative drivers in any observed eelgrass trends, but rather as components of a degrading landscape that may be contributing to trends in observed eelgrass cover (Klemas, 2001).

3.3 Results

3.3.1 Data quality of aerial photography

The overall quality of the aerial photography (Table 3.3) shows higher scores in recent years than in the earlier years, as defined by three parameters: tidal height; water clarity, or the amount of enhancement required to map eelgrass; and surface effects, or the amount of sun glint or wind ripples obscuring benthic features. These quality scores are out of a total of 12, and are reported in the following order when addressing all sites: Village Bay, Horton Bay, and Lyall Harbour. Early air photos from 1932 and 1950 (1932 scores = 8, 7, 7; 1950 scores = 8, 7, 6) were taken at high tide and required considerable use of digital enhancement, but were generally free of surface effects. Air photos from 1975 exhibited mixed qualities: Village Bay did not improve compared to previous years (Score = 8), while Horton Bay and Lyall Harbour improved in a combination of parameters (Scores = 9, 10). Aerial photography collected in 2004 was the best

for overall quality (Scores = 11, 11, 11), a result of having the lowest tide of any year, being mostly free of surface effects, and in general required minimal enhancement to interpret eelgrass features. Air photos from 2010 also exhibited high scores (Scores = 10, 8, 11) most due to minimal surface effects and low level of enhancement required; however, tidal height was higher at all sites relative to 2004. The 2016 UAV imagery exhibited mixed qualities: Village Bay achieved a score equal to that of 2004 (Score = 11) because high water clarity and the absence of surface effects made detection possible with no enhancements, while in Horton Bay and Lyall Harbour, water clarity and/or surface effects made interpreting the 2016 data difficult (Scores = 9, 10) relative to the 2004.

Table 3.3 Air photo quality scores for three sites from 1932 to 2016

Site	Factor	1932	1950	1975	2004	2010	2016
Village Bay	Tide	1	2	2	4	3	3
	Water clarity	3	2	2	3	4	4
	Surface effects	4	4	4	4	3	4
	Total	**8**	**8**	**8**	**11**	**10**	**11**
Horton Bay	Tide	1	2	3	4	1	3
	Water clarity	2	2	2	4	3	3
	Surface effects	4	3	4	3	4	3
	Total	**7**	**7**	**9**	**11**	**8**	**9**
Lyall Harbour	Tide	1	1	3	4	3	3
	Water clarity	3	2	3	3	4	3
	Surface effects	4	3	4	4	4	4
	Total	**8**	**6**	**10**	**11**	**11**	**10**

3.3.2 Long-term spatial-temporal trends in eelgrass area and fragmentation

Analysis of the eelgrass area and Shape Index suggests a downward trend in eelgrass condition over the time period studied. For the three study sites, eelgrass areal coverage declines by an average of 41.0% (Figure 3.2) suggesting a loss of eelgrass habitat, while Shape Index increases by 76.0% (Figure 3.3) suggesting increased fragmentation of the eelgrass habitat.

Village Bay showed the lowest rate of areal cover change between years compared to the larger sites (Figure 3.2). Specifically, there was a slight area increase from 1932 to 1950 when it reached a maximum extent of 2.24 ha, after which eelgrass area decreased through 2016 when a minimum extent of 1.67 ha was observed, representing a total change of -21.6%. Shape Index

ranged from a minimum in of 1.45 in 1932 to a maximum of 2.15 in 2016 in Village Bay, representing the largest change in Shape Index of the three sites with a 117.8% increase (Figure 3.3). As shown in Figure 4, the deep edge of the eelgrass meadow was fairly stable over time with retraction up to 2010 and expansion in 2016. Variation and eelgrass fragmentation in the intertidal area account for the majority of the increase in Shape Index (Figure 3.4).

Horton Bay experienced declines in eelgrass areal coverage over the entire study period, with a maximum extent of 3.78 ha in 1932 and a minimum extent of 1.90 ha in 2016, representing a total change of -49.7% (Figure 3.2). In Horton Bay, Shape Index ranged from 3.27 in 1932 to a maximum of 4.40 in 2016, an increase of 34.2% (Figure 3.3). These changes in areal coverage and Shape Index are represented graphically in Figure 3.5. Along the south shore, eelgrass exhibited some loss in 1950 but remained fairly stable from then on. The central region, on the other hand, was highly variable, with both gains and losses of large areas of eelgrass between mapping years until 2004-2016 where the general shape remained stable. Along the north shore of Horton Bay, there was an unbroken fringing eelgrass bed from 1932-1975, which became increasingly fragmented from 2004-2016 and appears to be associated with dock installation and boat traffic.

Similarly to Horton Bay, eelgrass areal coverage in Lyall Harbour decreased over the entire study period, from 4.95 ha in 1932 to 2.39 ha in 2016, representing a total change of -51.7%, which was the highest rate of change of the three sites studied (Figure 3.2). Shape Index began at 3.20 in 1932 and showed a slight decrease to 3.19 in 1950, and from that point increased to a maximum of 5.64 in 2016, representing a total increase of 75.9% (Figure 3.3). As shown in Figure 3.6, from 1932-1975, the edges of the bed were variable while a large section of interior bed remained stable. The time period from 1975-2004 experienced a large loss and significant increase in fragmentation, which worsened from 2004-2016. While the fringing eelgrass along the north shore of the site did decline and fragment, most of the loss and fragmentation occurs in the eastern region of the site, closer to the outflow of Lyall Creek.

3.3.3 Long-term changes in coastal environmental indicators

A dramatic increase in the number of shoreline alterations and activities was seen over time, accelerating between 1975 and 2004 (Figure 3.7 and Table 3.4). Shoreline activity in Village Bay (Figure 3.4) was primarily in the form of boats and moorage buoys, with a few docks and a small amount of built-land/rip-rap, as well as a significant ferry terminal installation after 1975.

No log booming appears to have occurred at this site during the time period of the analysis. In Village Bay, loss of eelgrass at the north end of the meadow coincides with the expansion of the ferry terminal between 1975 and 2004, and the recession of the deep edge with the increase in boat presence between 1975 and 2010. A small loss of eelgrass is observed around the installation of two docks between 2004 and 2010. Horton Bay experienced the highest rate of shoreline activity, being a very popular boat moorage site with many buoys and a public dock nearby. The site also showed some log booming intermittently throughout the study period. In Horton Bay, there is a strong indication of temporal eelgrass fragmentation as a result of boat traffic and dock building. Along the north shore of the bay, an area of fringing eelgrass between docks was seen to fragment and disappear between 1975 and 2010 following dock installation (Figure 3.5). This area of fragmentation is in the path of dinghy traffic between moored boats and the shore. Further, eelgrass loss was observed at two dock installations at the south-east edge of the site between 1950 and 1975, and again between 1975 and 2004. While the deep edge of the eelgrass in Horton Bay was quite variable between 1932 and 2004, it does not appear to be related to boat presence. Lyall Harbour (Figure 3.6), while being the largest site, experienced only slightly higher shoreline activity compared to the smallest site, Village Bay. In Lyall Harbour, log booming occurred in every year of study, and most of the boat presence concentrated around one large private dock attached to a large man-made piece of 'built land', built after 1975. In addition, few boats were anchored in the bay and no permanent buoys were identified, likely due to the distance from a public dock. In Lyall Harbour, much of the shoreline activity occurs out of direct proximity to the eelgrass meadow and changes in eelgrass habitat does not appear to be impacted by any particular activity.

Housing density increases over time in all sites (Figure 3.7), but the largest increase was seen in Village Bay (0.98 houses 100 ha^{-1} to 89.1 houses 100 ha^{-1}), which is the most accessible site and closest to the island's ferry terminal and amenities, with level topography good for residential buildings. Further, no forested or natural areas of the Village Bay watershed were protected and some of the area cleared for agricultural uses present in 1932 converts to residential over time, as is seen in the aerial photography. The relatively lower change in housing density in Horton Bay (1.8 houses 100 ha^{-1} to 17.6 houses 100 ha^{-1}) is likely a result of being a much further distance from the ferry terminal and the amenities of Mayne Island. Further, much of the agricultural area present in 1932 remained agricultural in the Horton Bay watershed, and another

large portion of mature forest was protected as a Regional Park in 1991 (Capital Regional District, 2017). The smallest change in residential housing density was observed in Lyall Harbour (0.61 houses 100 ha^{-1} to 10.6 houses 100 ha^{-1}). Lyall Harbour has steep topography, making it not ideal for building. A large portion of Lyall Harbour watershed was designated as part of the Gulf Islands National Park Reserve in 2003 (Parks Canada, 2017).

3.3.4 Relationship between eelgrass and environmental indicators

Pearson's R correlation models revealed very strong correlations (R>0.80) between eelgrass metrics and landscape-level coastal environmental indicators for all tested models except for the correlation between eelgrass Shape Index and shoreline activities in Village Bay (Table 3.5). There was a very strong negative correlation between housing density and eelgrass area at all three sites: Village Bay (-0.96), Horton Bay (-0.97), and Lyall Harbour (-0.86). Further, a strong positive correlation between housing density and eelgrass Shape Index was observed: Village Bay (0.82), Horton Bay (0.92), and Lyall Harbour (0.85). However, the p-value was not significant for Village Bay. There was a very strong negative correlation between shoreline activity and eelgrass area: Village Bay (-0.82), Horton Bay (-0.97), and Lyall Harbour (-0.98). Similarly to the previous model, the p-value was not significant for Village Bay. The lowest Pearson's R correlations were observed in the relationship between shoreline activity and eelgrass Shape Index for Village Bay (0.73) and Horton Bay (0.81), both of which did not achieve significant p-values. However, the strongest correlation observed for Lyall Harbour was between shoreline activity and eelgrass Shape Index (0.99).

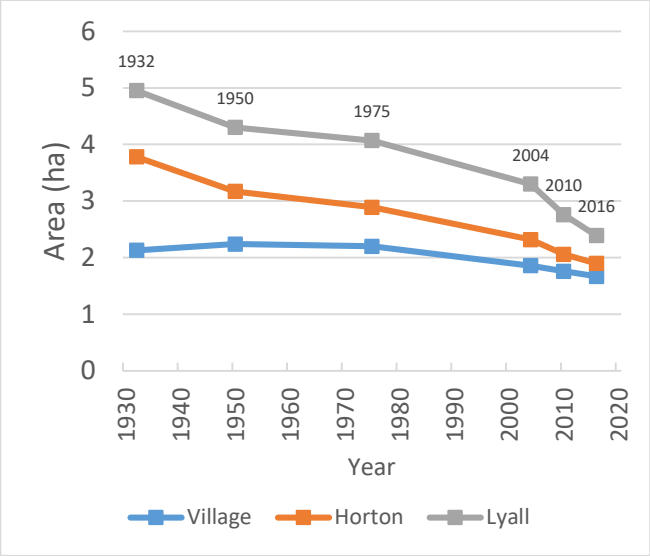

Figure 3.2 Eelgrass area (ha) over time period 1932-2016 in three sites in the Southern Gulf Islands

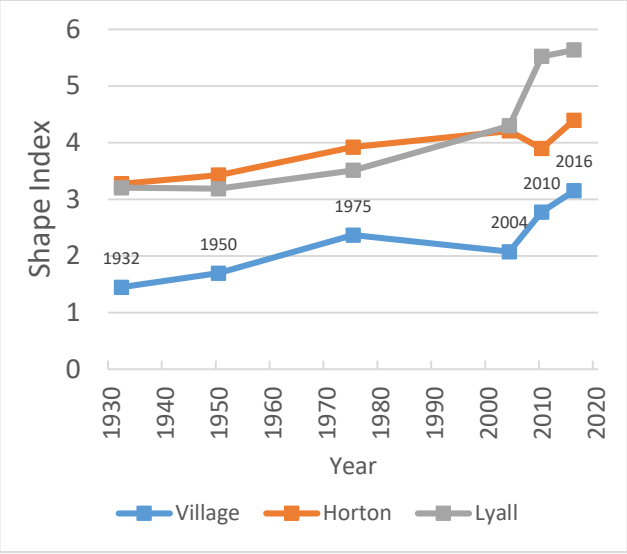

Figure 3.3 Shape Index over time period 1932-2016 of eelgrass meadows at the three study sites in the Southern Gulf Islands.

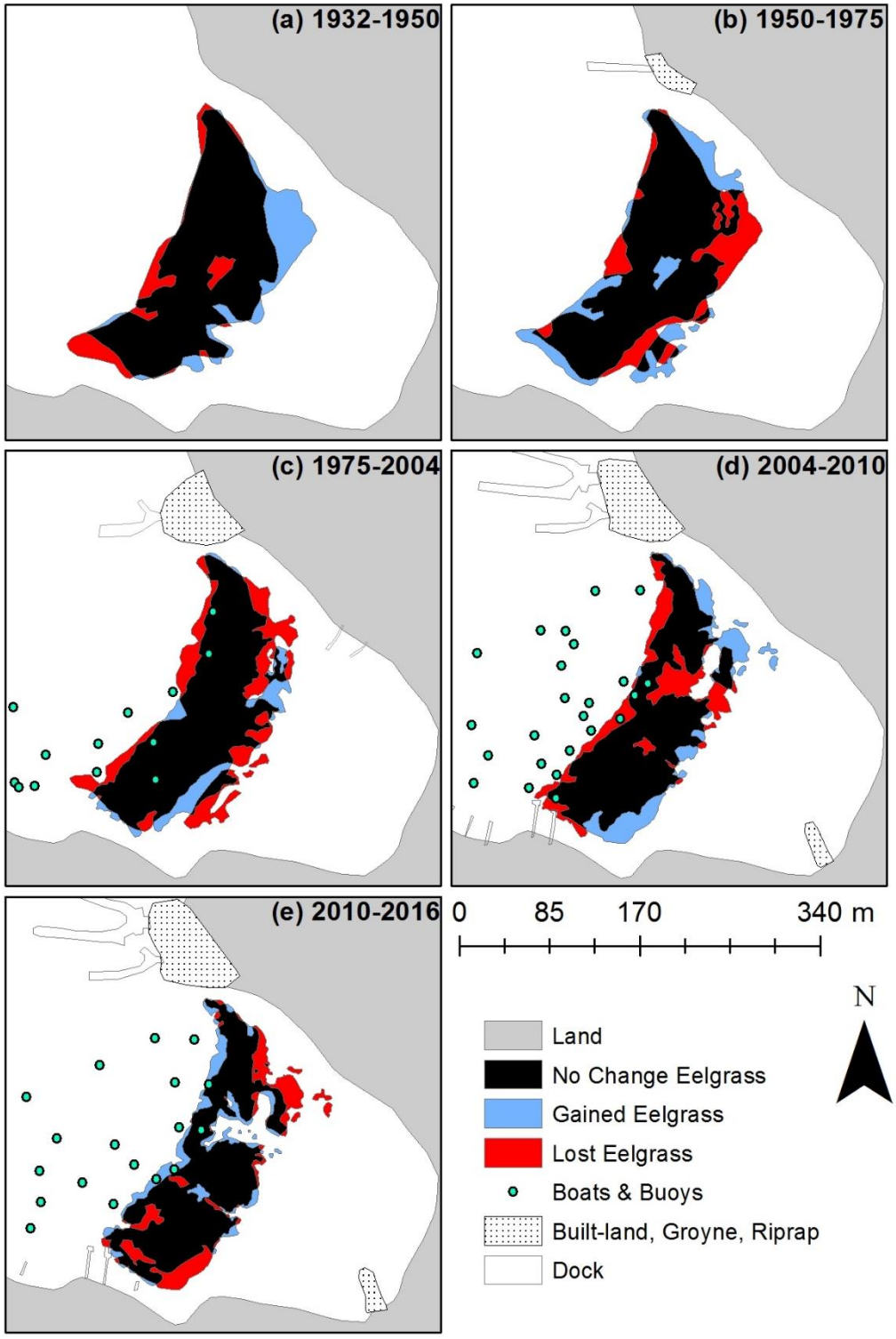

Figure 3.4 Changes in spatial distribution of eelgrass at Village Bay.

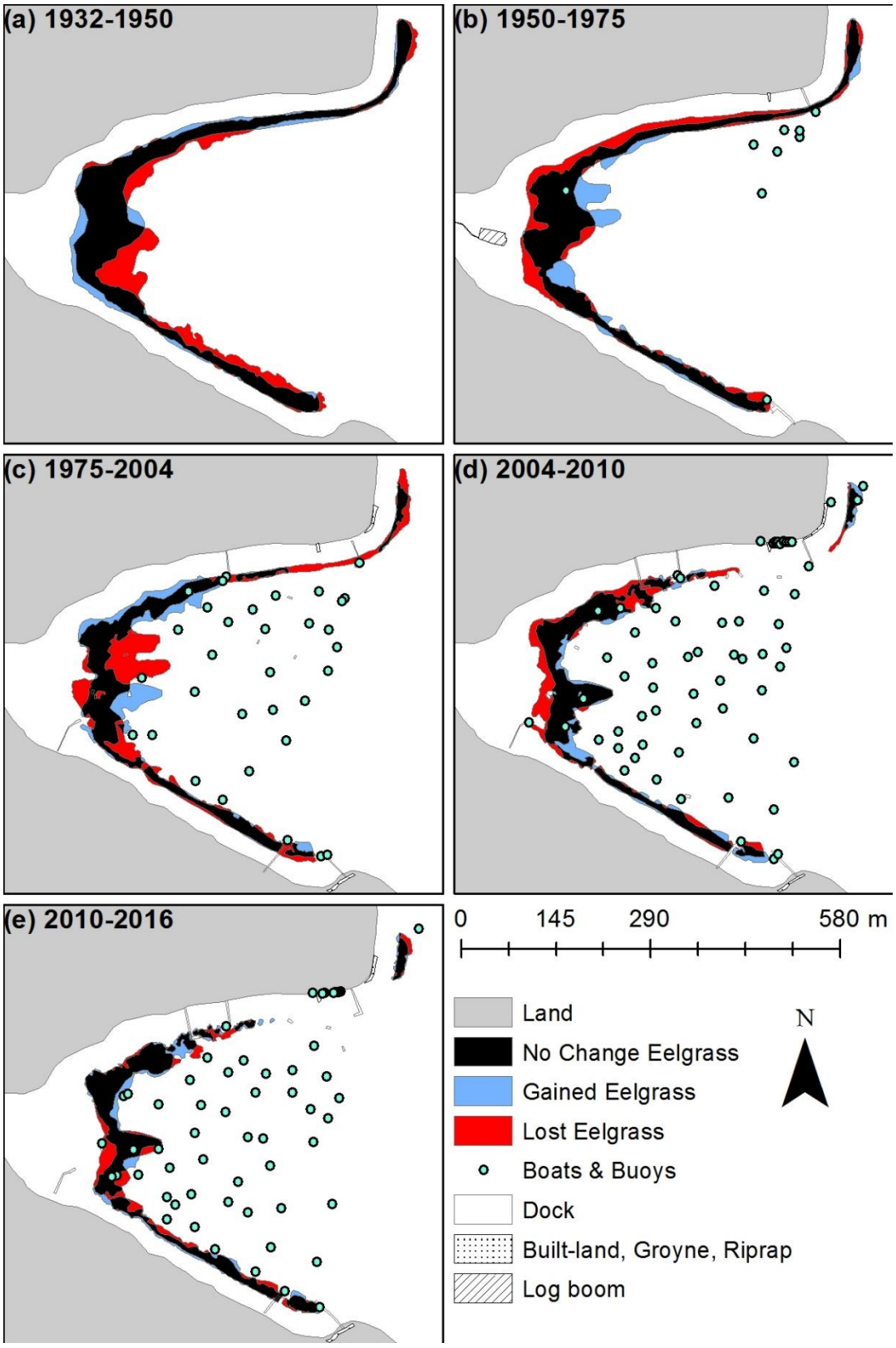

Figure 3.5 Changes in spatial distribution of eelgrass at Horton Bay

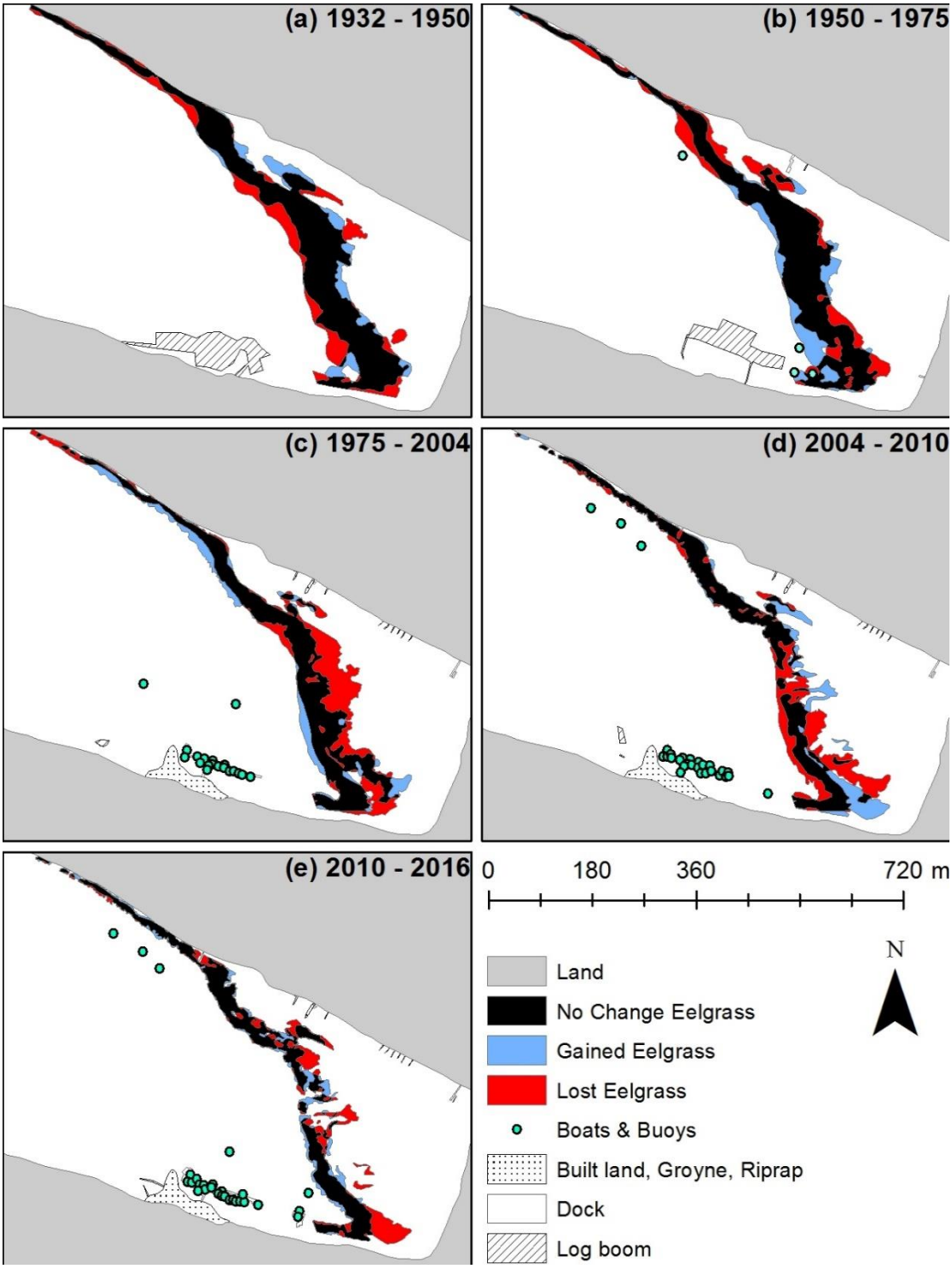

Figure 3.6 Changes in spatial distribution of eelgrass at Lyall Harbour

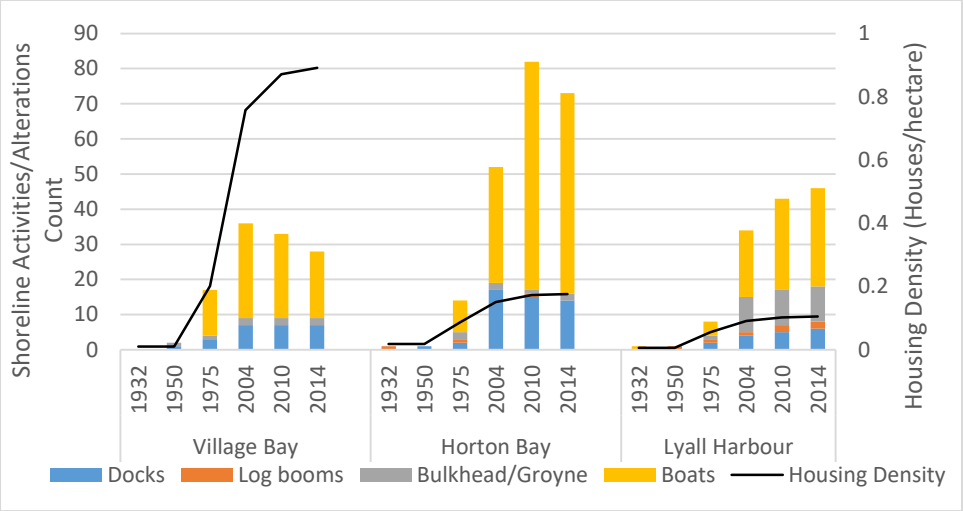

Figure 3.7 Indicators of coastal environmental health at each study site over the period of 1932 to 2014.

Table 3.4 Shoreline activity and alteration counts

	Year	Docks	Log booms	Builtland/Groyne/Riprap	Boats/Buoys
Village Bay	1932	0	0	0	0
	1950	1	0	1	0
	1975	3	0	1	13
	2004	7	0	2	27
	2010	7	0	2	24
	2014	7	0	2	19
Horton Bay	1932	0	1	0	0
	1950	1	0	0	0
	1975	2	1	2	9
	2004	17	0	2	33
	2010	15	1	1	65
	2014	14	0	2	57
Lyall Harbour	1932	0	0	0	1
	1950	0	1	0	0
	1975	2	1	1	4
	2004	4	1	10	19
	2010	5	2	10	26
	2014	6	2	10	28

*Table 3.5 Pearson's R values for Correlations between Housing Density and Shoreline Activities and eelgrass Percent Cover and Shape Index at three sites over time period 1932-2016 (all p-values <0.05 except where noted *)*

	Village Bay	Horton Bay	Lyall Harbour
Housing Density – Eelgrass Area	-0.96	-0.97	-0.86
Housing Density – Shape Index	0.82*	0.92	0.85
Shoreline Activity – Eelgrass Area	-0.82*	-0.97	-0.98
Shoreline Activity – Shape Index	0.73*	0.81*	0.99

3.4 Discussion

The discussion will first address the data quality and limitations of the aerial photography for long-term spatial-temporal eelgrass habitat assessment in order to frame the interpretation of the results. Then, the results of the analysis will be discussed and compared to other records of spatial-temporal eelgrass habitat change in the region. Finally, the implications of the observed eelgrass habitat change are discussed.

3.4.1 Data quality and limitations

Analysis of historic aerial photography is a common tool for identifying long-term spatial-temporal changes in seagrass habitats (Frederiksen et al., 2004a,b; Ball et al., 2014). However, the reliability of the seagrass maps produced from this aerial photography has several limitations, including availability of historic ground reference data, errors inherent to the interpretation of aerial photography, and issues in data quality for benthic habitat mapping (Ball et al., 2014; Finkbeiner et al., 2001; Rango et al., 2008). Further, when working with historic data it is important to consider the intended purpose of the aerial photography, which was generally intended for terrestrial applications, such as forestry and road building, and therefore considerations for benthic habitat mapping were not observed (Egan & Howell, 2005). In the present study, ground reference data was collected in 2016 along with the UAV imagery (Chapter 2) and some community mapping data was available from 2004 to 2015 (Wright et al., 2014), but reference data prior to 2004 does not exist. Therefore, the use of the produced historical maps has to consider the reliability index developed here (Table 3.3).

In Chapter 2, accuracy assessment of UAV-derived eelgrass maps showed that the majority of the classification error was a result of the omission of sparse and patchy eelgrass, with some error resulting through the commission of dark submerged vegetation such as green algae to the eelgrass class. Further, eelgrass mapping accuracy was found to decrease with increasingly unsuitable environmental conditions, such as sun glint and turbidity, which particularly inhibited the detection of deep eelgrass in some cases (Chapter 2). The relative degree to which these observed errors may affect the individual eelgrass maps in the present study are expected to be reflected in the reliability scores derived in Table 3.3. The tidal height, water clarity, and surface effects all act to augment the degree to which mapping errors occur, and influence the reliability of aerial photography for seagrass mapping (Finkbeiner et al., 2001; Table 2). The reliability of air

photos used for this analysis increased in recent years, in part because of improving technologies, but also in part because the timing of air photo acquisition for tidal height and environmental conditions appears to increase the reliability of the results (Pasqualini et al., 1997). Readers are advised to consider the results of this analysis with the understanding that there are greater uncertainties associated with the eelgrass maps derived from earlier years of aerial photography than with recent years.

3.4.2 Long-term spatial-temporal trends in eelgrass coverage

The results of this analysis show a downward trend in eelgrass area coverage and increasing shape complexity (Shape Index) at the study sites over the period of 1932 to 2016 (Figures 3.2 and 3.3). Overall, the three sites experienced an average decline in areal cover of -41.0% and an average increase in Shape Index of 76.0% over the 84 year study period. The eelgrass declines observed in this study were likely caused by multiple natural and anthropogenic stressors, which may act independently or simultaneously, including: changes in water quality; overproliferation of epiphytes and macroalgae; wave action and storms; disease; herbivore grazing; harbor building; and anchor, buoy, and propeller scarring (Gladstone & Courtenay, 2014; Patrick et al., 2014; Short & Burdick, 1996; Short & Wyllie-Echeverria, 1996; Unsworth et al., 2017; Valiela et al., 1992). While any number of these stressors may be acting upon the eelgrass at these sites, two landscape-level coastal environmental indicators, residential housing density and shoreline activities and alterations, were analyzed and revealed very strong correlations to changes in eelgrass coverage and Shape Index (Table 3.5; Klemas, 2001). While a direct causative effect between these landscape indicators and eelgrass coverage cannot be established by these simple correlations alone, the trend in these indicators and associated landscape changes suggest that the coastal marine environment of this region is likely becoming increasingly unfavourable for eelgrass.

The marked increase in housing density observed at these study sites in the Southern Gulf Islands was very strongly correlated to the metrics of eelgrass change in their associated nearshore areas (Table 3.5). In addition to the potential role of nitrogen sourced from residential septic systems on the observed changes in eelgrass habitat (Hauxwell et al., 2003; Short & Burdick, 1996), residential housing density is a good indicator of potential overall water quality impacts on eelgrass because of its coupling with other indicators of deteriorating coastal environmental health. As residential housing density increases, so does road density; impervious surface coverage;

deforestation; and agricultural land use practices, all of which affect water quality by increasing nutrient, sediment, and toxic pollutant inputs to coastal areas (Arnold & Gibbons, 1996; Basynat et al., 2000; Feist et al., 2017; Zebarth et al., 1998). However, it is important to note that the watersheds of these sites were not pristine at the beginning of the study period; all three sites had undergone extensive forest harvest prior to 1932 (Innes et al., 2008). A further consideration is that the watersheds of these sites are relatively undeveloped compared to other more urbanized areas of the Salish Sea such as the Fraser Valley (Shupe, 2013), which may be impacting the Salish Sea water quality as a whole. As such, the relationship observed between eelgrass areal cover, Shape Index, and residential housing density may in reality include the effects of many other land use practices on a larger geographic scale than analyzed in the present study.

Similarly to housing density, shoreline activities were strongly correlated to eelgrass areal coverage and Shape Index when considered (Table 3.5). While shoreline activities were analyzed as a total count in relation to the eelgrass metrics, the change maps in Figure 3.4-3.6 were valuable in assessing their spatial arrangement in order to assess the potential role of individual activities on eelgrass change. Eelgrass losses were observed specifically in relation to dock installation, boat mooring, and in pathways of boat traffic, similar to previous studies (Burdick & Short, 1999; Collins et al., 2010; Gladstone & Courtenay, 2014; Unsworth et al., 2017; Walker et al., 1989; Zieman, 1976). However, large changes in eelgrass extent were observed which appeared unrelated to any particular shoreline activity, especially in intertidal areas. One activity that is very specific to British Columbia but did not appear to directly impact the eelgrass at these sites is marine timber storage, known as “log booming”. In addition to direct physical damage and uprooting of eelgrass through log scouring and reduction of photosynthesis through shading, log booms also deposits large amounts of bark to the benthos, which smother eelgrass and change the chemical composition of the sediments (Sedell et al., 1991). While some log booming was present at the study sites, log booming was not extensive and there were no obvious areas of loss associated with a particular area of log booming.

3.4.3 Comparison to other records of eelgrass change

The change in eelgrass areal coverage observed in this study, -41.0% over the period of 1932 to 2016, represents a rate of change of -0.49% per year. This is consistent with an average worldwide decline of -29% (mean -1.5% per year; median -0.9% per year) from 1879 to 2006 as

calculated in a meta-analysis by Waycott et al. (2009). This is reflected in the many studies corroborating losses of *Zostera* spp. since the 1960's in Europe (Martin et al., 2010), Australia (Ball et al., 2014), South Africa (Pillay et al., 2011), and Atlantic North America (Short & Burdick, 1996). Further, the global projected trajectory of *Z. marina*, specifically, has been calculated at -1.4% per year (Short et al., 2011).

In the limited amount of research situated in British Columbia and Washington, similar losses in eelgrass coverage have been reported, corroborating the losses observed in the present study. Near Vancouver, BC, a 30% loss in eelgrass coverage between 1969 and 1984 was observed at Roberts Bank, suspected to be a result of dredging and filling for the construction of a causeway and coal-handling port (Harrison, 1990). In Washington, a long-term assessment based on pre-1900 and recent (1980's) hydrographic charts and aerial photographs found losses of 30% and 15% in Bellingham Bay and Snohomish River Delta, respectively, primarily caused by dredging and filling for port development (Thom & Hallum, 1990). Further, observations by professional aquatic ecologists and fishermen report substantial eelgrass declines throughout Puget Sound since the 1950s, along with the disappearance of black Brandt geese (*Branta bernicla nigricans*) and juvenile Dungeness crabs (*Metacarcinus magister*) (Thom & Hallum, 1990). Recent results from monitoring programs further indicate site-level declines throughout Puget Sound, however, sound-wide status estimates do not suggest widespread eelgrass declines in the Salish Sea (Gaeckle et al., 2008; Shelton et al., 2016). In these sound-wide assessments, it is important to note the disproportionate effect of large stable sites, which constitute approximately 30% of the total eelgrass area (Gaeckle et al., 2008).

The eelgrass at these study sites on the west coast of Canada do not appear to have been affected by the same wasting disease which decimated over 90% of eelgrass populations in Atlantic North America and Europe in the early 1930s (Dexter, 1985; Frederiksen et al., 2004a,b; Orth & Moore, 1984). The present results indicate that eelgrass areal coverage was highest in the earlier years of the study, 1932 and 1950, than at any time following. Unfortunately, the temporal resolution of analyzed data does not allow for detection of a large decline in eelgrass coverage during the 1932-1950 time frame; however, a large decline on the scale of that observed in the Atlantic is not suspected. In eelgrass populations decimated by wasting disease in the 1930s in Denmark, Frederiksen et al. (2004b) found very low eelgrass coverage in the earliest year of study

(1945 or 1954), substantial meadow recovery did not occur until the 1960/70s, and eelgrass coverage remained relatively high through the duration of the study period (1990s). Sites that were not affected by wasting disease exhibited an opposite temporal trend: high levels of eelgrass coverage in the earliest year of study (1954) and decline into the 1990s. When comparing the temporal patterns observed between these sites in Denmark and those of the present study, the eelgrass trends observed in the Southern Gulf Islands resemble the sites that were not affected by wasting disease in Frederiksen et al. (2004b). This finding would corroborate early anecdotal reports from scientific and government professionals from around Vancouver Island and Washington which state that no large-scale eelgrass declines were observed in the 1930s (Cottam, 1939). While no large-scale declines were observed, diseased plant tissue was found in Nanaimo, British Columbia in 1937 (Young, 1938). Wasting disease may be a contributing factor in the more recent declines in eelgrass coverage as the disease pathogen became more widely spread (Groner et al., 2016; Muehlstein, 1992; Sullivan et al., 2013).

3.4.4 Associated impacts on salmonids

The motivation behind this investigation centers on the question of whether or not deterioration in eelgrass habitats could be a factor in the decline in marine survival of juvenile salmonids (*Oncorhynchus* spp.). The results of the present study would suggest that loss and fragmentation of eelgrass habitat, as well as changes in watershed characteristics and increased use of the coastal zone, could certainly be a factor impacting juvenile Pacific salmon entering the marine environment. The importance of eelgrass habitat to juvenile salmon has been well studied (Kennedy et al. 2018; Semmens, 2008), and survival of hatchery-raised Chinook (*O. tshawytscha*) smolts has been linked to the amount of pristine estuarine habitat of their associated natal river (Magnusson & Hilborn, 2003). Pressure from industrial development is a threat to estuarine habitats and consequently juvenile salmon survival, as these locations are often highly desirable for shipping and port facilities. Carr-Harris et al. (2015) found the highest abundances of sockeye (*O. nerka*), chinook, and coho (*O. kisutch*) juveniles in the areas proposed for the development of two gas liquefaction terminals and a potash loading facility in the Skeena River Estuary, British Columbia.

In addition to the loss and fragmentation of eelgrass habitat, changes in the landscape-level coastal environmental indicators examined here could also be contributing to low survival of

juvenile salmon. There has been substantial research in the Salish Sea region, particularly Puget Sound, showing that premature death of adult salmon returning to urban streams is linked to toxic chemical contaminants in land-based runoff during the fall season (Feist et al., 2011; Spromberg et al., 2011). Spawner mortality is correlated to the proportion of roads, impervious surfaces, and commercial property within a watershed (Feist et al., 2017), which can also be considered landscape-level coastal environmental indicators associated with increases in housing density (Klemas, 2001). Toxic exposure in juvenile salmon increase their risk of predation (Kruzynski & Birtwell, 1994; Sandahl et al., 2007), while reducing toxic runoff through bioremediation in streams has been shown to improve juvenile salmon survival. (McIntyre et al., 2015). Further, increased use of the coastal zone, namely noise from boat traffic, has been shown to negatively impact coastal fishes (Celi et al., 2016; Nichols et al., 2015).

3.5 Conclusions

Eelgrass is a critical nearshore marine habitat in Canadian west coast waters, especially for juvenile Pacific salmon (Kennedy et al., 2018; Plummer et al., 2013). Because of the variable marine survival of juvenile salmon in recent decades (Beamish et al., 2003), there is concern that declining eelgrass habitats could play a role in the observed low marine survival. To assess long-term changes in eelgrass habitats and to identify if losses have occurred, historic aerial photography and UAV imagery over the study period of 1932 to 2016 were analyzed at three study sites in the Southern Gulf Islands. Metrics to assess eelgrass habitat change included eelgrass areal coverage and Shape Index, a proxy for fragmentation or meadow shape complexity. As well, these metrics of eelgrass habitat change were compared to two landscape-level coastal environmental indicators, residential housing density and shoreline activities. This analysis revealed overall areal coverage declined by an average of 41.0%, while meadow fragmentation as measured by Shape Index increased by an average of 76.0%. Further, these metrics of eelgrass habitat change were strongly correlated to residential housing density and shoreline activities, both of which increased dramatically over the study period. The results from this analysis highlight several instances where eelgrass loss appears to be associated with dock installation, boat moorage, and boat traffic. While these results certainly imply a deteriorating coastal environment, it is important to remember several limitations. When using historic aerial photography, the reliability of the data for benthic

habitat mapping must be considered. On the other hand, quantification of the landscape-level coastal environmental indicators can be done from the same historic aerial photography with a relatively high degree of confidence because of their ease of interpretation. Thus, while the analysis of eelgrass habitat change metrics are subject to the quality of the aerial photography for benthic habitat mapping, the dramatic increases in residential housing density and shoreline activities suggest a substantial increase in the magnitude of stress on the nearshore environment in the Salish Sea, which is likely to affect eelgrass habitats.

Chapter 4 – Summary and Conclusions

The goal of this research was to investigate the long-term trends in eelgrass habitat distribution in the Gulf Islands of the Salish Sea by analyzing a time series (1932-2016) of historic aerial photography and contemporary Unmanned Aerial Vehicle (UAV) imagery, and to consider the possible influence of landscape-level coastal environmental indicators of anthropogenic stress. To achieve this goal, two objectives were addressed:

1. Define the current (2016) eelgrass extent at the selected study sites using low-cost consumer-grade UAV technology and concurrent ground reference data. The results of this objective will provide a baseline for the analysis of historic aerial photography.
2. Assess the long-term spatial-temporal eelgrass habitat change from 1932 to 2016 using historic aerial photography and UAV imagery by considering how metrics of eelgrass change: areal cover and Shape Index. Examine the possible influence of residential housing density and shoreline activities on the long-term changes in eelgrass habitats at the selected study sites.

The first objective was addressed in Chapter 2, where the methods using a low-cost consumer-grade UAV for eelgrass mapping in three small coastal estuaries are described. UAV data collection was optimized for sun angle and tidal height, and other environmental variables such as cloud cover, Secchi depth, and wind speed were recorded during the flight. High mapping accuracies of 96.3%, 86.5%, and 89.7% for Village Bay, Horton Bay, and Lyall Harbour respectively were achieved on an eelgrass presence or absence basis. Overall mapping accuracy was found to be highly influenced by the environmental conditions present at the time of image acquisition. Village Bay, which experienced the most optimal environmental conditions, exhibited classification errors primarily as a result of omission of sparse patchy eelgrass. As environmental conditions became more variable in the larger sites, further classification errors were exhibited. In addition to the omission of sparse patchy eelgrass, Horton Bay had errors of commission of green algae to the eelgrass class, as well as omission of deep eelgrass where sun glint inhibited detection. Lyall Harbour provided excellent examples of opposite environmental conditions: half of the site had good water clarity but very high cloud cover, while the other half of the site experienced very

poor water clarity but clear sky conditions. Similar errors were experienced in Lyall Harbour involving omission of sparse patchy eelgrass, commission of dense patches of green algae, and omission of deep eelgrass where environmental conditions are poor.

In light of the results of Chapter 2, several benefits to using UAVs for eelgrass mapping were identified. First, since high mapping accuracies were achieved with the low-cost consumer-grade UAV platform used for data collection, it can be concluded that UAVs are a suitable method for mapping eelgrass habitats at the site-scale investigated here. Because of the low-cost and accessibility associated with UAVs, this method of eelgrass habitat assessment could be invaluable for repeated surveys over time to assess detailed spatial changes over smaller temporal scales than are normally examined (Barrell & Grant, 2015). The high resolution of the UAV imagery is a further benefit to its use, as it allows the visual interpretation of these habitats and differentiation between species that are normally difficult to separate based on spectral characteristics alone, such as eelgrass and green algae (O'Neill et al., 2011; Reshitnyk et al., 2014). UAVs are also highly flexible when it comes to scheduling image acquisition, and thus, flights can be conducted to optimize sun angle, tidal height, and other environmental parameters with relative ease compared to manned aircraft or satellite overpass.

However, because of the low altitude of flight, UAV orthomosaics can have inconsistent radiometric properties. At the sites surveyed in Chapter 2, flights took between 1.5 to 3 hours, and in that time sun angle and cloud cover can change substantially. While image-to-image colour balancing was applied prior to mosaicking, this did not remove localized cloud reflectance, or account for differences in illumination resulting from 20+° changes in sun angle between the start and end time of survey. As such, the object-based, manual classification approach for seagrass mapping with aerial photography using eCognition described by Lathrop et al. (2006) was adopted, combined with digital image enhancements in ENVI software. This method balanced the high visual interpretability of the UAV imagery with a time-efficient process for classifying target features with varying radiometric properties in different parts of the image as a result of changing sun angle, tidal height, water clarity, and cloud cover. Because of the small footprint of the imagery, UAV platforms are more suited to mapping eelgrass habitats at the site-specific scales examined in this research than at larger regional scales, for which manned aircraft or satellite platforms would be better suited. Consumer-grade UAV platforms show considerable promise for

mapping eelgrass habitats in British Columbia. However, further research is necessary to investigate the role of specific environmental conditions on the mapping accuracy, especially considering the fact that some environmental parameters clearly require adjustment to suit UAV acquisitions as compared to the guidelines suggested for manned aircraft. In addition, site characteristics, such as eelgrass density and the presence of other SAV, need to be considered in much greater detail than is examined here.

The UAV orthomosaics produced in Chapter 2 were resampled, along with historic aerial photography, to a consistent spatial resolution to assess long-term changes in eelgrass habitats over the study period of 1932 to 2016. Metrics to assess eelgrass habitat change included eelgrass areal coverage and Shape Index, a proxy for fragmentation or meadow shape complexity. Eelgrass delineations were produced through photointerpretation of digitally enhanced aerial photography. When using historic aerial photography, the reliability of the data for benthic habitat mapping must be considered, and as such, a reliability index was created considering the tidal height, water clarity, and surface effects. As well, these metrics of eelgrass habitat change were compared to two landscape-level coastal environmental indicators, residential housing density and shoreline activities, which were quantified by direct counts from the aerial photography.

This analysis revealed overall areal coverage declined by an average of 41.0%, while meadow fragmentation as measured by Shape Index increased by an average of 76.0%. Further, these metrics of eelgrass habitat change were strongly correlated to residential housing density and shoreline activities, both of which increased dramatically over the study period. The results from this analysis highlight several instances where eelgrass loss appears to be associated with dock installation, boat moorage, and boat traffic. While these results certainly imply a deteriorating coastal environment, it is important to remember several limitations, namely the lack of historic ground reference data and the low quality of historic data for benthic habitat mapping compared to more recent aerial photography. On the other hand, quantification of the landscape-level coastal environmental indicators can be done from the same historic aerial photography with a relatively high degree of confidence because of their ease of interpretation. Thus, while the analysis of eelgrass habitat change metrics are subject to the quality of the aerial photography for benthic habitat mapping, the dramatic increases in residential housing density and shoreline activities suggest a substantial increase in the magnitude of stress on the nearshore environment in the Salish

Sea, which is likely to affect eelgrass habitats. Based on the results of this analysis, the concern that declining eelgrass may play a role in the low and variable marine survival of juvenile salmon is well-founded

Results of this research can be applied in several specific ways:

(1) Chapter 2 was a first evaluation of the role of environmental conditions on the eelgrass mapping accuracy of consumer-grade UAV and digital camera technology, which provides a basis for further research to define specific guidelines for UAV mapping of eelgrass habitats.

(2) The methods for UAV image acquisition and processing described in Chapter 2 can be easily adopted by academics and community groups interested in mapping eelgrass at small spatial scales for operational monitoring, restoration site planning and monitoring, or ecological research. High resolution UAV imagery can be visually interpreted without the need for expensive software.

(3) As demonstrated in Chapter 3, historic aerial photography can be a valuable tool for assessing the historic distribution of eelgrass habitats. This type of information is invaluable to marine ecosystem restorationists for restoration site selection (Thom et al., 2014).

Bibliography

Anderson, K., & Gaston, K. J. (2013). Lightweight unmanned aerial vehicles will revolutionize spatial ecology. *Frontiers in Ecology and the Environment*, 11(3), 138–146.

Anderson, C. J., & Lockaby, B. G. (2011). Research Gaps Related to Forest Management and Stream Sediment in the United States. *Environmental Management*, 47(1), 303–313.

Andreadis, L., Glavas, E., & Tsalides, P. (1995). Image enhancement using colour information. *International Journal of Remote Sensing*, 16(12), 2285–2289.

Arnold, C. L., & Gibbons, C. J. (1996). Impervious Surface Coverage: The Emergence of a Key Environmental Indicator. *Journal of the American Planning Association*, 62(2), 243–258.

Babin, M., Morel, A., Fournier-Sicre, V., Fell, F., & Stramski, D. (2003). Light Scattering Properties of Marine Particles in Coastal and Open Ocean Waters as Related to the Particle Mass Concentration. *Limnology and Oceanography*, 48(2), 843–859.

Ball, D., Soto-Berelov, M., & Young, P. (2014). Historical seagrass mapping in Port Phillip Bay, Australia. *Journal of Coastal Conservation*, 18, 257–272.

Barrell, J., & Grant, J. (2015). High-resolution, low altitude aerial photography in physical geography: A case study characterizing eelgrass (*Zostera marina L.*) and blue mussel (*Mytilus edulis L.*) landscape mosaic structure. *Progress in Physical Geography*, 39(4), 440–459.

Basnyat, P., Teeter, L. D., Flynn, K. M., & Lockaby, B. G. (1999). Relationships between landscape characteristics and nonpoint source pollution inputs to coastal estuaries. *Environmental Management*, 23(4), 539–549.

Basnyat, P., Teeter, L., Lockaby, B. G., & Flynn, K. M. (2000). Land Use Characteristics and Water Quality: A Methodology for Valuing of Forested Buffers. *Environmental Management*, 26(2), 153–161.

Beamish, R. J., Pearsall, I. A., & Healey, M. C. (2003). A history of the research on the early marine life of Pacific salmon off Canada's Pacific coast. *N. Pac. Anadr. Fish Comm. Bull.*, 3, 1–40.

Beck, M. W., Heck, K. L., Able, K. W., Childers, D. L., Eggleston, D. B., Gillanders, B. M., Halpern, B., Hays, C., Hoshino, K., Minello, T. J., Orth, R. J., Sheridan, P. F., Weinstein, M. P. (2001). The Identification, Conservation, and Management of Estuarine and Marine Nurseries for Fish and Invertebrates. *BioScience*, 51(8), 633–641.

Bell, S. S., Fonseca, M. S., & Moten, L. B. (1997). Linking Restoration and Landscape Ecology. *Restoration Ecology*, 5(4), 318–323.

Blaschke, T., Hay, G. J., Kelly, M., Lang, S., Hofmann, P., Addink, E., Feitosa, R. Q., van der Meer, F., van der Werff, H., van Coillie, F., & Tiede, D. (2014). Geographic Object-Based Image Analysis - Towards a new paradigm. *ISPRS Journal of Photogrammetry and Remote Sensing*, 87, 180–191.

Blaschke, T. (2010). Object based image analysis for remote sensing. *ISPRS Journal of Photogrammetry and Remote Sensing*, 65, 2–16.

Bos, A. R., & Van Katwijk, M. M. (2007). Planting density, hydrodynamic exposure and mussel beds affect survival of transplanted intertidal eelgrass. *Marine Ecology Progress Series*, *336*, 121–129.

Bowden, D. A., Rowden, A. A., & Attrill, M. J. (2001). Effect of patch size and in-patch location on the infaunal macroinvertebrate assemblages of *Zostera marina* seagrass beds. *Journal of Experimental Marine Biology and Ecology*, 259, 133–154.

Bryson, M., Johnson-Roberson, M., Murphy, R. J., & Bongiorno, D. (2013). Kite Aerial Photography for Low-Cost, Ultra-high Spatial Resolution Multi-Spectral Mapping of Intertidal Landscapes. *PLoS ONE*, 8(9), 1–15.

Burdick, D. M., & Short, F. T. (1999). The effects of boat docks on eelgrass beds in coastal waters of Massachusetts. *Environmental Management*, 23(2), 231–240.

Burkholder, J. M., Tomasko, D. A., & Touchette, B. W. (2007). Seagrasses and eutrophication. *Journal of Experimental Marine Biology and Ecology*, 350, 46–72.

Capital Regional District. (2017). *Mount Parke Regional Park*. Available at https://www.crd.bc.ca/parks-recreation-culture/parks-trails/find-park-trail/mount-parke

Carr-Harris, C., Gottesfeld, A. S., & Moore, J. W. (2015). Juvenile Salmon usage of the Skeena River estuary. *PLoS ONE*, 10(3), 1–21.

Casella, E., Collin, A., Harris, D., Ferse, S., Bejarano, S., Parravicini, V., Hench, J. L., Rovere, A. (2017). Mapping coral reefs using consumer-grade drones and structure from motion photogrammetry techniques. *Coral Reefs*, 36, 269–275.

Celi, M., Filiciotto, F., Maricchiolo, G., Genovese, L., Quinci, E. M., Maccarrone, V., Mazzola, S., Vazzana, M., & Buscaino, G. (2016). Vessel noise pollution as a human threat to fish: assessment of the stress response in gilthead sea bream (*Sparus aurata*, Linnaeus 1758). *Fish Physiology and Biochemistry*, 42, 631–641.

Chavez Jr., P. (1996). Image-based atmospheric corrections – revisited and improved. *Photogrammetric Engineering and Remote Sensing*, 62(9), 1025–1036.

Collins, K. J., Suonpää, A. M., & Mallinson, J. J. (2010). The impacts of anchoring and mooring in seagrass, Studland Bay, Dorset, UK. *Underwater Technology*, 29(3), 117–123.

Costanza, R., D'Arge, R., de Groot, R., Farber, S., Grasso, M., Hannon, B., … van den Belt, M. (1997). The value of the world's ecosystem services and natural capital. *Nature*, 387(15), 253–260.

Cottam, C. (1939). The eelgrass situation on the American Pacific Coast. *Rhodora*, 41(487), 257-260.

Dekker, A., Brando, V., Anstee, J., Fyfe, S., Malthus, T., & Karpouzli, E. (2006). Remote Sensing of Seagrass Ecosystems: Use of Spaceborne and Airborne Sensors. In A. W. D. Larkum, R. J. Orth, & C. M. Duarte (Eds.), *Seagrasses: Biology, Ecology, and Conservation* (pp. 347 – 359). Dordrecht, The Netherlands: Springer.

Demers, M. C. A., Davis, A. R., & Knott, N. A. (2013). A comparison of the impact of "seagrass-friendly" boat mooring systems on *Posidonia australis*. *Marine Environmental Research*, 83, 54–62.

Dethier, M. N., Toft, J. D., & Shipman, H. (2017). Shoreline Armoring in an Inland Sea: Science-Based Recommendations for Policy Implementation. *Conservation Letters*, 10(5), 626–633.

Dexter, R. W. (1985). Changes in Standing Crop of Eelgrass, *Zostera marina* L., at Cape Ann, Massachusetts, since the Epidemic of 1932. *Rhodora*, 87(851), 357–366.

Dobson, J. E., Bright, E. A., Ferguson, R. L., Field, D. W., Wood, L. L., Haddad, K. D., Ireland, H., Jensen, J. R., Klemas, V. V., Orth, R. J., & Thomas, J. P. (1995). *Monitoring Submerged Land Using Aerial Photography*. *NOAA Coastal Change Analysis Program (C-CAP). NOAA technical report NMFS 123*.

Drake, L. A., Dobbs, F. C., & Zimmerman, R. C. (2003). Effects of epiphyte load on optical properties and photosynthetic potential of the seagrasses *Thalassia testudinum* Banks ex König and *Zostera marina* L. *Limnology and Oceanography*, 48(1), 456–463.

Duarte, C. M. (2002). The future of seagrass meadows. *Environmental Conservation*, 29(2), 192–206.

Duffy, J. P., Pratt, L., Anderson, K., Land, P. E., & Shutler, J. D. (2018). Spatial assessment of intertidal seagrass meadows using optical imaging systems and a lightweight drone. *Estuarine, Coastal and Shelf Science*, *200*, 169–180.

Elliott, M. (1984). *Mayne Island & the outer Gulf Islands, a history*. Mayne Island, BC: Gulf Islands Press.

Emmett, R., Llansó, R., Newton, J., Thom, R., Hornberger, M., Morgan, C., Levings, C., Copping, A., & Fishman, P. (2000). Geographic Signatures of North American West Coast Estuaries. *Estuaries*, 23(6), 765–792.

Feist, B. E., Buhle, E. R., Arnold, P., Davis, J. W., & Scholz, N. L. (2011). Landscape ecotoxicology of coho salmon spawner mortality in urban streams. *PLoS ONE*, 6(8), 1–11.

Feist, B. E., Buhle, E. R., Baldwin, D. H., Spromberg, J. A., Damm, S. E., Davis, J. W., & Scholz, N. L. (2017). Roads to ruin: Conservation threats to a sentinel species across an urban gradient. *Ecological Applications*, 27(8), 2382–2396.

Finkbeiner, M., Stevenson, B., & Seaman, R. (2001). *Guidance for Benthic Habitat Mapping: An Aerial Photographic Approach*. *NOAA Coastal Services Center*.

Fisheries and Oceans Canada. (2016). *Tides, currents, and water levels*. Retrieved from http://www.tides.gc.ca

Fletcher, R. S., Pulich, W., & Hardegree, B. (2009). A Semiautomated Approach for Monitoring Landscape Changes in Texas Seagrass Beds from Aerial Photography. *Journal of Coastal Research*, 25(2), 500–506.

Fonseca, M. S., & Cahalan, J. A. (1992). A preliminary evaluation of wave attenuation by four species of seagrass. *Estuarine, Coastal and Shelf Science*, 35, 565–576.

Forman, R. T. T., & Godron, M. (1981). Patches and Structural Components for a Landscape Ecology. *BioScience*, 31(10), 733–740.

Fraser, R. H., van der Sluijs, J., & Hall, R. J. (2017). Calibrating satellite-based indices of burn severity from UAV-derived metrics of a burned boreal forest in NWT, Canada. *Remote Sensing*, 9(279), 1–17.

Frederiksen, M., Krause-Jensen, D., Holmer, M., & Laursen, J. S. (2004a). Spatial and temporal variation in eelgrass (*Zostera marina*) landscapes: Influence of physical setting. *Aquatic Botany*, 78, 147–165.

Frederiksen, M., Krause-Jensen, D., Holmer, M., & Laursen, J. S. (2004b). Long-term changes in area distribution of eelgrass (*Zostera marina*) in Danish coastal waters. *Aquatic Botany*, 78, 167–181.

Fyfe, S. K. (2003). Spatial and temporal variation in spectral reflectance: Are seagrass species spectrally distinct? *Limnology and Oceanography*, 48(1), 464–479.

Getzin, S., Wiegand, K., & Schoning, I. (2012). Assessing biodiversity in forests using very high-resolution images and unmanned aerial vehicles. *Methods in Ecology and Evolution*, 3, 397–404.

GeoBC. (2015). *Digital orthomosaic aerial imagery of the Southern Gulf Islands, 2014*. https://www2.gov.bc.ca/gov/content/data/about-data-management/geobc/geobc-products

Georgia Strait Alliance. (2017). About the Strait. Available online at https://georgiastrait.org/issues/about-the-strait-2/

Giesen, W. B. J. T., van Katwijk, M. M., & den Hartog, C. (1990). Eelgrass condition and turbidity in the Dutch Wadden Sea. *Aquatic Botany*, 37, 71–85.

Gladstone, W., & Courtenay, G. (2014). Impacts of docks on seagrass and effects of management practices to ameliorate these impacts. *Estuarine, Coastal and Shelf Science*, 136, 53–60.

Groner, M. L., Burge, C. A., Kim, C. J. S., Rees, E., Van Alstyne, K. L., Yang, S., … Drew Harvell, C. (2016). Plant characteristics associated with widespread variation in eelgrass wasting disease. *Diseases of Aquatic Organisms*, 118, 159–168.

Guichard, F., Bourget, E., & Agnard, J. (2000). High-resolution remote sensing of intertidal ecosystems: A low-cost technique to link scale-dependent patterns and processes. *Limnology and Oceanography*, 45(2), 328–338.

Hansen, J. C. R., & Reidenbach, M. a. (2013). Seasonal Growth and Senescence of a *Zostera marina* Seagrass Meadow Alters Wave-Dominated Flow and Sediment Suspension Within a Coastal Bay. *Estuaries and Coasts*, 36, 1099–1114.

Harrison, P. G. (1990). Variations in Success of Eelgrass Transplants over a Five-years' Period. *Environmental Conservation*, 17(2), 157–163.

Hauxwell, J., Cebrián, J., & Valiela, I. (2003). Eelgrass *Zostera marina* loss in temperate estuaries: Relationship to land-derived nitrogen loads and effect of light limitation imposed by algae. *Marine Ecology Progress Series*, 247, 59–73.

Hedley, J. D., Harborne, a. R., & Mumby, P. J. (2005). Technical note: Simple and robust removal of sun glint for mapping shallow-water benthos. *International Journal of Remote Sensing*, 26(10), 2107–2112.

Hogrefe, K., Ward, D., Donnelly, T., & Dau, N. (2014). Establishing a Baseline for Regional Scale Monitoring of Eelgrass (*Zostera marina*) Habitat on the Lower Alaska Peninsula. *Remote Sensing*, 6, 12447–12477.

Holmer, M., Argyrou, M., Dalsgaard, T., Danovaro, R., Diaz-Almela, E., Duarte, C. M., … Tsapakis, M. (2008). Effects of fish farm waste on *Posidonia oceanica* meadows: Synthesis and provision of monitoring and management tools. *Marine Pollution Bulletin*, 56, 1618–1629.

Hossain, M. S., Bujang, J. S., Zakaria, M. H., & Hashim, M. (2015). The application of remote sensing to seagrass ecosystems: an overview and future research prospects. *International Journal of Remote Sensing*, 36(1), 61–114.

Hovel, K. A., Fonseca, M. S., Myer, D. L., Kenworthy, W. J., & Whitfield, P. E. (2002). Effects of seagrass landscape structure, structural complexity and hydrodynamic regime on macro-

faunal densities in North Carolina seagrass beds. *Marine Ecology Progress Series*, 243, 11–24.

Huang, A. C., Essak, M., & O'Connor, M. I. (2015). Top-down control by great blue herons *Ardea herodias* regulates seagrass-associated epifauna. *Oikos*, 124, 1492–1501.

Husson, E., Ecke, F., & Reese, H. (2016). Comparison of manual mapping and automated object-based image analysis of non-submerged aquatic vegetation from very-high-resolution UAS images. *Remote Sensing*, 8(724), 1–18.

Innes, T., Berst, P., & Reid, H. (2008). 1932 Historical Land-Cover Mapping: Comparison to 1950 and 2002 Land Status for the Gulf Islands National Park Reserve. Madrone Environmental Services LTD.

Jackson, E. L., Rowden, A. A., Attrill, M. J., Bossey, S. J., & Jones, M. B. (2001). The Importance of Seagrass Beds as a Habitat for Fishery Species. *Oceanography and Marine Biology*, 39, 269–303.

Jerlov, N. G. (1976). *Marine Optics*. Elsevier.

Karr, J. R., & Schlosser, I. J. (1978). Water Resources and the Land-Water Interface. *Science*, 201(4352), 229–234.

Kavzoglu, T., & Yildiz, M. (2014). Parameter-Based Performance Analysis of Object-Based Image Analysis Using Aerial and Quikbird-2 Images. *ISPRS Annals of Photogrammetry, Remote Sensing and Spatial Information Sciences*, 2(7), 31–37.

Kay, S., Hedley, J. D., & Lavender, S. (2009). Sun glint correction of high and low spatial resolution images of aquatic scenes: A review of methods for visible and near-infrared wavelengths. *Remote Sensing*, 1, 697–730.

Kennedy, L., Juanes, F., El-Sabaawi, R. (in press). Eelgrass as valuable near-shore foraging habitat for juvenile Pacific salmon in the early marine period. *Marine and Coastal Fisheries.*

Klemas, V. (2016). Remote Sensing of Submerged Aquatic Vegetation. In C. W. Finkl & C. Makowski (Eds.), *Seafloor Mapping along Continental Shelves: Research and Techniques for Visualizing Benthic Environments* (13th ed., pp. 125–140). Coastal Research Library. Switzerland: Springer, pp. 125–140.

Klemas, V. (2015). Coastal and Environmental Remote Sensing from Unmanned Aerial Vehicles: An Overview. *Journal of Coastal Research*, 31(5), 1260–1267.

Klemas, V. (2013). Using Remote Sensing to Select and Monitor Wetland Restoration Sites: An Overview. *Journal of Coastal Research*, 29(4), 958–970.

Klemas, V. (2001). Remote Sensing of Landscape-Level Coastal Environmental Indicators. *Environmental Management*, 27(1), 47–57.

Knudby, A., & Nordlund, L. (2011). Remote sensing of seagrasses in a patchy multi-species environment. *International Journal of Remote Sensing*, 32(8), 2227–2244.

Krause-Jensen, D., Greve, T. M., & Nielsen, K. (2005). Eelgrass as a bioindicator under the European water framework directive. *Water Resources Management*, 19, 63–75.

Kruzynski, G. M., & Birtwell, I. K. (1994). A Predation Bioassay to Quantify the Ecological Significance of Sublethal Responses of Juvenile Chinook Salmon (*Oncorhynchus tshawytscha*) to the Antisapstain Fungicide TCMTB. *Canadian Journal of Fisheries and Aquatic Sciences*, 51, 1780–1790.

Larkum, A. W. D., Orth, R. J., & Duarte, C. M. (2007). *Seagrasses: Biology, Ecology, and Conservation*. Dordrecht, The Netherlands: Springer.

Lathrop, R. G., Haag, S. M., Merchant, D., Kennish, M. J., & Fertig, B. (2014). Comparison of remotely-sensed surveys vs. in situ plot-based assessments of sea grass condition in Barnegat Bay-Little Egg Harbor, New Jersey USA. *Journal of Coastal Conservation*, 18, 299–308.

Lathrop, R. G., Montesano, P., & Haag, S. (2006). A Multi-scale Segmentation Approach to Mapping Seagrass Habitats Using Airborne Digital Camera Imagery. *Photogrammetric Engineering & Remote Sensing*, 72(6), 665–675.

Lee, K. S., & Park, J. I. (2008). An effective transplanting technique using shells for restoration of *Zostera marina* habitats. *Marine Pollution Bulletin*, 56, 1015–1021.

Levings, C. D., & Thom, R. M. (1994). Habitat changes in Georgia Basin: Implications for resource management and restoration. In *R. C. H. Wilson, R. J. Beamish, F. Aitkens, and J. Bell (eds.), Review of the Marine Environment and Biota of Strait of Georgia, Puget Sound, and Juan de Fuca Strait. British Columbia/Washington Symposium on the Marine Environment. Canadian Technical Report of Fisheries and Aquatic Sciences.* (Vol. 1948, pp. 330–351).

Longstaff, B. J., & Dennison, W. C. (1999). Seagrass survival during pulsed turbidity events: The effects of light deprivation on the seagrasses *Halodule pinifolia* and *Halophila ovalis*. *Aquatic Botany*, 65, 105–121.

Loos, E. A., & Costa, M. (2010). Inherent optical properties and optical mass classification of the waters of the Strait of Georgia, British Columbia, Canada. *Progress in Oceanography*, 87, 144–156.

Lyons, M., Roelfsema, C., Kovacs, E., Samper-Villarreal, J., Saunders, M., Maxwell, P., & Phinn, S. (2015). Rapid monitoring of seagrass biomass using a simple linear modelling approach, in the field and from space. *Marine Ecology Progress Series*, 530, 1–14.

Lyons, M. B., Phinn, S. R., & Roelfsema, C. M. (2012). Long term land cover and seagrass mapping using Landsat and object-based image analysis from 1972 to 2010 in the coastal

environment of South East Queensland, Australia. *ISPRS Journal of Photogrammetry and Remote Sensing*, 71, 34–46.

Magnusson, A., & Hilborn, R. (2003). Estuarine Influence on Survival Rates of Coho (*Oncorhynchus kisutch*) and Chinook Salmon (*Oncorhynchus tshawytscha*) Released from Hatcheries on the U.S. Pacific Coast. *Estuaries*, 26(4B), 1094–1103.

Marbà, N., Santiago, R., Díaz-Almela, E., Álvarez, E., & Duarte, C. M. (2006). Seagrass (*Posidonia oceanica*) vertical growth as an early indicator of fish farm-derived stress. *Estuarine, Coastal and Shelf Science*, 67, 475–483.

Marbà, N., & Duarte, C. M. (1998). Rhizome elongation and seagrass clonal growth. *Marine Ecology Progress Series*, 174, 269–280.

Martin, P., Sébastien, D., Gilles, T., Isabelle, A., de Montaudouin, X., Emery, É., Clare, N., & Christophe, V. (2010). Long-term evolution (1988-2008) of *Zostera* spp. meadows in Arcachon Bay (Bay of Biscay). *Estuarine, Coastal and Shelf Science*, 87, 357–366.

Masson, D. (2002). Deep Water Renewal in the Strait of Georgia. *Estuarine, Coastal and Shelf Science*, 54, 115–126.

Mayne Island Conservancy Society (MICS). (2016). *Eelgrass monitoring data.* http://mayneconservancy.ca/

McIntyre, J. K., Davis, J. W., Hinman, C., Macneale, K. H., Anulacion, B. F., Scholz, N. L., & Stark, J. D. (2015). Soil bioretention protects juvenile salmon and their prey from the toxic impacts of urban stormwater runoff. *Chemosphere*, 132, 213–219.

McMahon, K., Collier, C., & Lavery, P. S. (2013). Identifying robust bioindicators of light stress in seagrasses: A meta-analysis. *Ecological Indicators*, 30, 7–15.

Mount, R. (2005). Acquisition of Through-water Aerial Survey Images: Surface Effects and the Prediction of Sun Glitter and Subsurface Illumination. *Photogrammetric Engineering & Remote Sensing*, 71(12), 1407–1415.

Muehlstein, L. K. (1992). The host – pathogen interaction in the wasting disease of eelgrass, *Zostera marina*. *Canadian Journal of Botany*, 70, 2081–2088.

Nagendra, H., Lucas, R., Honrado, J. P., Jongman, R. H. G., Tarantino, C., Adamo, M., & Mairota, P. (2013). Remote sensing for conservation monitoring: Assessing protected areas, habitat extent, habitat condition, species diversity, and threats. *Ecological Indicators*, 33, 45–59.

Nahirnick, N., Hunter, P., Costa, M., Schroeder, S., Sharma, T. (2018, *in preparation*). Benefits and challenges of UAV imagery for eelgrass (*Zostera marina*) mapping in small estuaries of the Salish Sea. *Remote Sensing*.

Nakaoka, M. & Aioi, K. (1999) Growth of the seagrass *Halophila ovalis* at dugong trails compared to existing within-patch variation in a Thailand intertidal flat. *Marine Ecology Progress Series,* 184, 97–103.

Neckles, H. A., Kopp, B. S., Peterson, B. J., & Pooler, P. S. (2012). Integrating Scales of Seagrass Monitoring to Meet Conservation Needs. *Estuaries and Coasts*, 35, 23–46.

Negri, A. P., Flores, F., Mercurio, P., Mueller, J. F., & Collier, C. J. (2015). Lethal and sub-lethal chronic effects of the herbicide diuron on seagrass. *Aquatic Toxicology*, 165, 73–83.

Nichols, T. A., Anderson, T. W., & Širović, A. (2015). Intermittent noise induces physiological stress in a coastal marine fish. *PLoS ONE*, 10(9), 1–13.

O'Neill, J. D., & Costa, M. (2013). Mapping eelgrass (*Zostera marina*) in the Gulf Islands National Park Reserve of Canada using high spatial resolution satellite and airborne imagery. *Remote Sensing of Environment*, 133, 152–167.

O'Neill, J. D., Costa, M., & Sharma, T. (2011). Remote Sensing of Shallow Coastal Benthic Substrates: In situ Spectra and Mapping of Eelgrass (*Zostera marina*) in the Gulf Islands National Park Reserve of Canada. *Remote Sensing*, 3, 975–1005.

Olesen, B., & Sand-Jensen, K. (1994). Patch dynamics of eelgrass *Zostera marina*. *Marine Ecology Progress Series*, 106, 147–156.

Orth, R. J., Carruthers, T. J. B., Dennison, W. C., Duarte, C. M., Fourqurean, J. W., Heck, K. L., … Williams, S. L. (2006). A Global Crisis for Seagrass Ecosystems. *Bioscience*, 56(12), 987–996.

Orth, R. J., & Moore, K. A. (1984). Distribution and Abundance of Submerged Aquatic Vegetation in Chesapeake Bay: An Historical Perspective. *Estuaries*, 7(4B), 531–540.

Paine, D. P & Kaiser, J.D. (2012). Aerial Photography and Image Interpretation (3rd ed.). Hoboken, NJ: John Wiley & Sons, Inc.

Parks Canada. (2017). *Gulf Islands National Park Reserve*. Available at https://www.pc.gc.ca/en/pn-np/bc/gulf.

Parks Canada. (2015). *Gulf Islands National Park Reserve aerial photography*. https://www.pc.gc.ca/en/pn-np/bc/gulf

Paneque-Gálvez, J., McCall, M. K., Napoletano, B. M., Wich, S. A., & Koh, L. P. (2014). Small drones for community-based forest monitoring: An assessment of their feasibility and potential in tropical areas. *Forests*, 5, 1481–1507.

Pasqualini, V., Pergent-Martini, C., Pergent, G., Agreil, M., Skoufas, G., Sourbes, L., & Tsirika, A. (2005). Use of SPOT 5 for mapping seagrasses: An application to *Posidonia oceanica*. *Remote Sensing of Environment*, 94, 39–45.

Pasqualini, V., Pergent-Martini, C., Fernandez, C., & Pergent, G. (1997). The use of airborne remote sensing for benthic cartography: Advantages and reliability. *International Journal of Remote Sensing*, 18(5), 1167–1177.

Patrick, C. J., Weller, D. E., Li, X., & Ryder, M. (2014). Effects of Shoreline Alteration and Other Stressors on Submerged Aquatic Vegetation in Subestuaries of Chesapeake Bay and the Mid-Atlantic Coastal Bays. *Estuaries and Coasts*, *37*, 1516–1531.

Patrick, C. J., Weller, D. E., & Ryder, M. (2016). The Relationship Between Shoreline Armoring and Adjacent Submerged Aquatic Vegetation in Chesapeake Bay and Nearby Atlantic Coastal Bays. *Estuaries and Coasts*, 39(1), 158–170.

Pereira, E., Bencatel, R., Correia, J., Félix, L., Gonçalves, G., Morgado, J., & Sousa, J. (2009). Unmanned Air Vehicles for Coastal and Environmental Research. *Journal of Coastal*, 2(2009), 1557–1561.

Penhale, P. A., & Smith, W. O. (1977). Excretion of Dissolved Organic Carbon by Eelgrass (*Zostera marina*) and its Epiphytes. *Limnology and Oceanography*, 22(3), 400–407.

Phillips, R. C. (1984). *The ecology of eelgrass meadows in the Pacific Northwest: A community profile. U.S. Fish and Wildlife Service*.

Phinn, S., Roelfsema, C., Dekker, A., Brando, V., & Anstee, J. (2008). Mapping seagrass species, cover and biomass in shallow waters: An assessment of satellite multi-spectral and airborne hyper-spectral imaging systems in Moreton Bay (Australia). *Remote Sensing of Environment*, 112, 3413–3425.

Pillay, D., Branch, G. M., Griffiths, C. L., Williams, C., & Prinsloo, A. (2010). Ecosystem change in a South African marine reserve (1960-2009): Role of seagrass loss and anthropogenic disturbance. *Marine Ecology Progress Series*, 415, 35–48.

Plummer, M. L., Harvey, C. J., Anderson, L. E., Guerry, A. D., & Ruckelshaus, M. H. (2013). The Role of Eelgrass in Marine Community Interactions and Ecosystem Services: Results from Ecosystem-Scale Food Web Models. *Ecosystems*, 16, 237–251.

Precision Identification & Environment Canada. (2002). *Methods for Mapping and Monitoring Eelgrass Habitat in British Columbia.*

Rango, A., Laliberte, A., & Winters, C. (2008). Role of aerial photos in compiling a long-term remote sensing data set. *Journal of Applied Remote Sensing*, 2(23541), 1–21.

Reshitnyk, L., Robinson, C. L. K., & Dearden, P. (2014). Evaluation of WorldView-2 and acoustic remote sensing for mapping benthic habitats in temperate coastal Pacific waters. *Remote Sensing of Environment*, 153, 7–23.

Riemann, B., & Hoffman, E. (1991). Ecological consequences of dredging and bottom trawling in the Limfjord, Denmark. *Marine Ecology Progress Series*, 69, 171–178.

Robbins, B. D., & Bell, S. S. (1994). Seagrass landscapes: A terrestrial approach to the marine subtidal environment. *Trends in Ecology and Evolution*, 9, 301–304.

Robinson, C. L. K., & Yakimishyn, J. (2013). The persistence and stability of fish assemblages within eelgrass meadows (*Zostera marina*) on the Pacific coast of Canada. *Canadian Journal of Fisheries and Aquatic Sciences*, 70, 775–784.

Robinson, C. L. K., Yakimishyn, J., & Dearden, P. (2011). Habitat heterogeneity in eelgrass fish assemblage diversity and turnover. *Aquatic Conservation: Marine and Freshwater Ecosystems*, 21, 625–635.

Robinson, C. L. K., & Yakimishyn, J. (2005). Monitoring for the Ecological Integrity of Eelgrass Beds (*Zostera marina*) in Canada's Coastal National Parks of British Columbia. Parks Canada Resource Conservation technical report (internal document), 1-89.

Roelfsema, C. M., Lyons, M., Kovacs, E. M., Maxwell, P., Saunders, M. I., Samper-Villarreal, J., & Phinn, S. R. (2014). Multi-temporal mapping of seagrass cover, species and biomass: A semi-automated object based image analysis approach. *Remote Sensing of Environment*, 150, 172–187.

Roelfsema, C., Phinn, S. R., Udy, N., & Maxwell, P. (2009). An integrated field and remote sensing approach An Integrated Field and Remote Sensing Approach for Mapping Seagrass Cover, Moreton Bay, Australia. *Journal of Spatial Science*, 54(1), 45–62.

Ruesink, J. L., Hong, J. S., Wisehart, L., Hacker, S. D., Dumbauld, B. R., Hessing-Lewis, M., & Trimble, A. C. (2010). Congener comparison of native (*Zostera marina*) and introduced (*Z. japonica*) eelgrass at multiple scales within a Pacific Northwest estuary. *Biological Invasions*, 12, 1773–1789.

Salo, T., Pedersen, M. F., & Boström, C. (2014). Population specific salinity tolerance in eelgrass (*Zostera marina*). *Journal of Experimental Marine Biology and Ecology*, 461, 425–429.

Sandahl, J. F., Baldwin, D. H., Jenkins, J. J., & Scholz, N. L. (2007). A sensory system at the interface between urban stormwater runoff and salmon survival. *Environmental Science and Technology*, 41, 2998–3004.

Sandbrook, C. (2015). The social implications of using drones for biodiversity conservation. *Ambio*, 44(4), 636–647.

Saturna Island Marine Research and Education Society (SIMRES). (2016). *Eelgrass monitoring data*. http://saturnamarineresearch.ca/

Schweizer, D., Armstrong, R. A., & Posada, J. (2005). Remote sensing characterization of benthic habitats and submerged vegetation biomass in Los Roques Archipelago National Park, Venezuela. *International Journal of Remote Sensing*, 26(12), 2657–2667.

Sedell, J. R., Leone, F. N., & Duval, W. S. (1991). Chapter 9. Water transportation and storage of logs. In: Influences of Forest and Rangeland Management on Salmonid Fishes and their Habitats. *American Fisheries Society Special Publication*, 19, 325–368.

Semmens, B. X. (2008). Acoustically derived fine-scale behaviors of juvenile Chinook salmon (*Oncorhynchus tshawytscha*) associated with intertidal benthic habitats in an estuary. *Canadian Journal of Fisheries and Aquatic Sciences*, 65, 2053–2062.

Shafer, D. J. (1999). The Effects of Dock Shading on the Seagrass *Halodule wrightii* in Perdido Bay, Alabama. *Estuaries*, 22(4), 936–943.

Shelton, A. O., Francis, T. B., Feist, B. E., Williams, G. D., Lindquist, A., & Levin, P. (2016). Forty years of seagrass population stability and resilience in an urbanizing estuary. *Journal of Ecology*, 105(2), 458–470.

Short, F. T., Coles, R., Fortes, M. D., Victor, S., Salik, M., Isnain, I., Andrew, J., & Seno, A. (2014). Monitoring in the Western Pacific region shows evidence of seagrass decline in line with global trends. *Marine Pollution Bulletin*, 83(2), 408–416.

Short, F. T., Polidoro, B., Livingstone, S. R., Carpenter, K. E., Bandeira, S., Bujang, J. S., Calumpong, H. P., Carruthers, T. J. B., Coles, R. G., Dennison, W. C., Erftemeijer, P. L. A., Fortes, M. D., Freeman, A. S., Jagtap, T. G., Kamal, A. G. M., Kendick, G. A., Kenworthy, W. J., La Nafie, Y. A., Nasution, I. M., Orth, R. J., Prathep, A., Sanciangco, J. C., van Tussenbroek, B., Vergara, S. G., Waycott, M., & Zieman, J. C. (2011). Extinction risk assessment of the world's seagrass species. *Biological Conservation*, 144, 1961–1971.

Short, F. T., Burdick, D. M., & Kaldy, J. E. (1995). Mesocosm experiments quantify the effects of eutrophication on eelgrass, *Zostera marina*. *Limnology and Oceanography*, 40(4), 740–749.

Short, F. T., & Burdick, D. M. (1996). Quantifying Eelgrass Habitat Loss in Relation to Housing Development and Nitrogen Loading in Waquoit Bay, Massachusetts. *Estuaries*, 19(3), 730–739.

Short, F. T., & Wyllie-Echeverria, S. (1996). Natural and human-induced disturbance of seagrasses. *Environmental Conservation*, 23(1), 17–27.

Shupe, S. (2013). Statistical and spatial analysis of land cover impact on selected Metro Vancouver, British Columbia watersheds. *Environmental Management*, 51, 18–31.

Simenstad, C. A., & Cordell, J. R. (2000). Ecological assessment criteria for restoring anadromous salmonid habitat in Pacific Northwest estuaries. *Ecological Engineering*, 15, 283–302.

Spromberg, J. A., & Scholz, N. L. (2011). Estimating the future decline of wild coho salmon populations resulting from early spawner die-offs in urbanizing watersheds of the Pacific Northwest, USA. *Integrated Environmental Assessment and Management*, 7(4), 648–656.

Sullivan, B. K., Sherman, T. D., Damare, V. S., Lilje, O., & Gleason, F. H. (2013). Potential roles of *Labyrinthula* spp. in global seagrass population declines. *Fungal Ecology*, 6, 328–338.

Tallis, H. M., Ruesink, J. L., Dumbauld, B., Hacker, S., & Wisehart, L. M. (2009). Oysters and Aquaculture Practices Affect Eelgrass Density and Productivity in a Pacific Northwest Estuary. *Journal of Shellfish Research*, 28(2), 251–261.

Thom, R. M., Gaeckle, J. L., Buenau, K. E., Borde, A. B., Vavrinec, J., Aston, L., Woodruff, D. L. (2014). Eelgrass (*Zostera marina* L.) Restoration in Puget Sound: Development and Testing of Tools for Optimizing Site Selection. Pacific Northwest National Laboratory.

Thom, R. M., & Hallum, L. (1990). *Long-term changes in the areal extent of tidal marshes, eelgrass meadows and kelp forests of Puget Sound*. *Final Report to Office of Puget Sound, Region 10 U.S. Environmental Protection Agency.*

Thom, R. M., Diefenderfer, H. L., Vavrinec, J., & Borde, A. B. (2012). Restoring Resiliency: Case Studies from Pacific Northwest Estuarine Eelgrass (*Zostera marina* L.) Ecosystems. *Estuaries and Coasts*, 35, 78–91.

Transport Canada. (2016). *Getting permission to fly your drone*. Retrieved from https://www.tc.gc.ca/eng/civilaviation/opssvs/getting-permission-fly-drone.html

Turner, D., Lucieer, A., & Watson, C. (2012). An automated technique for generating georectified mosaics from ultra-high resolution Unmanned Aerial Vehicle (UAV) imagery, based on Structure from Motion (SFM) point clouds. *Remote Sensing*, 4, 1392–1410.

United States Naval Observatory. *Sun or Moon Altitude/Azimuth Table.* http://aa.usno.navy.mil/data/docs/AltAz.php

University of British Columbia Geographic Information Center. (2016). Aerial photography of Southern Gulf Islands. Available at http://gic.geog.ubc.ca/

Unsworth, R. K. F., Williams, B., Jones, B. L., & Cullen-Unsworth, L. C. (2017). Rocking the Boat: Damage to Eelgrass by Swinging Boat Moorings. *Frontiers in Plant Science*, 8, 1–11.

Valiela, I., Foreman, K., LaMontagne, M., Hersh, D., Costa, J., Peckol, P., DeMeo-Andreson, B., D'Avanzo, C., Babione, M., Sham, C., Brawley, J., & Lajtha, K. (1992). Couplings of

Watersheds and Coastal Waters: Sources and Consequences of Nutrient Enrichment in Waquoit Bay, Massachusetts. *Estuaries*, 15(4), 443–457.

van Katwijk, M. M., Thorhaug, A., Marbà, N., Orth, R. J., Duarte, C. M., Kendrick, G. A., Althuizen, I. H. J., Balestri, E., Bernard, G., Cambridge, M. L., Cunha, A., Durrance, C., Giesen, W., Han, Q., Hosokawa, S., Kiswara, W., Komatsu, T., Lardicci, C., Lee, K., Meinesz, A., Nakaoka, M., O'Brien, K., Paling, E. I., Pickerell, C., Ransijn, A. M. A., & Verduin, J. J. (2016). Global analysis of seagrass restoration: The importance of large-scale planting. *Journal of Applied Ecology*, 53(2), 567–578.

van Katwijk, M. M., Bos, A. R., Kennis, P., & de Vries, R. (2010). Vulnerability to eutrophication of a semi-annual life history: A lesson learnt from an extinct eelgrass (*Zostera marina*) population. *Biological Conservation*, 143, 248–254.

Ventura, D., Bruno, M., Jona, G., Belluscio, A., & Ardizzone, G. (2016). A low-cost drone based application for identifying and mapping of coastal fish nursery grounds. *Estuarine, Coastal and Shelf Science*, 171, 85–98.

Walker, D. I., Lukatelich, R. J., Bastyan, G., & McComb, A. J. (1989). Effect of boat moorings on seagrass beds near Perth, Western Australia. *Aquatic Botany*, 36, 69–77.

Wan, H., Wang, Q., Jiang, D., Fu, J., Yang, Y., & Liu, X. (2014). Monitoring the invasion of Spartina alterniflora using very high resolution unmanned aerial vehicle imagery in Beihai, Guangxi (China). *Scientific World Journal*, 2014, 14–16.

Ward, D. H., Reed, A., Sedinger, J. S., Black, J. M., Derksen, D. V., & Castelli, P. M. (2005). North American Brant: Effects of changes in habitat and climate on population dynamics. *Global Change Biology*, *11*, 869–880.

Waycott, M., Duarte, C. M., Carruthers, T. J. B., Orth, R. J., Dennison, W. C., Olyarnik, S., Calladine, A., Fourqurean, J. W., Heck, K. L., Hughs, A. R., Kendrick, G. A., Kenworthy, W. J., Short, F. T., & Williams, S. L. (2009). Accelerating loss of seagrasses across the globe threatens coastal ecosystems. *Proceedings of the National Academy of Sciences*, 106(30), 12377–12381.

Wilber, C.G. (1983). Turbidity in the Aquatic Environment: an Environmental Factor in Fresh and Oceanic Waters. Springfield, IL: C.C. Thomas Publishing Ltd.

Wood, N., & Lavery, P. (2000). Monitoring seagrass ecosistem health - The role of perception in defining health and indicators. *Ecosystem Health*, *6*(2), 134–148.

Wozniak, B., & Dera, J. (2007). *Light absorption in sea water* (Vol. 33).

Young, E. L. (1938). Labyrinthula on Pacific Coast Eel-grass. *Canadian Journal of Research*, 16c(3), 115-117.

Zebarth, B. J., Hii, B., Liebscher, H., Chipperfield, K., Paul, J. W., Grove, G., & Szeto, S. Y. (1998). Agricultural land use practices and nitrate contamination in the Abbotsford Aquifer, British Columbia, Canada. *Agriculture, Ecosystems and Environment*, 69, 99–112.

Zieman, J. C. (1976). The ecological effects of physical damage from motor boats on turtle grass beds in Southern Florida. *Aquatic Botany*, 2, 127–139.

Appendix A – Distribution of training and validation data in Village Bay, Horton Bay, and Lyall Harbour

Village Bay

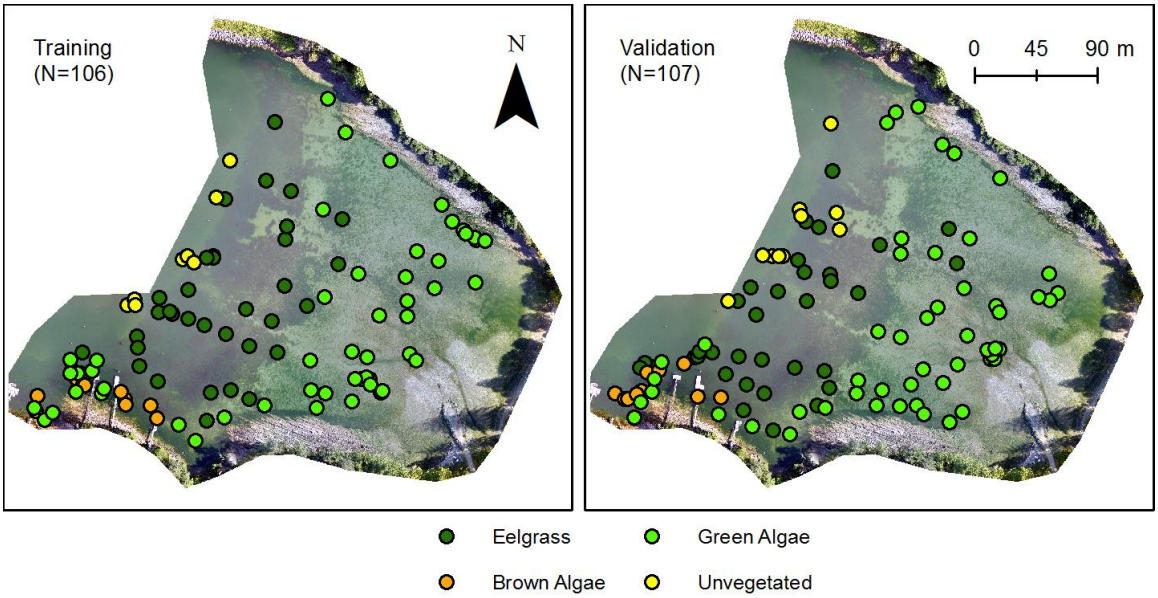

Horton Bay

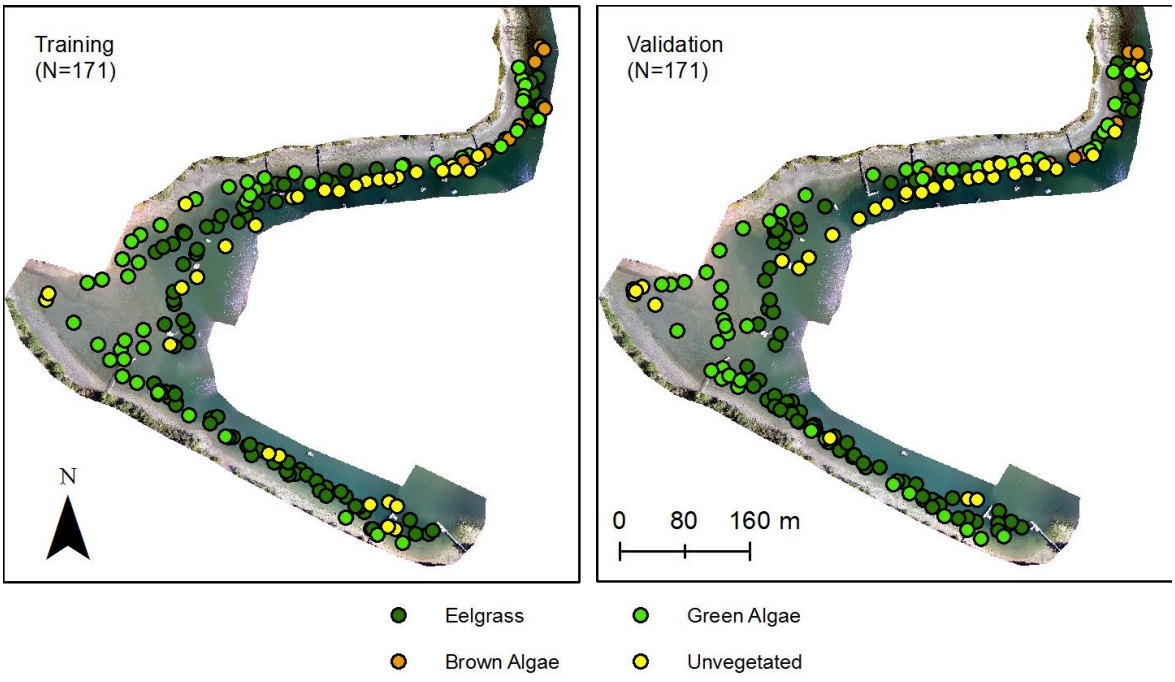

Lyall Harbour

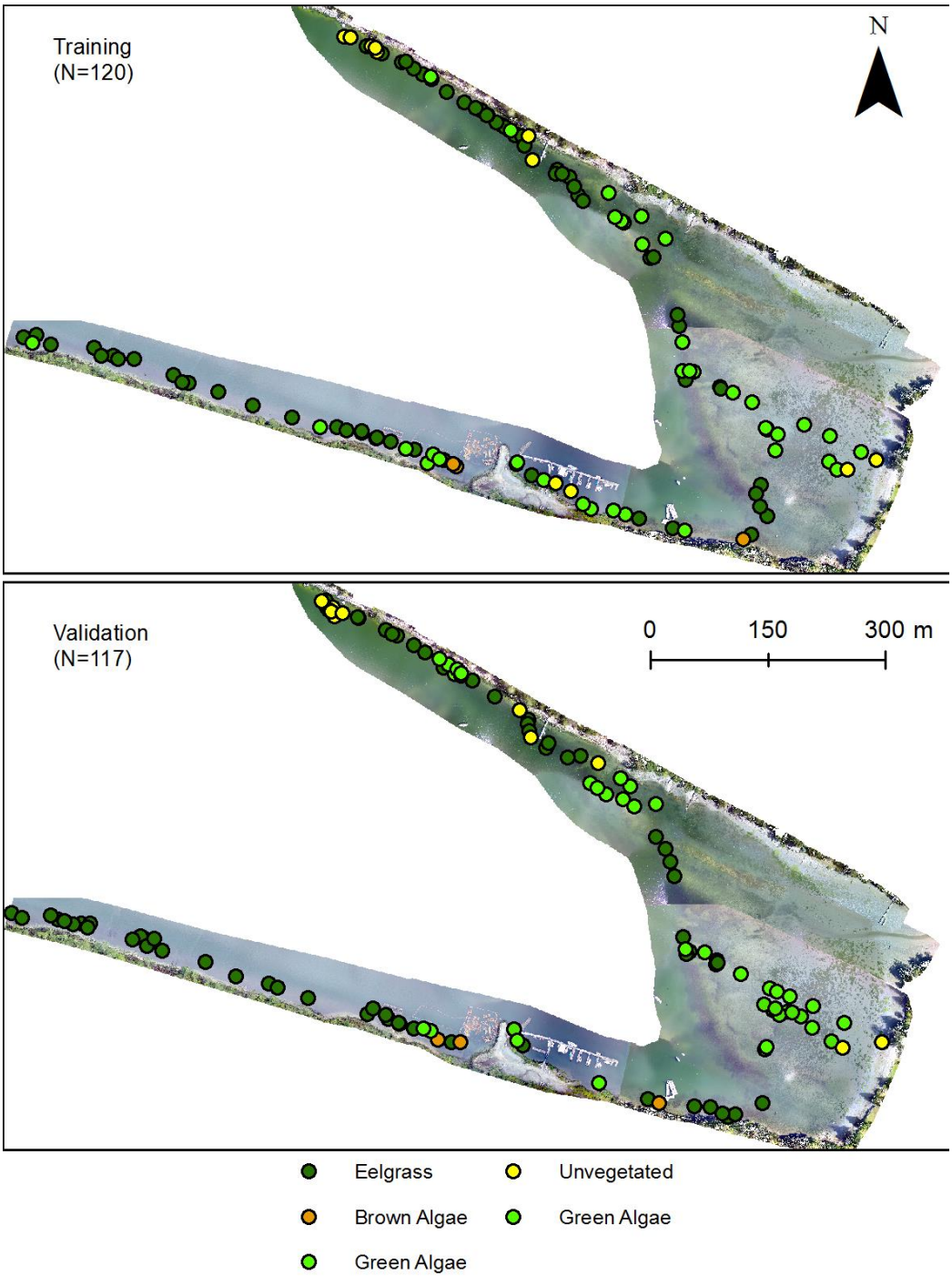

Appendix B – Optimizing UAV Flight Times for Benthic Habitat Mapping

The following SAS code was written as a term project in Geography 524 and was used to optimize tidal height and sun angle for Village Bay, Mayne Island, for the summer 2016 field season (May to August) in order to create a schedule for UAV air photo acquisition. In order to acquire optimal air photos of benthic habitats, flights should be conducted within two hours of the lowest tide of the day, and between sun angles of 30° to 45°.

This analysis included two datasets: tidal height predictions and sun angle calculations for the study period of May to August 2016. Predicted hourly tidal heights were downloaded from the Department of Fisheries and Oceans website for Village Bay (STN#7414). The resulting tidal dataset contained columns for year, month, day, hour, and height in meters for each hourly observation. Sun angle and azimuth data were downloaded from the Astronomical Applications Department of the U.S. Naval Observatory for Victoria, BC. Ten minute increments of sun altitude and azimuth from prior to sunrise to after sunset were saved as individual daily files with columns of time (HH:MM), altitude (°), and azimuth (° E of N).

The general methodological steps for this analysis included: (1) read in datasets into SAS and format appropriately; (2) flag +/- 2 hours on either side of low tide; (3) extract sun altitudes between 30° and 45°; (4) match up appropriate sun altitudes with flagged tidal heights; and (5) create a flight calendar for the 2016 field season. Additionally, plots were created to show tidal height and sun angle for each day for visualization. SAS was used for this analysis, commented code is found in the following box:

```
/* PROGRAM NAME: GEOG 524 PROJECT
   DESCRIPTION: optimizes sun and tide for benthic air photos
   WRITTEN BY: Natasha Nahirnick
   DATE: April 12, 2016

   INPUT FILES:
      hourly tidal height predictions (YEAR, MONTH, DAY, HOUR, HEIGHT)
      Daily 10-minute incremented sun altitude and azimuth (TIME (HH:MM),
ALTITUDE, AZIMUTH)
*/

/* ****** TIDAL DATA ****** */
/* read in tide data all of 2016 and format dates */
data tide_2016;
      infile "E:\NK-524\project_data\2016_tides.txt" delimiter =", ";
      input yr mo dy hr ht;
      date = mdy(mo,dy,yr);
      format date YYMMDD10.;
      time = hms(hr,0,0);
      format time HHMM.;
run;
```

```
/* subset tides to only four summer months */
data tide_summer;
      set tide_2016;
      where date between '1may2016'd and '31aug2016'd;
run;

/* calculate stats for height by day, assign time stamp to id min heights*/
proc means data = tide_summer;
      class date;
      var ht;
      /* creates new variable min_time id the min heights */
      output out = tide_stats minid(ht(time)) = min_time min= ;
run;

/* drop TYPE & FREQ and create a flag variable = 1 */
data min_tides;
      set tide_stats;
      drop _TYPE_ _FREQ_;
      flag = 1;
run;

/*creates new dataset where min tides are flagged in full summer 2016 */
proc SQL;
      create table tide_min_merge as
      select A.*, B.flag
      from tide_summer A left join min_tides B
      on A.date = B.date and A.time = B.min_time
      order by date;
quit;


/* flags +/- 2 hours on either side of low tide. Flag is set at 1 for min
tides by previous datastep, fullflag used to mark 2 hours either side of flag
= 1 */
data flag_sides;
      set tide_min_merge nobs=nobs;
            fullflag=0;
            if flag=1 then do;
                  current=_N_;
                  prev2=current-2;
                  prev1=current-1;
                  next1=current+1;
                  next2=current+2;

                  if prev2 > 0 then do;
                        set tide_min_merge point=prev2;
                        fullflag=1;
                        output;
                  end;

                  if prev1 > 0 then do;
                        set tide_min_merge point=prev1;
                        fullflag=1;
                        output;
                  end;

                  set tide_min_merge point=current;
```

```
                  fullflag=1;
                  output;

                  if next1 <= nobs then do;
                        set tide_min_merge point=next1;
                        fullflag=1;
                        output;
                  end;

                  if next2 <= nobs then do;
                        set tide_min_merge point=next2;
                        fullflag=1;
                        output;
                  end;

            end; /* flag loop */
run;

/* ******SUN***** */
/* read the sun altitude and azimuth data */
%let dir=E:\NK-524\project_data\Da_Scrapa\SummerData\;
%macro sun;
      %let merge_string=;
      %do month = 5 %to 8;
            %do day = 01 %to 31; /* if May, July or Aug, do day 1 to 31, else
to 30 */
                  %if &month = 6 & &day = 31 %then %goto skipout; /* specific
case where June has 30 days and all other have 31 */
                        data sun_&month._&day;
                              format hr Z2.0 /* keep leading zeros */
                                    mi Z2.0  ;
                        infile "&dir.sun_&month._&day." end=last; /* no
extension in sun files */
                              input @1 hr 2. @4 mi 2. alt az;
                              time = hms(hr,mi,0);
                              format time HHMM.;
                              year = 2016;
                              date = mdy(&month,&day,year);
                              format date YYMMDD10.;
                  run;

                  %let merge_string = &merge_string sun_&month._&day;
                  %put &merge_string;
                  %skipout: %let junk=1;
            %end;
      %end;
      data full_sun;
            set &merge_string;
      run;

%mend sun;

%sun;


/* extract times where altitude is between 30 and 45 degrees*/
data sun_good;
```

```
      set full_sun;
      where alt between 30 and 45;
      drop hr mi year;
run;

/* joins the OPTIMAL sun and tide tables together -> output is where optimal
sun and tide date and times match */
proc SQL;
      create table sun_tide_merge as
      select A.*, B.ht
      from sun_good A, flag_sides B
      where A.date = B.date and A.time = B.time
      order by date;
quit;

/* sort optimal times by date and time*/
proc sort data = sun_tide_merge out = sun_tide_sort;
      by date time;
run;


/* ****** DATA TRANSFORM FOR PROC CALENDAR ******* */
/* calculate frequency of obs by day (# of hours we have to fly) and identify
min time (start_time) of each day (minid(date(time)))*/
proc means data = sun_tide_sort noprint;
      by date;
      class time;
      output out=means_sun_tide minid(date(time)) = start_time;
run;

/* keep only the date, freq (# of flight hours), and start time */
data cal_stats;
      set means_sun_tide;
      where _TYPE_ = 0;
      keep date _FREQ_ start_time;
      rename _FREQ_ = flight_hours;
run;

/* calculate the mean alt az and ht for the optimal times
to display in calendar */
proc means data= sun_tide_sort noprint;
      by date;
      class time;
      var alt az ht;
      output out = mean_test;
run;

/* keep only the alt az and ht stats for type 1 (daily) */
data mean_bits;
      set mean_test;
      where _TYPE_ = 0 and _STAT_ = 'MEAN';
      drop time _FREQ_ _TYPE_ _STAT_;
run;

/* merge all the calendar data together, reorder variables */
data cal_dat;
      retain date start_time flight_hours ht alt az;
```

```
      merge cal_stats mean_bits;
run;

/* CALENDAR: displays start time (min time per day), flight hours (freq of
obs per day), average height, altitude, azimuth */
proc calendar data=cal_dat legend;
      start date;
      var start_time flight_hours ht alt az;
run;


/* ***** PLOTTING ******* */

/* Convert from date and time variables to datetime variable to plot time
series of tides */
data tide_date_time;
      set tide_summer;
      sasdatetime=dhms(date,0,0,time);
      format sasdatetime datetime13.;
run;

/* plot tidal height versus datetime variable. example: first week of May*/
proc gplot data = tide_date_time;
      plot ht*sasdatetime;
      where mo = 5 and dy <= 7;
run;
quit;


/* convert sun date and time to datetime */
data sun_date_time;
      set full_sun;
      sasdatetime=dhms(date,0,0,time);
      format sasdatetime datetime13.;
run;

/* plot sun altitude versus datetime variable. Example: month of June */
proc gplot data = sun_date_time;
      plot alt*sasdatetime;
      where '1jun2016'd <= date <= '30jun2016'd;
run;
quit;


/* Plot sun and tide on same chart */
/* merge full sun angle and tide height datasets to plot*/
proc SQL;
      create table sun_tide_merge_full as
      select A.*, B.ht
      from full_sun A, tide_summer B
      where A.date = B.date and A.time = B.time
      order by date;
quit;


/* sorts the merged sun and tide dataset by date and time*/
proc sort data = sun_tide_merge_full out = sun_tide;
```

```
      by date time;
run;

/* plotting sun and tides on the same plot*/
axis1 minor = none
      label=(angle=90 h=2 'Tidal Height (m)');
axis2 minor = none
      label=(angle=270 h=2 'Sun Altitude (d)');
axis3 label=(h=2 'Time');
symbol1 interpol=join width=4 color=blue;
symbol2 interpol=join width=4 color=red;

proc gplot data = sun_tide;
      plot ht*time / vaxis=axis1 haxis=axis3 legend;
      plot2 alt*time / vaxis=axis2 legend;
      by date;
run;

quit;
```

The result of this analysis consists of a calendar of flight windows for the 2016 field season for optimal benthic habitat air photo acquisition. For each day, the information listed includes: start time of optimal flight window (start_time), the number of hours in the flight window (flight_hours), and the average tidal height (ht), sun altitude (alt), and sun azimuth (az) during the optimal flight window.

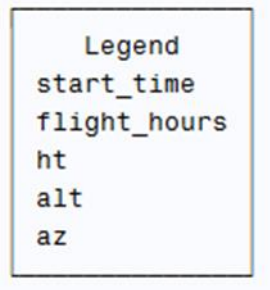

May 2016

Sunday	Monday	Tuesday	Wednesday	Thursday	Friday	Saturday
1 15:00 2 1.65 37.6 248.35	2	3 8:00 2 1.5 34.75 106.5	4 8:00 2 1.2 35 106.3	5 8:00 2 1.05 35.2 106.1	6 8:00 2 1.05 35.45 105.9	7 9:00 1 0.9 40.4 112.3
8	9	10 15:00 1 0.7 44.1 243.6	11 15:00 2 0.8 39.6 250.8	12 15:00 2 0.85 39.8 251	13 15:00 2 1.15 39.9 251.2	14 15:00 2 1.55 40.1 251.4
15 15:00 2 1.95 40.3 251.6	16 8:00 2 1.55 37.35 103.85	17 8:00 2 1.35 37.5 103.65	18 8:00 2 1.25 37.65 103.4	19 8:00 2 1.15 37.75 103.2	20 8:00 2 1.15 37.95 103.05	21 9:00 1 1 42.9 109.3
22 9:00 1 1.2 43 109.2	23 9:00 1 1.3 43.2 109	24	25	26	27 16:00 1 1.1 37.4 260.4	28 16:00 1 1 37.5 260.5
29 16:00 1 1.2 37.7 260.6	30 16:00 1 1.6 37.8 260.7	31 8:00 2 1.6 39.1 101.1				

June 2016

Sunday	Monday	Tuesday	Wednesday	Thursday	Friday	Saturday
			1 8:00 2 1.15 39.15 101	2 8:00 2 0.8 39.2 100.8	3 8:00 2 0.6 39.3 100.65	4 8:00 2 0.6 39.3 100.55
5 9:00 1 0.6 44.3 106.8	6 9:00 1 1 44.3 106.6	7	8	9	10 16:00 1 1.2 38.9 261.3	11 16:00 1 1.3 39 261.4
12 16:00 1 1.6 39.1 261.4	13 8:00 2 1.75 39.6 99.5	14 8:00 2 1.45 39.6 99.4	15 8:00 2 1.25 39.5 99.3	16 8:00 2 1 39.5 99.25	17 8:00 2 0.9 39.5 99.2	18 8:00 2 0.85 39.5 99.1
19 8:00 2 0.95 39.5 99.05	20 9:00 1 0.9 44.3 105.3	21 9:00 1 1.1 44.3 105.2	22	23	24	25 16:00 1 1.3 39.6 260.9
26 16:00 1 1.3 39.6 260.8	27 16:00 1 1.4 39.6 260.8	28 8:00 1 1.8 34.1 92.6	29 8:00 1 1.3 34 92.6	30 8:00 2 1 38.9 98.85		

July 2016

Sunday	Monday	Tuesday	Wednesday	Thursday	Friday	Saturday
					1 8:00 2 0.6 38.8 98.85	2 8:00 2 0.45 38.7 98.95
3 8:00 2 0.5 38.6 98.95	4 8:00 2 0.8 38.5 99	5 9:00 1 0.9 43.3 105.3	6	7	8	9 16:00 1 1.6 39.2 259.3
10 16:00 1 1.6 39.2 259.2	11	12 8:00 1 1.8 32.8 93.3	13 8:00 1 1.5 32.6 93.4	14 8:00 2 1.3 37.4 99.85	15 8:00 2 1.05 37.3 99.95	16 8:00 2 0.9 37.15 100.1
17 8:00 2 0.75 37 100.2	18 8:00 2 0.8 36.85 100.4	19 8:00 2 0.95 36.7 100.5	20 9:00 1 1 41.5 107	21 9:00 1 1.3 41.3 107.1	22	23
24	25 16:00 1 1.6 37.4 256.6	26	27	28 8:00 1 1.3 30.5 95.7	29 8:00 2 1 35.15 102.3	30 8:00 2 0.65 34.95 102.5
31 8:00 2 0.5 34.8 102.7						

August 2016

Sunday	Monday	Tuesday	Wednesday	Thursday	Friday	Saturday
	1 9:00 1 0.5 39.5 109.4	2 9:00 1 0.7 39.3 109.6	3 9:00 1 1 39.1 109.8	4 9:00 1 1.5 38.9 110.1	5	6
7 15:00 1 1.7 44 239.6	8 15:00 2 1.9 39.15 246.6	9	10	11	12	13 9:00 1 1.3 37.1 112.5
14 9:00 1 1 36.9 112.8	15 9:00 1 0.8 36.7 113.1	16 9:00 2 0.75 40.75 121.25	17 9:00 2 0.75 40.5 121.55	18 9:00 2 0.85 40.25 121.85	19 9:00 2 1.1 40 122.15	20 10:00 1 1.3 44 130.3
21 10:00 1 1.8 43.7 130.6	22 15:00 1 1.8 39.7 236.7	23	24	25	26	27
28 9:00 1 1 33.7 117.2	29 9:00 2 0.9 37.55 125.35	30 9:00 2 0.85 37.25 125.65	31 9:00 2 0.95 37 126			

Appendix C – Matrix for interpreting benthic habitats in UAV imagery

Cover type	Tone/Colour	Texture	Shadow	Context
Eelgrass	Dark green, slightly red hue where epiphytes heavy	Medium, 'sinuous' blade texture	Present	Bathy range, sandy substrates, reference to community mapping
Green algae	Medium green when dense, bright when sparse over bright sand	Fine, 'flat'	Not present	Accumulate generally on landward side of eelgrass meadow because gets "stuck" as tide goes out
Brown algae (*L. saccharina*)	Dark Purple-red	Fine, 'flat'	Not present	Small patches mixed in green algae
Brown algae (*S. muticum*)	Medium to bright orange-brown	Medium	Present	Small patches arranged in linear groups on rocky substrates
Bare	Bright in shallow to medium in deep. Brighter than SAV	Very fine	Not present	Between eelgrass and shore, past deepwater edge of eelgrass

Appendix D – Additional sites mapped by UAV not included in analysis

During data collection in the summer of 2016, UAV imagery and kayak videography were collected at a total of eight sites. While several of these sites did not have good quality historic aerial photography and were thus excluded from long-term change assessment, all of these additional sites experienced poor UAV image stitching and geometric outcomes as a result of the UAV technology used. The XAircraft X650 UAV was already 6-8 years old when the data was collected, and as such it did not support geotagged imagery. All consumer-grade "off-the-shelf" UAV platforms available on the market today will support geotagged imagery, which will always provide full-coverage orthomosaics, even when water visibility was poor or in deep water with no distinct features. By selecting the sites that had the best orthomosaic coverage and geometry to write a manuscript for publication, it was possible to address specifically the "benefits and challenges" of UAV eelgrass mapping without having to discuss why poor mapping outcomes were experienced from using the wrong technology. While only three of these sites, Village Bay, Horton Bay, and Lyall Harbour, were used for analyses, the other five sites constituted a considerable investment of time and effort spent within the context of the graduate research.

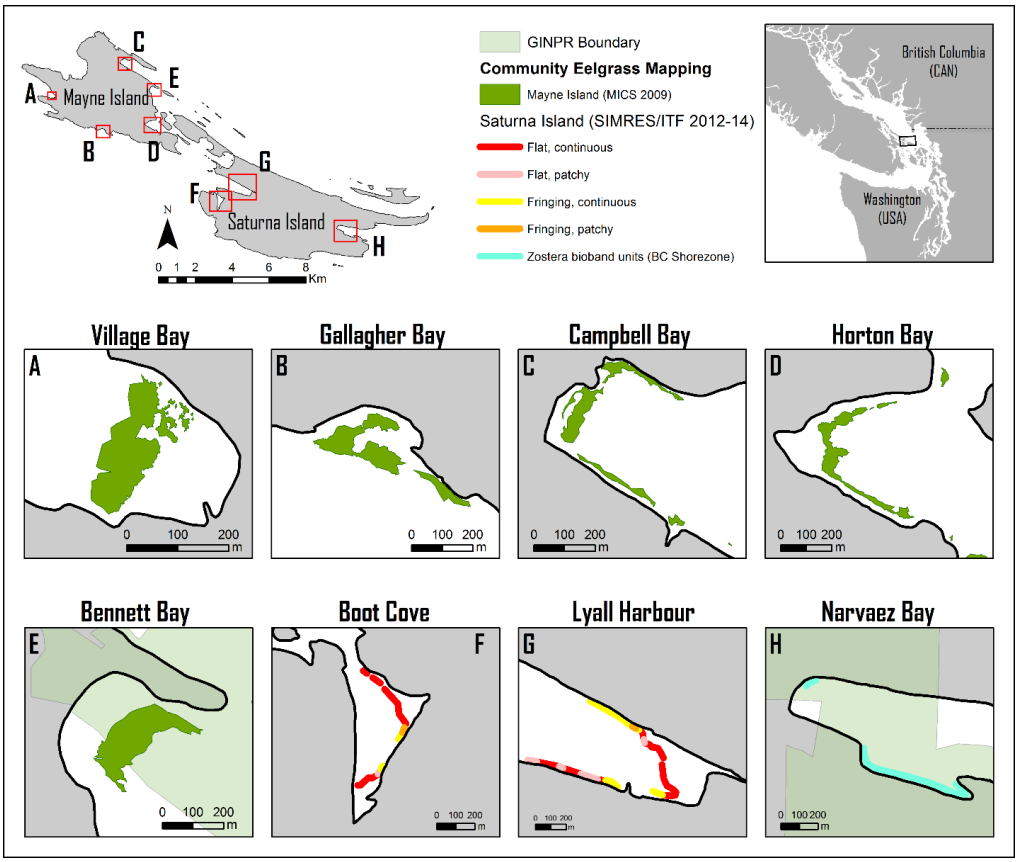

Gallagher Bay

This site was not part of the original field data collection plan. However, since the MICS eelgrass mapping site for the 2016 season was Gallagher Bay, there was an opportunity to compare the eelgrass mapped by kayak and dive survey to the UAV data. Data was collected at Gallagher Bay on June 29 and again on July 21 to cover more area with hopefully better environmental conditions. Imagery collected on both days are presented here with mapped eelgrass, because while the June 29 survey experienced better eelgrass detection, the July 21 survey covered more area. A total of 0.67 ha and 1.32 ha of eelgrass was mapped on June 29 and July 21, respectively. A small patch of suspected *Z. japonica* was located in the high intertidal. When comparing the two dates, there appears to be a loss of eelgrass in the shallow intertidal, perhaps because of smothering caused by the substantial collection of *Ulva* spp. at this site, which increases between the two dates. Image stitching is seen to fail in the deep regions of the orthomosaic.

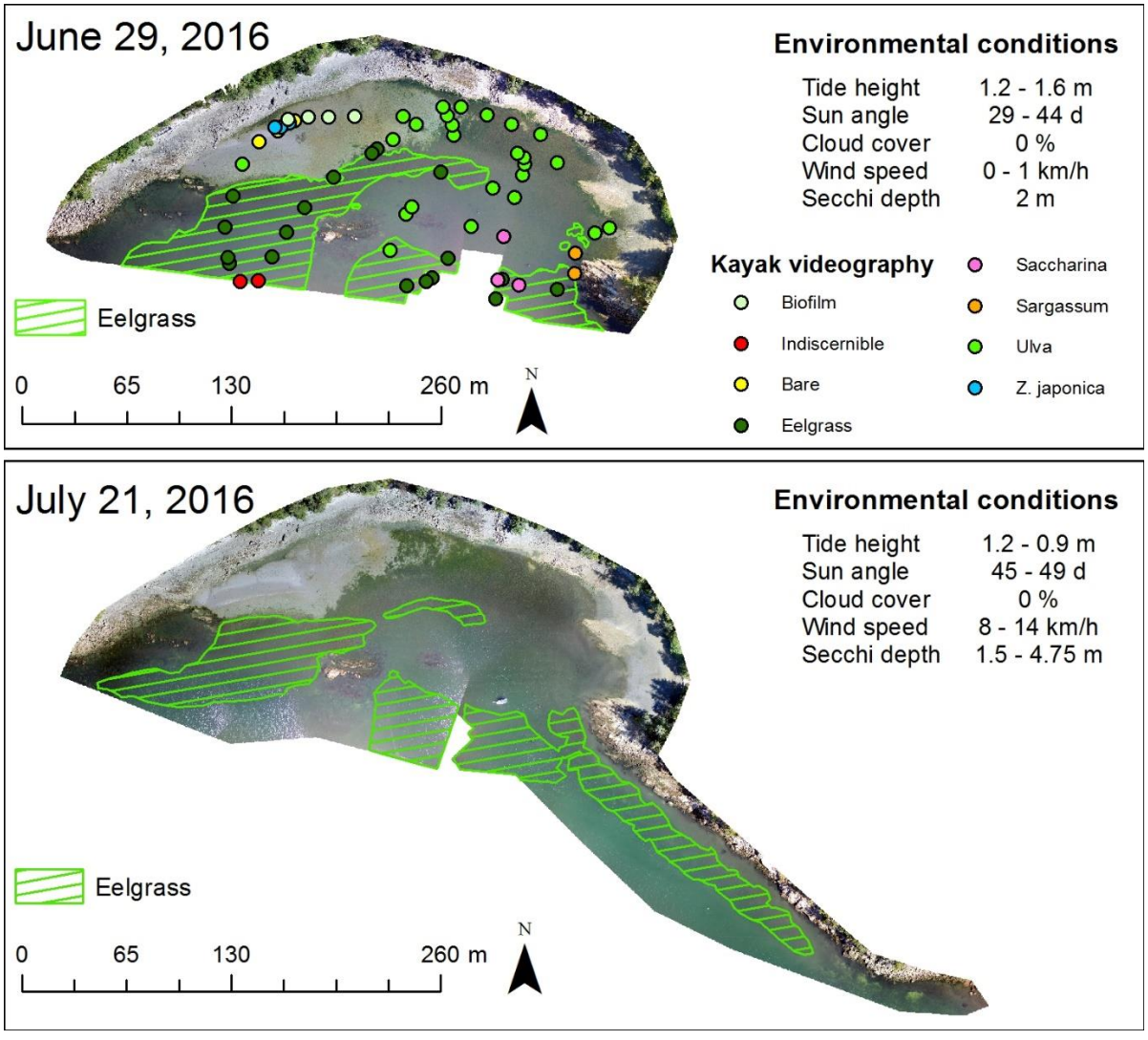

Campbell Bay

Campbell Bay was surveyed a total of three times: once on June 27, and twice consecutively on the morning of July 18. The first flight on June 27 only covered the larger patch at the center of the bay, and the first flight of July 18 experienced very cloudy conditions. As such, the second survey of July 18 was chosen as the mapping photomosaic because eelgrass was much easier to detect with the clearer sky conditions. Some geometric errors were apparent at Horton Bay, as is seen along the south shore where kayak videography points do not line up with mapped eelgrass. A total of 1.09 ha of eelgrass was mapped at Campbell Bay. While full coverage orthomosaics were produced, this site experienced poor geometric fidelity as a result of the placement of ground control points. This issue is demonstrated clearly along the south shore of the site, where kayak videography data indicates eelgrass presence approximately 20m north of where the UAV orthomosaic shows the eelgrass is.

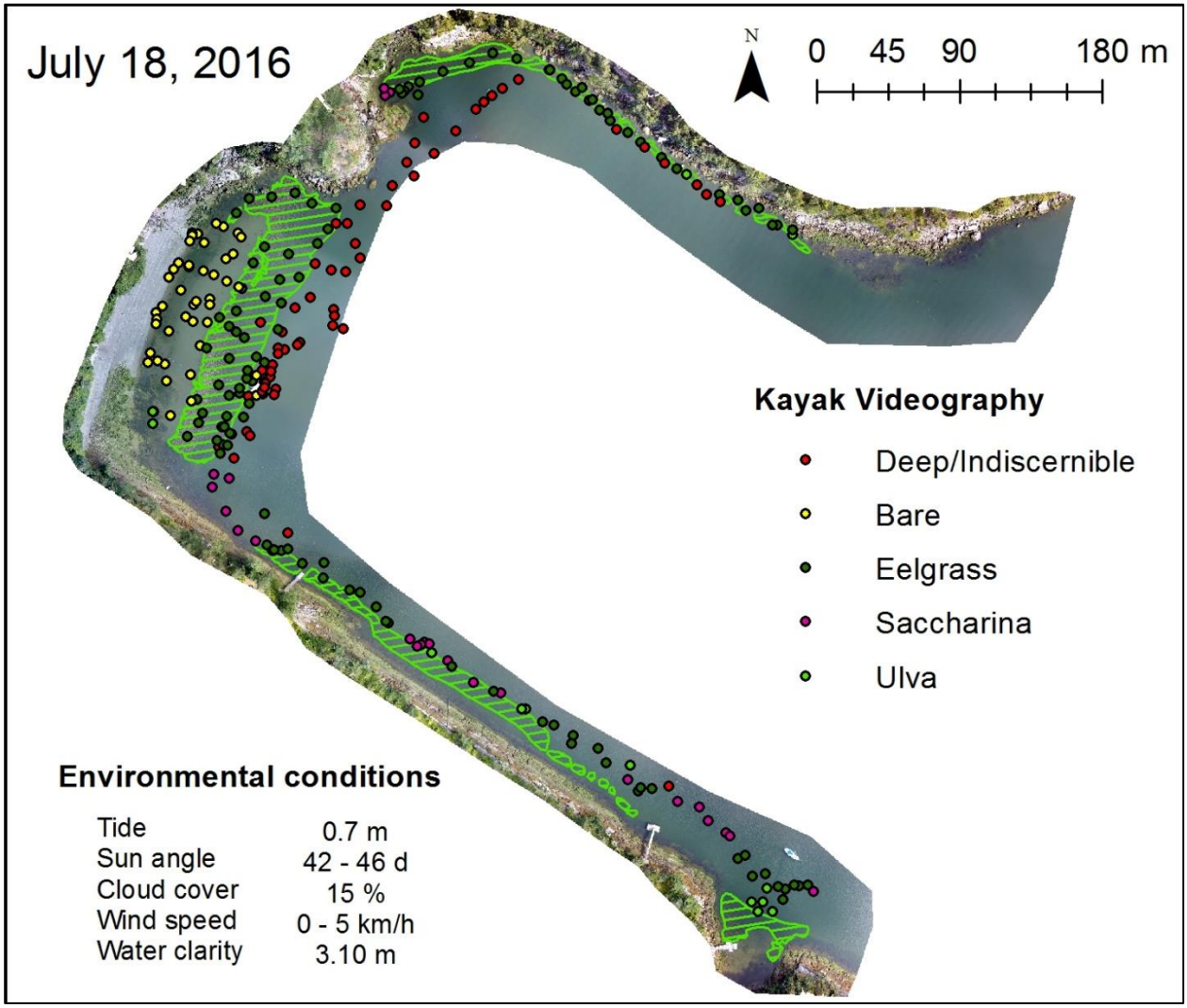

Bennett Bay

The eelgrass in Bennett Bay consists of a main flat and continuous meadow with a small patchy fringe to the north-east. A total of 2.7 ha of eelgrass was mapped by UAV. While we experienced good water clarity conditions at this site, the sky was completely overcast for the majority of the survey. Deep, homogenous parts of the eelgrass bed provide few distinct features for image stitching, and thus in combination with the significant cloud reflectance, image stitching failed in the deep parts of the bay. Mapped eelgrass goes to the edge of the stitched photomosaic, but when compared to the MICS mapping there is likely more eelgrass beyond this deep boundary. There was a large patch of eelgrass on the north-east side of the main bed, indicated by the kayak videography, which was not previously mapped by MICS. Unfortunately, cloud cover prevented image stitching and eelgrass detection in this area, so a polygon was simply traced around the kayak points. Image stitching is seen to have failed along the deep region of the eelgrass.

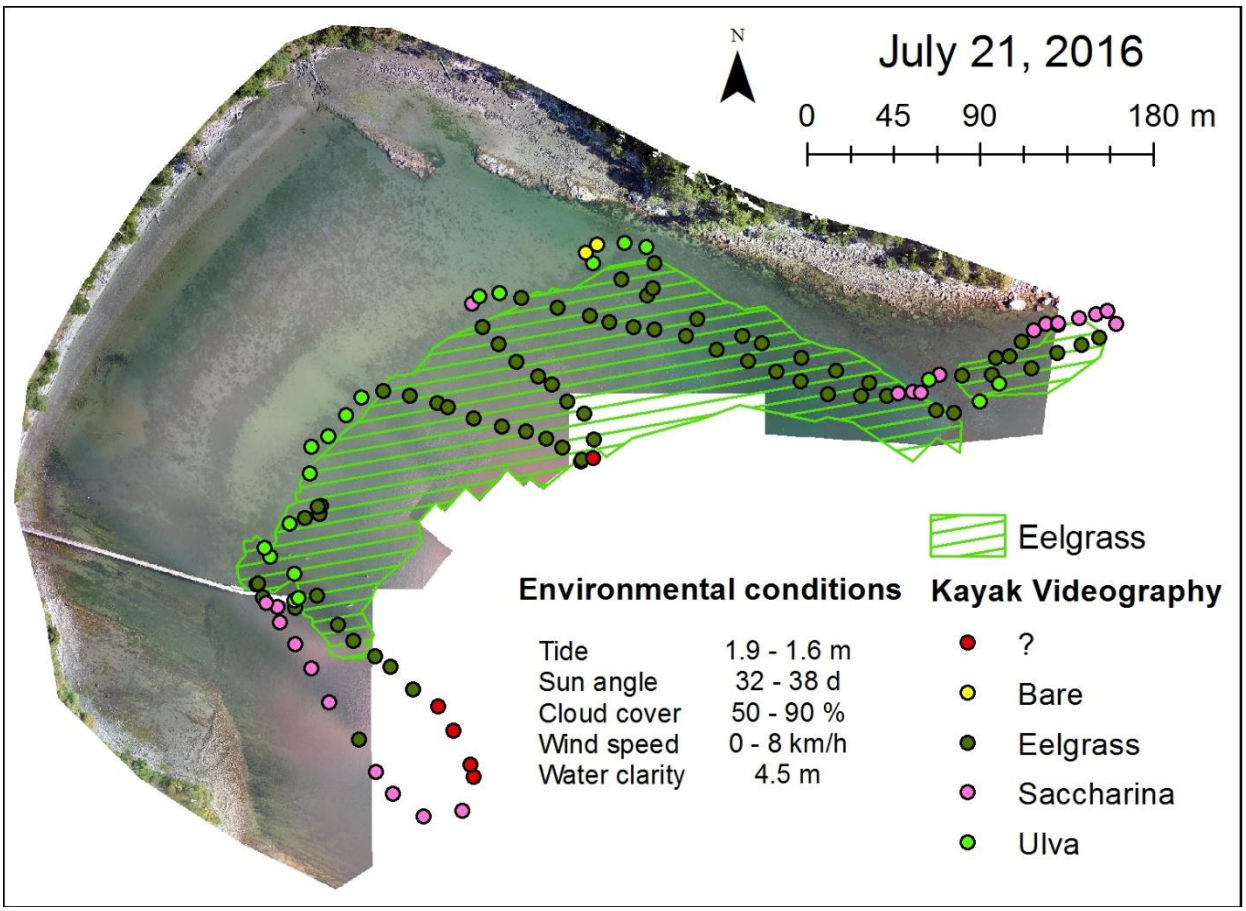

Boot Cove

Eelgrass in Boot Cove consists of two small meadows in the “toe” and “heel”. A total of 0.45 ha of eelgrass was mapped by UAV. Cloud conditions were highly variable throughout this survey, with portions being quite clear and others requiring significant image enhancement to detect the eelgrass beneath the cloud reflectance. The eelgrass patch at the toe of the “boot” was in part defined by drawing a polygon around the kayak points where the imagery failed to stitch.

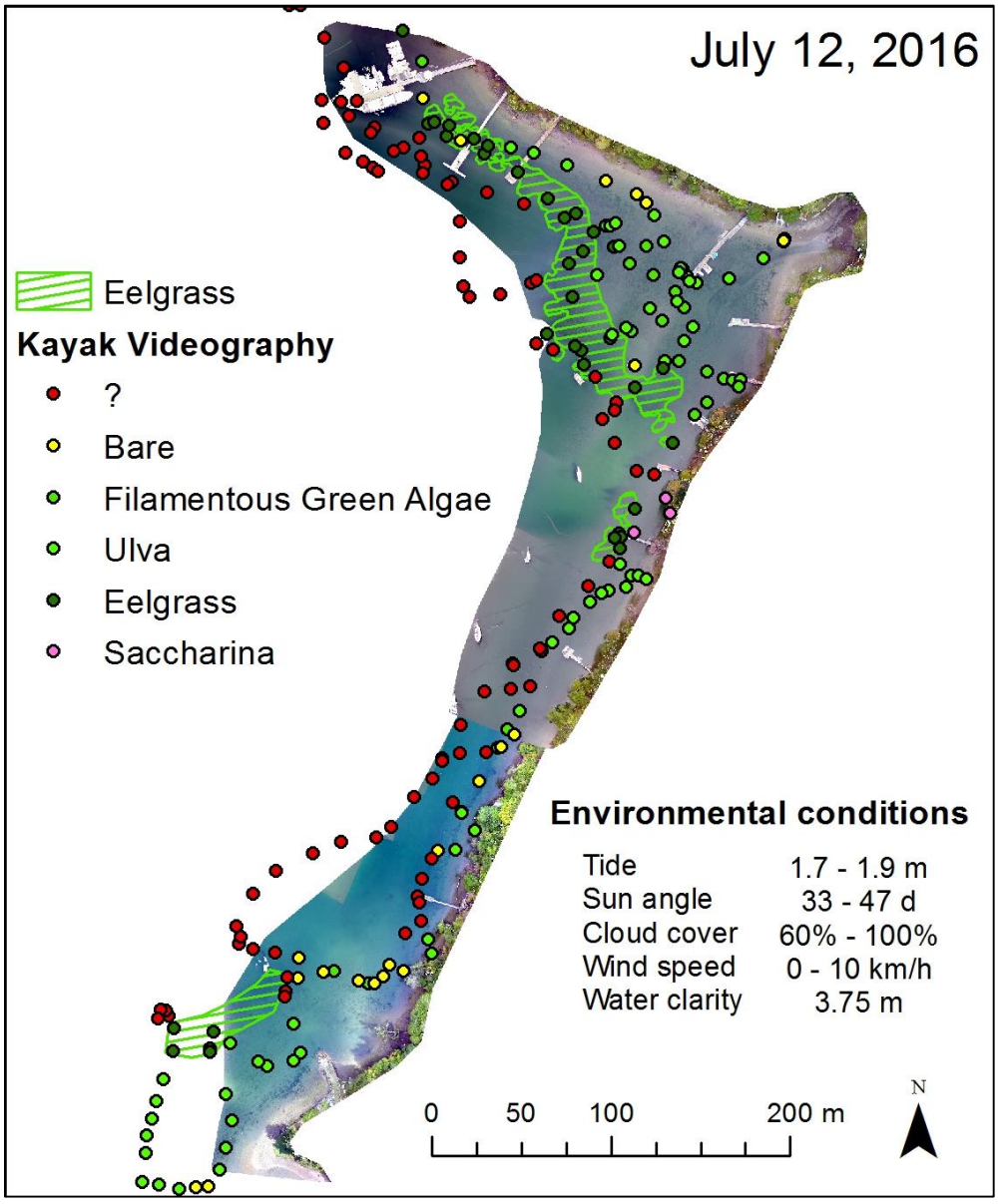

Narvaez Bay

UAV eelgrass mapping in Narvaez Bay was exploratory, as no previous mapping has been conducted at this site by SIMRES or Parks Canada. UAV and kayak data was collected with guidance from the "*Zostera* bioband units" from the BC Shorezone, as well as on observations made in the field from kayak. Unfortunately, while three separate eelgrass beds were located in the kayak video and UAV imagery was collected of all three, the environmental conditions at the time of acquisition, as well as the lack of geotagged imagery, made production of a full-coverage UAV orthomosaic impossible. The results of patchy cloud cover with intermittent sun can be seen in the east end of Little Bay, where "striping" occurs when the imagery is stitched together. On the west end of Little Bay, the photos failed to mosaic due to poor image overlap and lack of geotagging. A total of 1.7 ha of eelgrass is mapped using a combination of UAV imagery, kayak videography, and aerial photography from 2004 and 2010. The large bed on the north shore of Narvaez Bay did not match the "Zostera bioband unit" placement and thus when the bed was discovered, we did not know to collect imagery as far and as deep as would be necessary to capture the entire bed.